HYBRID MACROCYCLES FOR SUPRAMOLECULAR ASSEMBLIES

A Dissertation
Presented to
The Academic Faculty

by

Walter Philip Watson

In Partial Fulfillment
of the Requirements for the Degree
Doctor of Philosophy in the
School of Polymer, Textile and Fiber Engineering

Georgia Institute of Technology
April 2005

HYBRID MACROCYCLES FOR SUPRAMOLECULAR ASSEMBLIES

Approved by:

Dr. Haskell Beckham, Advisor
School of Polymer Textile & Fiber
   Engineering
Georgia Institute of Technology

Dr. Anselm Griffin
School of Polymer Textile & Fiber
   Engineering
Georgia Institute of Technology

Dr. Johannes Leisen
School of Polymer Textile & Fiber
   Engineering
Georgia Institute of Technology

Dr. David Collard
School of Chemistry & Biochemistry
 Georgia Institute of Technology

Dr. Joseph Schork
School of Chemical & Biomolecular
   Engineering
Georgia Institute of Technology

Date Approved: April 15, 2005

ACKNOWLEDGEMENTS

To my research advisor, Dr. Haskell Beckham, for knowing when to let me muddle through things and learn something in the process, even when I don't find what I was looking for, and when to share his insights and get me to try something new.

To my research group, especially Bryan White, Swati Singla, Tiejun Zhao, Chris Hubbel, Tami Mace, and undergraduate intern Angela Camp, for some great discussions and even greater laughs.

To my committee, comprised of Drs. Collard, Griffin, Leisen, and Schork, for their guidance and input into my research.

Most especially, to my wife Cathy, with many thanks for her love and support throughout my graduate studies.

TABLE OF CONTENTS

LIST OF TABLES

LIST OF FIGURES

LIST OF ABBREVIATIONS

BPP-LED	Bipolar pulse pair and longitudinal eddy current delay
CaH	Calcium hydride
$CHCl_3$	Chloroform
CMC	Critical micelle concentration
DEG	Diethylene glycol
DMSO	Dimethyl sulfoxide
DOSY	Diffusion ordered NMR spectroscopy
DSC	Differential scanning calorimetry
DTBP	Di-*tert*-butyl peroxide
GPC	Gel permeation chromatography
HCl	Hydrochloric acid
IR	Infrared
KOH	Potassium hydroxide
LCCC	Liquid chromatography at the critical condition
LC PEAT	Liquid chromatography at the point of the exclusion-adsorption transition
MALDI-TOF MS	Matrix-assisted laser desorption/ionization time-of-flight mass spectrometry
MEK	Methyl ethyl ketone
N_2	Nitrogen gas
NaH	Sodium hydride
NMR	Nuclear magnetic resonance

P2VP	Poly(2-vinylpyridine)
PE	Poly(ethylene)
PDMS	Poly(dimethyl siloxane)
PDMS-POE	Poly(dimethyl siloxane)-*block*-poly(oxyethylene)
PHVE	Poly(hydroxyethyl vinyl ether)
POE	Poly(oxyethylene)
PS	Poly(styrene)
PS-DEG	Poly(styrene)-*block*-diethylene glycol
PS-POE	Poly(styrene)-*block*-poly(oxyethylene)
QELS	Quasielastic light scattering
THF	Tetrahydrofuran
T_g	Glass transition temperature
T_m	Melting temperature

SUMMARY

Hybrid macrocycles, which chimerically integrate multiple chemical compositions and architectures, provide an effective way to impart new properties to polymers that are not found in their linear or homocyclic analogues. This dissertation addresses the incorporation of hydrophilic blocks into hydrophobic polymer, as either a poly(dimethyl siloxane)-*block*-poly(oxyethylene) (PDMS-POE) tadpole with a hydrophobic "head" and a hydrophilic "tail" or as a diblock poly(styrene)-*block*-diethylene glycol hydrophobic-hydrophilic macrocycle. The supramolecular association properties of both kinds of cycles were studied: the PDMS-POE tadpoles in forming micelles, and the PS-DEG macrocycles were threaded with linear polymer to form polyrotaxanes.

The first part of this dissertation focuses on the synthesis and characterization of tadpole macrocycles consisting of a PDMS "head" and POE "tail." Linear α,ω-dihydroxy PDMS was cyclized under dilute conditions with dichloromethylsilane forming a hydrosilane-functionalized PDMS macrocycle. This cycle was then reacted with an α-allyl,ω-methoxy POE oligomer via radical hydrosilylation, resulting in an amphiphilic tadpole. The structure of the tadpole and its precursors were confirmed with gel permeation chromatography (GPC), matrix-assisted laser desorption/ionization time-of-flight mass spectrometry (MALDI-TOF MS), IR, ^{1}H, ^{13}C, and ^{29}Si NMR spectroscopy. Micelle formation in polar and nonpolar solvents was observed by surface tensiometry to determine the critical micelle concentration and quasielastic light scattering (QELS) to measure the size of aggregates. The polymer was found to form larger micelles in polar

solution than nonpolar solution, since the tadpole shape forced the aggregates to pack differently.

The second part of the dissertation concerns the synthesis of a hybrid macrocycle from α,ω-dibromo PS and DEG ditosylate. The PS was synthesized via atom transfer radical polymerization, which allowed for the preparation of oligomeric PS having a narrow molecular weight distribution and functionalized end groups. The two components were reacted in dilute solution, then analyzed with GPC, MALDI-TOF MS, and ^{1}H and ^{13}C NMR, as well as diffusion-ordered NMR spectroscopy (DOSY). Next, styrene was polymerized with a bulky free-radical initiator in the presence of the PS-DEG macrocycles. The cycles were statistically trapped by the growing polymer chains, resulting in polyrotaxanes. The assembly was confirmed by DOSY and the amount of threading calculated to be 13 wt% by ^{1}H NMR. DSC analysis was employed to confirm that the linear and cyclic components were part of the same phase, showing a single T_g of 79 °C.

CHAPTER I

INTRODUCTION

1.1   Motivation and Objectives

Macrocyclic polymers possess several different properties than their linear

counterparts, including different viscosities, diffusion coefficients, thermal transitions,

and miscibilities, making them of interest to the scientific community.[1-7] Originally, the

preparation involved methods like ring-chain equilibribration, which resulted in low

yields and poor control of ring size. Advances in cyclization techniques including "click

chemistry" and self-assembly, however, have made it possible to prepare macrocycles in

large amounts and good yield. Furthermore, topologies more advanced than the simple

ring are now possible, including bridged macrocycles, theta cycles, tadpoles, and other

shapes[8-10] depicted in Figure 1.1.
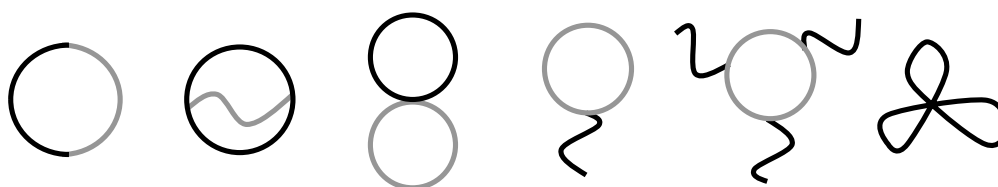
Figure 1.1 –   Examples of macrocycles with advanced topologies. From left to right:
diblock macrocycle, theta macrocycle, conjoined macrocycles, tadpole
macrocycle, branched macrocycle, and knot.

Concurrent with advances in cyclization methods, improvements have been made in

separating cyclic products from their linear byproducts and starting materials. With

solvent fractionation, a decision always had to be made between high purity and high yield, but automated systems like liquid chromatography at the point of the exclusion-adsorption transition (LC PEAT)[11-13] now allow for much higher resolution. Still other schemes use endgroups on linear species[14] or the differences in linear and cyclic topologies[15] to chemically detect and sequester noncyclic impurities.

When combined with the existing tools for the preparation of block copolymers, a new topological class can be created, known as hybrid macrocycles. These molecules consist of a hybrid chemical composition stemming from their block copolymer nature, but the constraints placed on the moieties as a result of their architectures lead to potentially useful properties, especially at interfaces – as a compatibilizer between two immiscible polymeric phases, as a surfactant in solution, or as an additive to alter a polymer surface in response to an environmental stimulus.

For most commercial polymeric systems, it is necessary to incorporate multiple properties, instead of relying on the characteristics of a single polymer. The properties are combined by a variety of methods, ranging from chemical methods such as copolymerization and network formation, to physical means such as blending existing polymers. Copolymers can exist in random, block, and graft topologies, but developing and implementing the chemistry necessary to produce these systems can be expensive and time-consuming. For many end uses, polymer blends offer the most cost-effective solution.

Blending polymers can be accomplished by either layering or mixing. Multilayered or laminate systems are used to act as barriers or to provide an increase in impact resistance,[16] as well as for the fabrication of sensitive optical devices.[17] Otherwise, the

blends stem from mixing the component polymers in solution or in the molten state. Blending polymers can allow the strengths of one component to compensate for weaknesses in another, and sometimes the components synergistically interact, improving the properties further.[18]

Unfortunately, few polymers are completely miscible with each other and able to blend homogeneously. Miscibility requires a negative free energy of mixing, according to the Gibbs Free Energy equation, but blending two polymers typically does not increase the entropy of the system. Therefore, a favorable change in free energy depends on an exothermic enthalpy of mixing. If the polymers interact with each other by hydrogen bonding, dipole-dipole interactions, or ionic bonding, the enthalpy is negative and mixing is favored. Most polymers only interact via weak Van der Waals forces, however, leading to an enthalpy that is zero or positive, resulting in demixing.[18,19]

As the components phase separate in this thermodynamically unstable system, the morphology begins to coarsen. For laminate systems, the layers start to pull apart, and in blends the additives begin to form large domains within the matrix polymer, resulting in poorer physical properties because of the lack of stress transfer across the interfaces between the domains.[20] To alleviate this problem, compatibilizers have been developed with the goals of reducing the interfacial energy between the phases, providing stability against phase separation, and improving interfacial adhesion.[21]

Many different types of compatibilizers have been developed, including random copolymers, graft copolymers, and diblock copolymers. For a hypothetical blend of polymers A and B, the compatibilizer could be a polymer prepared from monomers of A and B. An alternative compatibilizer could be prepared from monomers X and Y, where

X is very incompatible with A and Y is very incompatible with B. In both cases, the compatibilizer has a driving force to situate at the A-B interface, but the XY copolymer potentially has an even stronger thermodynamic drive to do so.[18,19] Once either polymer reaches the interface, the chains stretch across and act like stitches, entangling with the polymer on either side.

As the number of blocks in the compatibilizer increase, so does the number of times the interface is crossed.[18,20] Diblock copolymers cross the interface only once, triblocks twice, tetrablocks three times, and so on. Random copolymers cross the interface multiple times, becoming pancake-like in structure, and only act as stabilizers at higher molecular weights than their blocky bretheren.[22]

Graft copolymers, conversely, are divided into two subspecies: wet brush and dry brush. Wet brush graft copolymers have a low grafting density and low homopolymer molecular weight, allowing for deep penetration into the interface. At the other extreme is dry brush, which resembles a neat block copolymer lamella and has a low degree of penetration. Furthermore, the interfacial tension reduction scales with the degree of polymerization of the wet brush, but is independent of the molecular weight of the dry brush.[23]

Although many kinds of compatibilizers have been developed, obstacles still remain. The primary issue is that preparing many of these unique structures is costly, making them unattractive to industrial adoption. Secondly, the compatibilizer must be able to diffuse in a reasonable amount of time to the interface between the blend components, which can be especially problematic for graft copolymers.[24] The final hurdle is micellization – instead of traveling to the interface, the compatibilizers form micelles in

the polymer matrix that end up disrupting the morphology further, instead of stabilizing it.[19,25,26] Block copolymers are especially prone to forming micelles, but other topologies can do so as well. One current workaround is the preparation of elaborate gradient copolymers, where the composition changes along the chain length.[27] Another strategy is to add monomers that quickly diffuse to and then polymerize at the interface, but this path is difficult to precisely control and prone to side-reactions.[28]

A different architecture that has not been considered for compatibilizers is the hybrid macrocycle. As mentioned above, macrocycles from homopolymers have been demonstrated to possess different physical properties than their linear counterparts, including faster diffusion coefficients and increased miscibility in polymer blends, making them ideal candidates for blend stabilization.[29] By constructing the macrocycles from block copolymers, the self-assembly properties of the block copolymer can be altered by cyclization. Furthermore, topologically advanced cyclic derivatives can also be prepared, paving the way for even more tailored properties. For example, multiarmed macrocycles could combine many of the benefits of graft compatibilizers with the benefits of cyclization.

In addition to acting as compatibilizers between polymers in the solid state, hybrid macrocycles can act as micelles, stabilizing polymers in solution. By controlling the topology of the surfactant, the micelles can adopt more advanced shapes than a spherical arrangement. Micelles from hybrid macrocycles have been shown to behave like lyotropic liquid crystals, with the surfactant concentration and the relative amounts of each polymer block affecting the solution behavior.[10] Columnar and lamellar micelles are especially favored, depending on the exact topology of the polymer.[30] Furthermore,

changing the solvent quality and polarity can cause the macrocycle to adopt new conformations, resulting in solvent-switchable systems.[31]
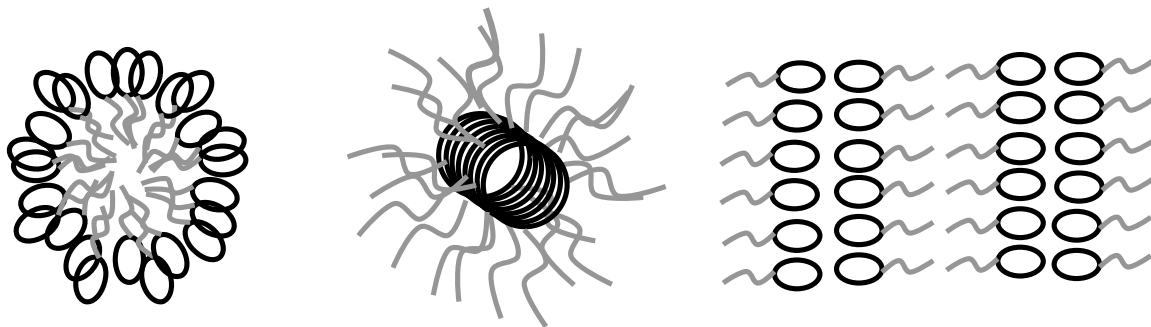
Figure 1.2 – Examples of micelles formed by hybrid macrocycles. From left to right: spherical, columnar, and lamellar micelles.

By selecting the appropriate design, hybrid macrocyclic systems self-assemble and serve as the basis for new kinds of nanoparticles, hydrogels, and microreactors, as well as potentially mimicking the self-assembly of biological macromolecules. By using the topology and chemical composition to tailor the interactions, nanoparticles can be designed that can form the basis for soft lithographic techniques to enable the fabrication of ultra-small electronic devices.[32] Similarly, crosslinking amphiphilic hybrid macrocycles could result in new kinds of hydrogels that swell anisotropically, allowing them to more efficiently fill cracks and holes in bone and cartilage, then act as scaffolds for the growth of new tissue.[33] Finally, micelles from hybrid macrocycles can lead to more design choices in the development of nanoreactors, furthering the possibilities of nanofabrication in polymer matrices.[34]

A final end use for hybrid macrocycles is in the field of surface modification. Currently, surface modification is accomplished by replacing the base polymer formulation with a copolymer, or by blending small homopolymers or copolymers into

the base polymer matrix. Replacing the base polymer formulation with a copolymer results in the additive being present not only at the surface, where it is needed, but also in the bulk, where it can significantly alter physical properties such as strength and thermal transitions. Blends can allow the additive to segregate to the surface, but poor miscibility in the base polymer can lead to leaching from the surface into the environment, with possible toxic effects. The increased miscibility of the hybrid macrocycles can reduce leaching, and the chain ends on topologies such as the tadpole or multiarmed cycle would have an additional entropic drive to surface segregate.

In addition to providing simple surface modification, hybrid macrocycles with solvent-switchable configurations could aid in the development of smart surfaces, which are able to respond in a controlled and reproducible change in their environment.[35] The stimulus could be thermal, electrical, photonic, or chemical, among others. A variety of arms could be grafted onto a macrocycle that is miscible with the base polymer, resulting in a modular library of additives that could all surface segregate for a complex coating, such as the kind needed to trap a host of toxic metals for water decontamination.[35]

Another advantage that hybrid macrocycles offer over their linear counterparts is the option of forming supramolecular assemblies called polyrotaxanes. Polyrotaxanes, also known simply as rotaxanes, consist of macrocycles threaded with linear polymer,[36,37] as illustrated in Figure 1.2. While these assemblies can be prepared in a modular fashion, similarly to blends, they differ in that the two species are mechanically linked, and can be prevented from dethreading by the presence of sterically bulky blocking groups. This architecture can alleviate issues like surface blooming in surface modification applications.
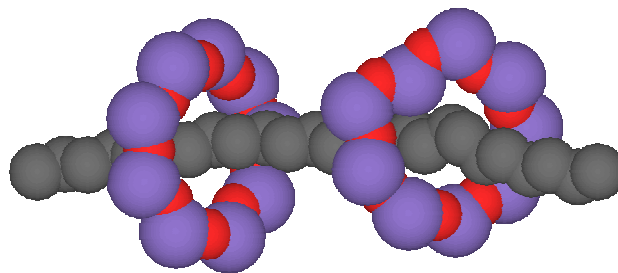
Figure 1.3 –   A simple diagram of a polyrotaxane.

Rotaxanes can be prepared by either self-assembly or statistical threading.   In self-assembly, intermolecular forces result in a thermodynamic drive that causes macrocycles to thread linear polymer in high yield, approaching one macrocycle for every repeat unit.[38]   This occurs between only a small number of linear and cyclic polymers, so the majority of potentially useful rotaxane systems must be synthesized statistically to overcome neutral or unfavorable interactions.   In this method, monomers are polymerized in the presence of a high concentration macrocycles, which rely on Le Chatelier's principle to increase the odds that a cycle will be trapped by the growing polymer.   The very nature of this method, unfortunately, leads to much lower threading levels.[39]

One particular challenge with statistical rotaxanations is that, while the monomer and macrocycle can easily coexist in the same phase, the presence of the polymer tends to cause phase separation, reducing threading levels when the linear and cyclic polymer are chemically different species.   Using a hybrid macrocycle that incorporates blocks of polymer that are miscible with the linear species can retard phase separation, allowing for a greater extent of threading.   Others have speculated that hybrid macrocyclic surfactants would also improve threading yields.   Self-assembling in a columnar conformation could increase the probability of threading multiple cycles.   Furthermore, threading in micelles

of cyclic polymer could couple rotaxanes with many of the benefits of emulsion polymerization, including processability and kinetic control.[40]

The aim of this work is to establish synthetic routes to different kinds of hybrid macrocycles, and then to measure their supramolecular associations as micelles and/or rotaxanes. By linking hydrophobic and hydrophilic blocks, the solution properties of the resultant polymer can be modified, granting it amphiphilic behavior. Similarly, by adding blocks to the macrocycle that resemble the linear polymer in a rotaxane, the unfavorable thermodynamics of mixing will be reduced and threading levels will be increased.

1.2   Materials and Methods

Linear poly(dimethylsiloxane) (PDMS) was chosen as a precursor for the cyclic component of the amphiphilic tadpole molecule. Not only have many cyclization and purification schemes already been developed for PDMS,[14,41,42] but silicon chemistry also offers many ways of creating new bonds that are insensitive to nucleophilic substitutions occurring in the cyclization step. Therefore, the macrocycle could be cyclized with a hydrosilane group present, without needing additional steps for protection and deprotection. Furthermore, PDMS has a low surface energy (20 mN/m),[43] and its low glass transition temperature (-144 to -123 °C)[43] allows the polymer chains to be very mobile; both of these characteristics are an asset to many potential applications in polymer blends. Finally, PDMS is extremely hydrophobic, and can be combined with a large range of more polar polymers to grant amphiphilic behavior. Conversely, poly(oxyethylene) (POE) is a very polar species which can increase the polarity of a

system upon incorporation. Like PDMS, POE has a low T_g (-72 to -65 °C),[43] and incorporates functionalized endgroups that can be utilized in further chemical reactions. The molecular weights of the PDMS and POE polymers were chosen so that each had the same number of repeat units, in order to balance the hydrophilic and hydrophobic blocks of the tadpole.

Poly(styrene) (PS) was chosen because it terminates almost expressly by coupling during free-radical polymerization, facilitating rotaxanation by allowing the use of initiators that can double as blocking groups to prevent dethreading. It can also be synthesized by controlled radical polymerization techniques that result in low molecular weight, low polydispersity, functionalized polymer for macrocyclic precursors. Diethylene glycol ditosylate was then selected to act as a coupling agent in the cyclization of the functionalized PS, increasing the polarity of the resultant macrocycle. More importantly, it kept the total number of backbone atoms below 42, the empirically established upper limit in size that the blocking group/initiator *meso*-4,4-bis(*p-tert*-butylphenyl)-4-phenylbutyl 4,4'-azobis[4-cyanopentanoate] will stop from dethreading.[44]

Rotaxanes from linear PS and cyclic POE have been cyclized previously, but with low threading ratios. The addition of a cosolvent allowed styrene and POE to exist in the same phase, but diluting the concentration of macrocycles also decreased the probability of threading occurring during polymerization. Furthermore, as the polymer chains grew, the POE would begin to phase separate from the styrene and polystyrene, reducing the likelihood of further rotaxanation. It is hypothesized that, by including styrene blocks in the macrocycle, these unfavorable thermodynamic interactions would be reduced and threading levels increased.

1.3 Scope of Dissertation

In keeping with the objectives in Section 1.1, the present study was divided into 5 chapters. Chapter 2 deals with the synthesis and purification of functionalized PDMS, the primary obstacle in making the PS-POE tadpole. Originally, 2 kinds of functionalized macrocycles were planned – those with hydrosilane functionality and those with vinylsilane functionality. Unfortunately, the vinyl group proved to be a target for side reactions, making the route with the hydrosilane species more attractive for further reactions. Analytical techniques like IR and NMR spectroscopy, GPC, and matrix-assisted laser desorption/ionization time of flight spectrometry (MALDI-TOF MS) were used to ascertain the purity of the cyclic product.

Chapter 3 covers the functionalization of linear α-methoxy,ω-hydroxy POE for the second precursor of the amphiphilic tadpole and its subsequent linking to the PDMS macrocycle. Initially, the linking was to be accomplished by a platinum-catalyzed hydrosilylation reaction – a standard procedure for reacting a hydrosilane group and a vinyl group to form a silicon-carbon bond – but using several platinum catalysts under a variety of conditions did not result in a PDMS-POE tadpole. After some model reactions involving α,ω-dihydrosilyl PDMS and α-methoxy,ω-allyl POE to form a triblock POE-PDMS-POE polymer, a radical hydrosilylation pathway was selected to form the tadpole. The product was studied by GPC and multinuclear NMR to fully characterize its structure. Concurrently, differential scanning calorimetry (DSC), surface tensiometry, and quasielastic light scattering (QELS) were employed to study the physical and solution properties of the polymer.

The second hybrid macrocyclic system, a PS-DEG cycle, is discussed in Chapter 4, as well as the preparation of a rotaxane from it and linear PS. A low molecular weight, low polydispersity, difunctional PS was prepared via the controlled radical polymerization technique known as atom transfer radical polymerization. The PS was then cyclized under dilute conditions with a diethylene glycol ditosylate linker. GPC, MALDI-TOF MS, multinuclear NMR, and 2D diffusion-ordered NMR spectroscopy (DOSY) were employed to characterize the macrocycle. The macrocycle was threaded statistically during the polymerization of PS with an initiator containing sterically bulky groups that prevent the cycles from dethreading from the rotaxane. GPC, multinuclear NMR, and DOSY NMR were used to confirm threading and quantitate the amount of macrocycles present in the PS matrix. Thermal characterization was studied by DSC.

1.4   References

(1)   Iatrou, H.; Hadjicristidis, N.; Meier, G.; Frielinghous, H.; Monkenbusch, M. *Macromolecules* **2002**, *35*, 5426.

(2)   Cates, M. E.; Deutsch, J. M. *J. Phys.* **1986**, *47*, 2121.

(3)   Faust, A. B.; Sremcich, P. S.; Gilmer, J. W.; Mays, J. W. *Macromolecules* **1989**, *22*, 1250.

(4)   Santore, M. M.; Han, C. C.; McKenna, G. B. *Macromolecules* **1992**, *25*, 3416.

(5)   Nachlis, W. L.; Bendler, J. T.; Kambour, R. P.; MacKnight, W. J. *Macromolecules* **1995**, *28*, 7869.

(6)   Khokhlov, A. R.; Nechaev, S. K. *J. Phys.* **1996**, *6*, 1547.

(7)   Lecommandoux, S.; Borsali, R.; Schapacher, M.; Deffieux, A.; Narayanan, T.; Rochas, C. *Macromolecules* **2004**, *37*, 1843.

(8)   Frisch, H. L.; Wasserman, E. *J. Am. Chem. Soc.* **1961**, *83*, 3789.

(9)   Tezuka, Y.; Oike, H. *Prog. Polym. Sci.* **2002**, *27*, 1069.

(10)   Khandpur, A. K.; Farster, J. S.; Bates, F. S.; Hamley, I. W.; Ryan, A. J.; Brass, W.; Almdal, K.; Mortensen, K. *Macromolecules* **1995**, *28*, 8796.

(11)   Lepoittevin, B.; Dourges, M. A.; Masure, M.; Hemery, P.; Baran, K.; Cramail, H. *Macromolecules* **2000**, *33*, 8218.

(12)   Cho, D.; Park, S.; Kwon, K.; Chang, T.; Roovers, J. *Macromolecules* **2001**, *34*, 7570.

(13)   Lee, H. C.; Lee, H.; Lee, W.; Chang, T.; Roovers, J. *Macromolecules* **2000**, *33*, 8119.

(14)   White, B. M.; Watson, W. P.; Barthelme, E. E.; Beckham, H. W. *Macromolecules* **2002**, *35*, 5345.

(15)   Singla, S.; Zhao, T.; Beckham, H. *Macromolecules* **2003**, *36*, 6945.

(16)   Cole, P. J.; Cook, R. F.; Macosko, C. W. *Macromolecules* **2003**, *36*, 2808.

(17)   Weber, M. F.; Stover, C. A.; Gilbert, L. R.; Nevitt, T. J.; Ouderkirk, A. J. *Science* **2000**, *287*, 2451.

(18)   Koning, C.; Van Duin, M.; Pagnoulle, C.; Jerome, R. *Prog. Polym. Sci.* **1998**, *23*, 707.

(19)   Viglis, T. A.; Noolandi, J. *Macromolecules* **1990**, *23*, 2941.

(20)   Eastwood, E. A.; Dadmun, M. D. *Macromolecules* **2002**, *35*, 5069.

(21)   Anastasiadis, S. H.; Gancarz, I.; Koberstein, J. T. *Macromolecules* **1989**, *22*, 1449.

(22)   Lee, M. S.; Lodge, T. P.; Macosko, C. W. *J. Poly. Sci. Part B: Polym. Phys.* **1997**, *35*, 2835.

(23)   Hu, W.; Koberstein, J. T.; Lingelser, J. P.; Gallot, Y. *Macromolecules* **1995**, *28*, 8209.

(24)   Furgiuele, N.; Lebovitz, A. H.; Khait, K.; Torkelson, J. M. *Macromolecules* **2000**, *33*, 225.

(25)   Lebovitz, A. H.; Khait, K.; Torkelson, J. M. *Macromolecules* **2002**, *35*, 8672.

(26)   Adedeji, A.; Lyu, S.; Macosko, C. W. *Macromolecules* **2001**, *34*, 8663.

(27)   Kim, J. K.; Gray, M. K.; Zhou, H.; Nguyen, S. T.; Torkelson, J. M. *Macromolecules* **2005**, *38*, 1037.

(28)   Lu, Q.-W.; Macosko, C. W.; Horrion, J. *Macromol. Symp.* **2003**, *198*, 221.

(29)   Singla, S. *Topological Effects on Properties of Multicomponent Polymer Systems.* School of Polymer, Textile and Fiber Engineering, Georgia Institute of Technology, 2004.

(30)   Brandys, F. A.; Pugh, C. *Macromolecules* **1997**, *30*, 8153.

(31)   Höger, S.; Morrison, D. L.; Enkelmann, V. *J. Am. Chem. Soc.* **2002**, *124*, 6734.

(32)   Xia, Y.; Whitesides, G. M. *Angew. Chem. Int. Ed.* **1998**, *37*, 550.

(33)   Weiss, F.; Finkelmann, H. *Macromolecules* **2004**, *37*, 6587.

(34)   Liu, T.; Burger, C.; Chu, B. *Prog. Polym. Sci.* **2003**, *28*, 5.

(35)   Gray, H. N.; Jorgensen, B.; McClaughtery, D. L.; Kippenberger, A. *Ind. Eng. Chem. Res.* **2001**, *40*, 3540.

(36)   Gibson, H. W.; Bheda, M. C.; Engen, P. T. *Prog. Polym. Sci.* **1994**, *19*, 843.

(37)   Nepogodiev, S. A.; Stoddart, J. F. *Chem. Rev.* **1998**, *98*, 1959.

(38)   Harada, A.; Kamachi, M. *Macromolecules* **1990**, *23*, 2821.

(39)   Harrison, I. T. *J.C.S. Perkin I* **1974**, 301.

(40)   Pugh, C.; Bae, J.-Y.; Scott, J. R.; Wilkins, C. L. *Macromolecules* **1997**, *30*, 8139.

(41)   Semlyen, J. A. *Cyclic Polymers*; Elsevier: New York, 1986.

(42)   Grubb, W. T.; Osthoff, R. C. *J. Am. Chem. Soc.* **1955**, *77*, 1405.

(43)   Brandrup, J.; Immergut, E. H.; Grulke, E. A., Eds. *Polymer Handbook*; 4th ed.; John Wiley & Sons, Inc.: New York, 1999.

(44)   Lee, S.-H.; Engen, P. T.; Gibson, H. W. *Macromolecules* **1997**, *30*, 337.

CHAPTER II

SYNTHESIS AND CHARACTERIZATION OF FUNCTIONALIZED CYCLIC POLY(DIMETHYLSILOXANE)

2.1 Introduction

2.1.1. Cyclization Methods

Macrocyclic polymers possess different viscosities, glass transition temperatures, and second virial coefficients than their linear analogues, which propel their interest in the scientific community.[1-7] While several schemes exist for the preparation of macrocycles, they can be grouped in three categories: ring-chain equilibration, bond insertion, and ring closure, all pictured in Figure 2.1. In ring-chain equilibration, a thermodynamic equilibrium exists between ring formation, accomplished by either backbiting or reaction of the endgroups to form a reversible bond, and ring opening to produce linear species. Bond insertion begins with a small macrocycle and, as the name indicates, adds repeat units until the cycle becomes large enough to be considered a macromolecule.

The final scheme, ring closure, encompasses a family of coupling reactions that are illustrated in Figure 2.1(c)-(e). The closure can be accomplished through either unimolecular means or involve two separate species with complementary functionality to make the ring. The third path to ring closure cyclization employs uses ring-closing metathesis, in which a metal catalyst joins together two vinyl-functionalized endgroups to
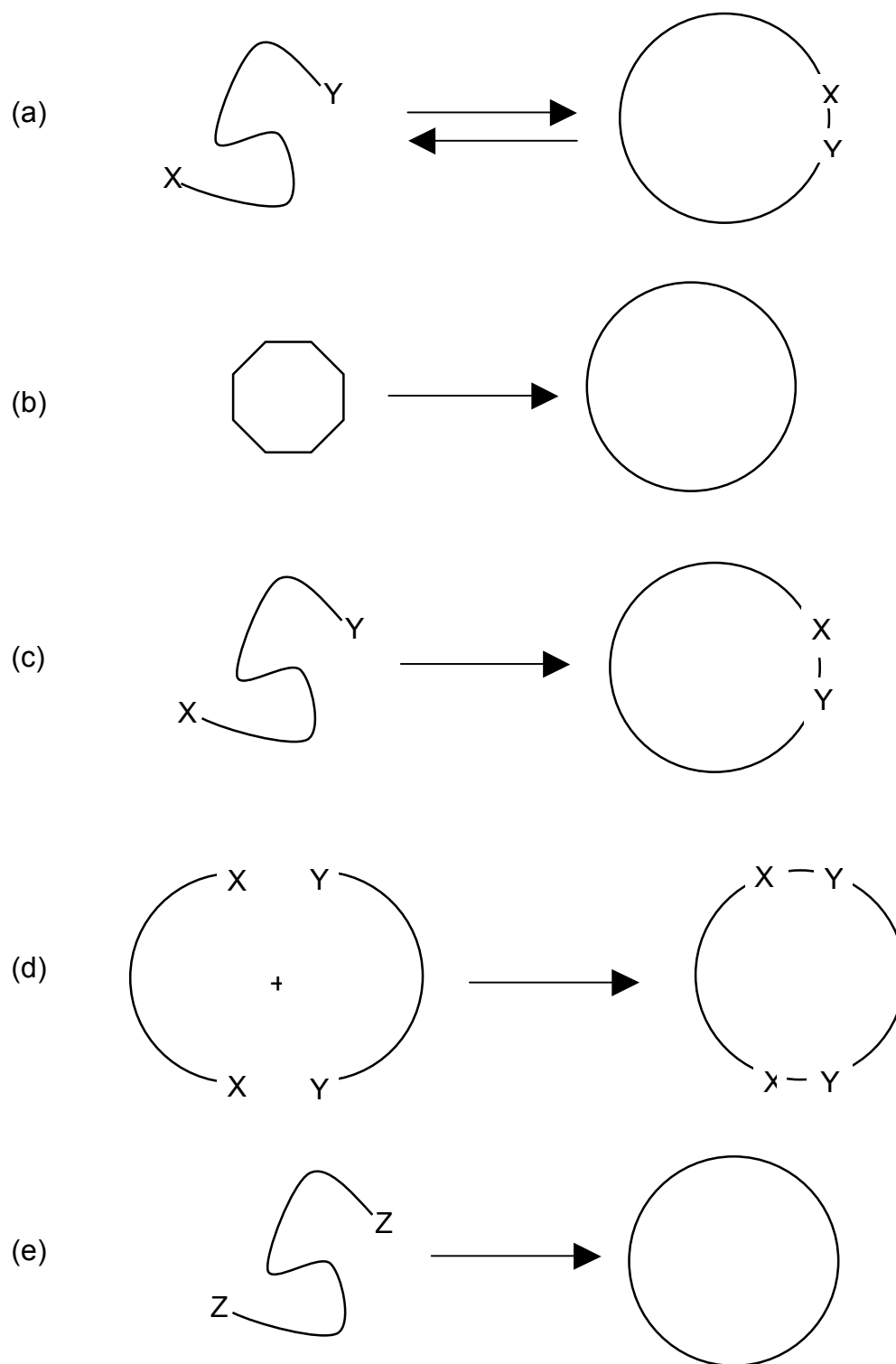
Figure 2.1 – Synthetic schemes for polymer cyclization. (a) Ring-chain equilibrium for linear polymer with complementary reactive endgroups X and Y. (b) Bond insertion to increase the size of a small cycle. (c) Ring closure by unimolecular coupling of an α,ω-heterodifunctional polymer with complementary reactive endgroups X and Y. (d) Ring closure via

16

bimolecular coupling of two α,ω-homodifunctional polymers with complementary reactive endgroups X and Y. (e) Ring closure by unimolecular coupling of allyl groups Z by metathesis condensation.

form a macrocycle containing a double bond, evolving ethylene gas as a byproduct. Unlike the bonds formed in ring-chain equilibration, these reactions are non-reversible.

Some of the earliest research into the synthesis of cyclic PDMS involved ring-chain equilibration.[8-11] Mixtures of linear and cyclic PDMS were heated in the presence of potassium hydroxide or refluxed in concentrated toluene solutions to give a broad range of linear and cyclic products caused by silanolate ions attacking a silicon atom on a PDMS chain and cleaving the existing silicon-oxygen bond in a backbiting reaction to produce a PDMS ring and a smaller linear molecule.[12] These reactions, however, suffered from the inability to produce cycles over 30,000 g/mol and resulted in a broad distribution of cycle sizes – anywhere from 4 to 17 repeat units, with the majority of the cycles consisting of thermodynamically favored sizes of 4 to 6 repeat units,[10] making this scheme unfit for the high-yield preparation of large macrocycles with narrow polydispersities.

The next synthetic path, bond insertion, has one advantage over ring-chain equilibrium and ring closure: since all the products are cyclic, linear byproducts do not need to be isolated and removed from the system. Bond insertion schemes have been employed using organoboranes,[13-15] olefin metathesis,[16] and radical[17] mechanisms. The organoborane path begins with a small cyclic alkane containing a thexylborane substituent that is treated with an ylide, adding the anionic portion of the ylide to the cycle. Units containing alkanes and alkenes have been successfully incorporated, with the M_n of the macrocycle ranging from 1,133 to 26,050 g/mol and polydispersities from

1.37 to 2.9. Unfortunately, the molecular weight of the product is difficult to control,[15] and this chemistry has not yet been proven to work with a large number of systems, including siloxanes.

Olefin metathesis uses a transition-metal catalyst such as ruthenium to swap the carbons in two sets of double bonds. When the double bonds are located at the endgroups of a polymer, ethylene gas is evolved as a byproduct, but when the double bonds are part of 2 different cyclic backbones, the smaller cycle is opened and incorporated into the larger one. Perhaps the most elegant scheme involves the conversion of cyclooctene into cyclic polyethylene with M_n values ranging from 9,000 to 35,000 g/mol and PDIs around 2.0.[16] The main drawback to metathesis reactions involving PDMS is that the catalysts do not react with vinylsilane groups, even when a thermodynamically stable 6-membered ring structure could result.[18]

A final method of ring insertion uses a radical intermediate and can work with polymers that terminate predominantly by coupling. The cyclic initiator consists of 20 backbone atoms, including two thioester groups. Application of heat, ultraviolet light, or γ-ray irradiation splits the initiator into 2 stable sulfur radicals. The radicals initiate the polymerization of monomer, and then terminate by coupling to reform the cycle. Block macrocycles can also be formed, since the thioester groups can be induced to cleave again and polymerize a new monomer. This pathway has been successfully employed to prepare cyclic poly(methyl acrylate) and poly(methyl acrylate)-*block*-(*N*-isopropylacrylamide) macrocycles of M_n 5,730 and 9,600 g/mol, respectively, with PDIs of approximately 1.3. Since radicals interfere with certain silane functionalities, however, a radical method might not be the best mechanism for silicones.[19,20]

Ring closure schemes encompass several synthetic paths that have been used to cyclize many varieties of polymers. Poly(oxyethylene) (POE) has been cyclized 2 different ways, each providing a different kinds of linkage. Booth et al. deprotonated α,ω-dihydroxy POE with a base in a dichloromethane solvent; the hydroxylate ions then displaced the chlorine groups of the solvent, converting a dichloromethane molecule into an acyl linkage for the macrocycle.[21,22] Another method involves deprotonating the endgroups, as before, but reacting tosyl chloride at one end. The hydroxylate ion at the other end of the POE displaces the tosylate group, resulting in a more stable ether linkage.[23,24]

The cyclizations of poly(styrene) (PS)[25,26] and poly(2-vinylpyridine) (P2VP)[27] differ from those of POE in that these cycles were prepared directly from their respective monomers, instead of preformed linear polymer. In each case, a difunctional ionic initiator was used to prepare a polymer with living ionic endgroups under dilute conditions. Next, a difunctional linking agent was added – dichlorodimethylsilane[25] or 1,3-bis(1-phenylethylenyl)benzene[28] for PS, and α,α'-dibromo-p-xylene for P2VP – to result in the cycle. PS cycles were reported in yields as high as 55%, but yields for the P2VP cycles were not reported. Although extreme care must be taken to shield the ions in these schemes from the atmosphere, their living nature allows for an extraordinary amount of control over the molecular weight and size distribution produced.

The bimolecular ring closing reaction of linear PDMS has also been accomplished, resulting in higher yields of larger cycles than ring-chain equilibration. Similarly to the cyclization of POE, PDMS can be reacted with a dichlorosilane linking agent under dilute conditions, resulting in a dimethylsiloxy linkage and a cyclic yield of 77%.[29] The only

drawback to this method is that the silanolate endgroups still have the potential to engage in intramolecular backbiting reactions that can compete with reacting with the dichlorosilane.[30] Bimolecular cyclization of PDMS also has been accomplished while totally avoiding any backbiting reactions, however, by reacting an α,ω-dihydrosilyl PDMS with methyl 3,5-diallyloxybenzoate under dilute conditions in the presence of a platinum catalyst, producing a pair of very stable Si-C bonds to link the ends together.[31]

Additionally, many ring closure reactions can benefit from templating interactions, which have been documented to increase yields by up to 16% for poly(oxyethylene)[32,33] and π-conjugated macrocycles.[34] One of the most promising ring closure schemes using templates, however, is Tezuka and Oike's self assembly and covalent fixation for cyclization results in quantitative yield. This method has been successful in preparing poly(oxyethylene),[35] poly(styrene),[36] and poly(tetrahydrofuran),[37-39] in homocyclic and hybrid topologies, and will be discussed further in Chapter V. The only ring closure scheme that has not been able to work with PDMS to date is ring closing metathesis,[16,40-42] for reasons mentioned above.

2.1.2. Purification Methods

Perhaps the greatest challenge in the synthesis of macrocyclic polymers is the separation of linear and cyclic molecules in the product mixture. The only exceptions to this are the bond insertion schemes, which only leave small molecules as byproducts, and ring closure by self-assembly and covalent fixation, which occurs in quantitative yield. Originally, the species were separated by fractionation with a nonsolvent such as methanol, but similarities in solubilities resulted in low resolution, requiring a trade-off

between purity and yield[43] – high-purity cycles could be recovered in low yield, while higher cyclic yields meant the inclusion of more linear polymer contaminants.

Advances in technology brought about preparative HPLC[44] and GPC,[45] which allow for the automation of the separation process in batches of up to a few grams at a time while separating by either polarity or size. In many cases, unfortunately, the differences between the linear and cyclic species still are not great enough to provide sufficient resolution between the moieties, returning things to the high-purity-or-high-yield dilemma.[46] One modification to this technique, known alternately as liquid chromatography at the critical condition (LCCC)[28,47] or liquid chromatography at the point of exclusion-adsorption transition (LC PEAT)[26] offers the highest resolution to date. It separates polymers by operating at the transition point of size exclusion and adsorption modes of liquid chromatography, causing the linear and cyclic species to elute separately. This technique, however, does not work with all mixtures of linear and cyclic polymers.[48]

Other methods have been adopted that depend on chemical and topological means to separate linear and cyclic molecules in solution with high degrees of specificity. White et al.'s method uses an ion-exchange resin prepared from crosslinked polystyrene with quaternized ammonium salts randomly substituted on phenyl groups throughout the polymer.[29] Linear PDMS molecules with silanolate endgroups then react with the resin and subsequently are removed from solution, and a simple filtration leaves a purified solution of PDMS macrocycles.

Similarly, Singla et al. used the well-documented complexation of linear POE and α-cyclodextrin[49-60] to separate linear and cyclic POE moieties.[24] In this case, saturated aqueous solutions of the polymer mixture and cyclodextrin are mixed; the linear POE

forms insoluble complexes with cyclodextrin that are collected by centrifugation and filtration. The mixture of cyclic POE and uncomplexed cyclodextrin was dissolved in ethyl acetate and filtered to result in pure cyclic POE.

From the many options listed above, one path was chosen – to couple linear α,ω-dihydroxy PDMS under dilute conditions with a dichlorosilane. This approach had been successfully employed previously by White et al. to prepare PDMS macrocycles in high yield, and the linear and cyclic species could be separated easily by using an ion-exchange resin. The deciding factor, however, proved to be the possibility of using different dichlorosilanes such as dichloromethylhydrosilane and dichloromethylvinylsilane to introduce functional groups into the macrocycle.

2.2 Experimental Section

2.2.1. Materials

All reagents were used without further purification unless otherwise specified. Sodium hydride (dry, 95%), dichloromethylvinylsilane (97%), dichloromethylhydrosilane (98%), tetrahydrofuran (THF, anhydrous, 99.9%, inhibitor-free), chloroform-d (99.8 atom % D), and THF-d_8 (99.5 atom % D) were purchased from the Aldrich Chemical Co. α,ω-dihydroxy poly(dimethyl siloxane) (PDMS, M_n 1,520 g/mol, PDI 1.55 as determined by MALDI-TOF MS) was procured from Gelest, and macroporous ion-exchange resin AG MP-1M (1 mequiv/mL, 0.7 g/mL, 100-200 mesh, chloride form) was obtained from Bio-Rad Laboratories and dried at room temperature under a vacuum of 500 mTorr for 16 hours before use. Magnesium sulfate (anhydrous),

toluene (reagent grade), and THF (HPLC, inhibitor-free) were purchased from Fisher Scientific.

2.2.2. Instrumentation

GPC was conducted in THF (1 mL/min) at 303 K on three Waters Styragel columns (5 μm beads: HR 1, 100 Å; HR 3, 1000 Å; HR 4, 10000 Å) that were connected to a Waters 2690 separations module and Waters 2410 refractive index detector. Injections of 100 – 200 μL were made from 10 wt% solutions.

MALDI-TOF mass spectrometry was carried out on a Micromass TofSpec 2E with dithranol serving as the matrix and silver trifluoroacetate used for ionization. Solutions of the polymer (10 mg/mL), matrix (10 mg/mL), and silver trifluoroacetate (2 mg/mL) were mixed in the order listed in volume ratios of 1:1:1, 1:10:1, and 1:100:1. Aliquots of 1 – 2 μL were withdrawn and used to collect mass spectrograms, and the ones with the highest signal/noise ratio were reported.

NMR spectra were measured on a Bruker AMX 400 in chloroform-d ($CDCl_3$) and THF-d_8 in concentrations of approximately 1 wt%.

IR spectra were collected on a Bruker Vector 22 FTIR at a resolution of 4 cm^{-1} with samples supported on potassium bromide discs.

Differential scanning calorimetry was performed on a Seiko Instruments DSC 220C under nitrogen purge with samples weighing 10 – 15 mg sealed in aluminum pans and heated at a rate of 10 °C/min. The power and temperature scales of the calorimeter were calibrated against the enthalpies of fusion and melting temperatures of pure indium and tin.

2.2.3. Synthesis of Hydrosilane-functionalized Cyclic PDMS

A 250-mL round bottom flask, inert gas inlet, and magnetic stir bar were dried overnight at 120 °C, then evacuated and purged with nitrogen 3 times. Using a cannula, 200 mL of anhydrous THF was charged into a flask, and then 0.102 g NaH (4.04 mmol) was added under positive nitrogen flow and suspended in the solvent by vigorous stirring. A gastight syringe was purged 3 times with nitrogen and used to inject 5.0 mL PDMS (4.9 g, 3.2 mmol) dropwise into the reaction flask for a 0.016 M solution. The solution was stirred for 9 hours until the PDMS was deprotonated and the solution grew clear.

A purged gastight syringe was used to add 2.1 mL dichloromethylhydrosilane, followed by 7.9 mL anhydrous THF, into a similarly oven-dried and inert-gas-purged 25-mL flask with stir bar and gas inlet. From this solution, 1 mL was withdrawn (0.21 mL dichloromethylhydrosilane, 2.0 mmol) and added dropwise to the reaction flask containing the activated linear PDMS. The reaction was allowed to proceed 16 hours, and then was quenched by 5.03 g of vacuum-dried ion-exchange resin added to the system under positive nitrogen flow.

After 6 hours, the solution was filtered through a 0.45-μm membrane to remove the resin, and the product was dried by rotary evaporation. Next, the product was dissolved in toluene (200 mL) and washed with distilled water (3 × 200 mL) to extract residual sodium salts, then dried over magnesium sulfate. Toluene was removed by rotary evaporation, and the PDMS was heated at a temperature of 120 °C and pressure of 500 mTorr for 16 hours to remove any low molecular weight cyclic byproducts. The product M_n and PDI as calculated by MALDI-TOF MS were 1,300 g/mol and 1.21, respectively, with 3.19 g of the light yellow oil recovered (76.7% yield). ^{1}H NMR (CDCl$_3$, ppm): 0.3

(Si-CH$_3$), 4.7 (Si-H). ^{29}Si NMR (CDCl$_3$, ppm): -19.17 (Si-H), -22.00 (Si-CH$_3$). FT-IR (cm^{-1}): 2964 (C-H stretch), 2904 (C-H stretch), 2160 (Si-H), 1470 (C-H bend), 1407 (Si-C), 1261 (Si-O), 1129 (Si-O-Si), 823 (Si-C) DSC: No thermal transitions were observed from -150 to 150 °C.

2.2.4. Synthesis of Vinylsilane-functionalized Cyclic PDMS

A 250-mL round bottom flask, inert gas inlet, and magnetic stir bar were dried overnight at 120 °C, then evacuated and purged with nitrogen 3 times. Using a cannula, 200 mL of anhydrous THF was charged into a flask, and then NaH (0.1056 g, 4.18 mmol) was added under positive nitrogen flow and suspended in the solvent by vigorous stirring. A gastight syringe was purged 3 times with nitrogen and used to inject 4.0 mL PDMS (3.8 g, 2.5 mmol) dropwise into the reaction flask for a 0.013 M solution. The solution was stirred for 24 hours until the PDMS was deprotonated and the solution grew clear.

A purged gastight syringe was used to add 29.1 mL anhydrous THF, followed by 0.9 mL dichloromethylvinylsilane, into a similarly oven-dried and inert gas-purged 50-mL flask with stir bar and gas inlet. From this solution, 10 mL was withdrawn (0.30 mL dichloromethylvinylsilane, 2.3 mmol) and added dropwise to the reaction flask containing the activated linear PDMS. The reaction was allowed to proceed 24 hours, and then was quenched by 4.17 g of vacuum-dried ion-exchange resin added to the system under positive nitrogen flow.

After 6 hours, the solution was filtered through a 0.45-μm membrane to remove the resin, and the product was dried by rotary evaporation. Next, the product was dissolved in toluene (200 mL) and washed with distilled water (3 × 200 mL) to extract residual sodium salts, then dried over magnesium sulfate. Toluene was removed by rotary

evaporation, and the PDMS was heated at a temperature of 120 °C and pressure of 500 mTorr for 16 hours to remove any low molecular weight cyclic byproducts. ^{1}H NMR (THF-d_8, ppm): 0.1 (Si-CH$_3$), 0.9 (Cl$_2$Si-CH$_3$), 1.3 (Si-CH-CH$_2$-Si), 5.7-6.1 (Si-CH=CH$_2$).

2.3 RESULTS AND DISCUSSION

2.3.1. Hydrosilane-functionalized Cyclic PDMS

The reaction depicted in Figure 2.2 was monitored by IR and NMR spectroscopy, GPC, and MALDI-TOF MS to study the cyclization process. A comparison of IR spectra of the starting material and product in Figure 2.3 shows the disappearance of the O-H stretch at 3500 cm^{-1} in the product, coupled with a new peak at 2160 cm^{-1} for a Si-H bond.
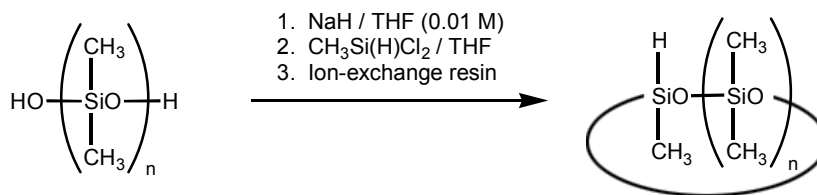
Figure 2.2 – Synthesis of a hydrosilane-functionalized PDMS macrocycle from linear α,ω-dihydroxy PDMS and dichloromethylhydrosilane.

The ^{1}H and ^{29}Si NMR spectra of the linear starting material and cyclic product in Figure 2.4 shows similar results: the peak for the hydroxyl proton from the silanol endgroups (δ_H = 2.9 ppm, δ_{Si} = -20.97 ppm) is absent in the product, replaced by one from the hydrosilane group (δ_H = 4.7 ppm, δ_{Si} = -19.17 ppm). A peak for water in the chloroform solvent can be seen around δ_H = 1.5 ppm.
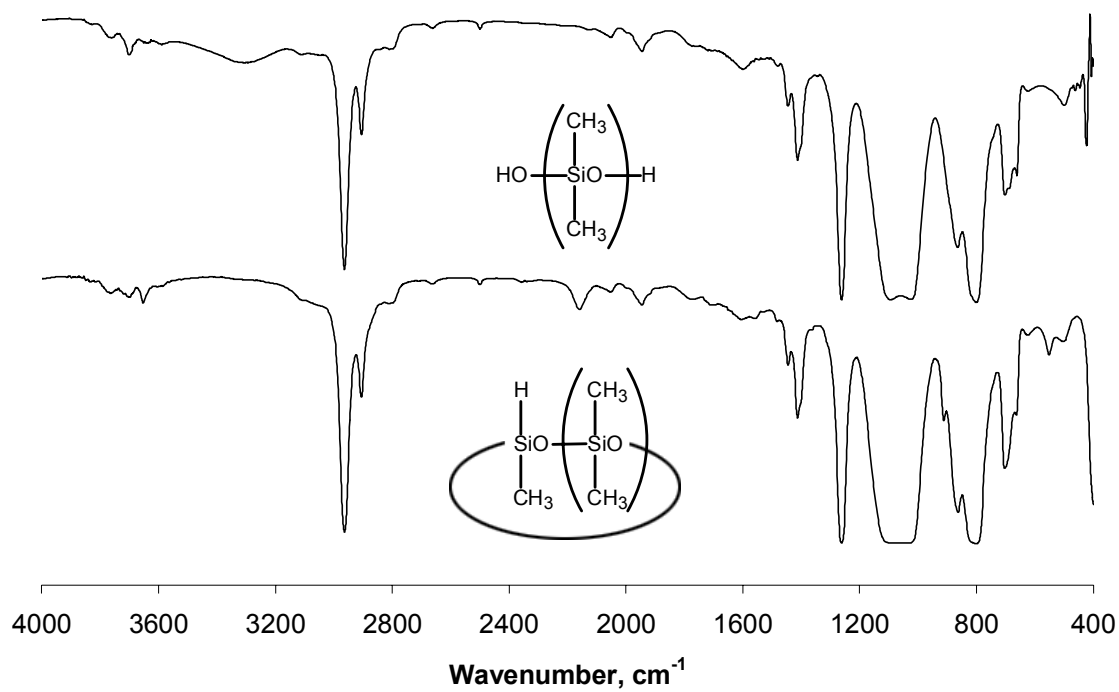
Figure 2.3 – IR spectra of linear and hydrosilane-functionalized cyclic PDMS.
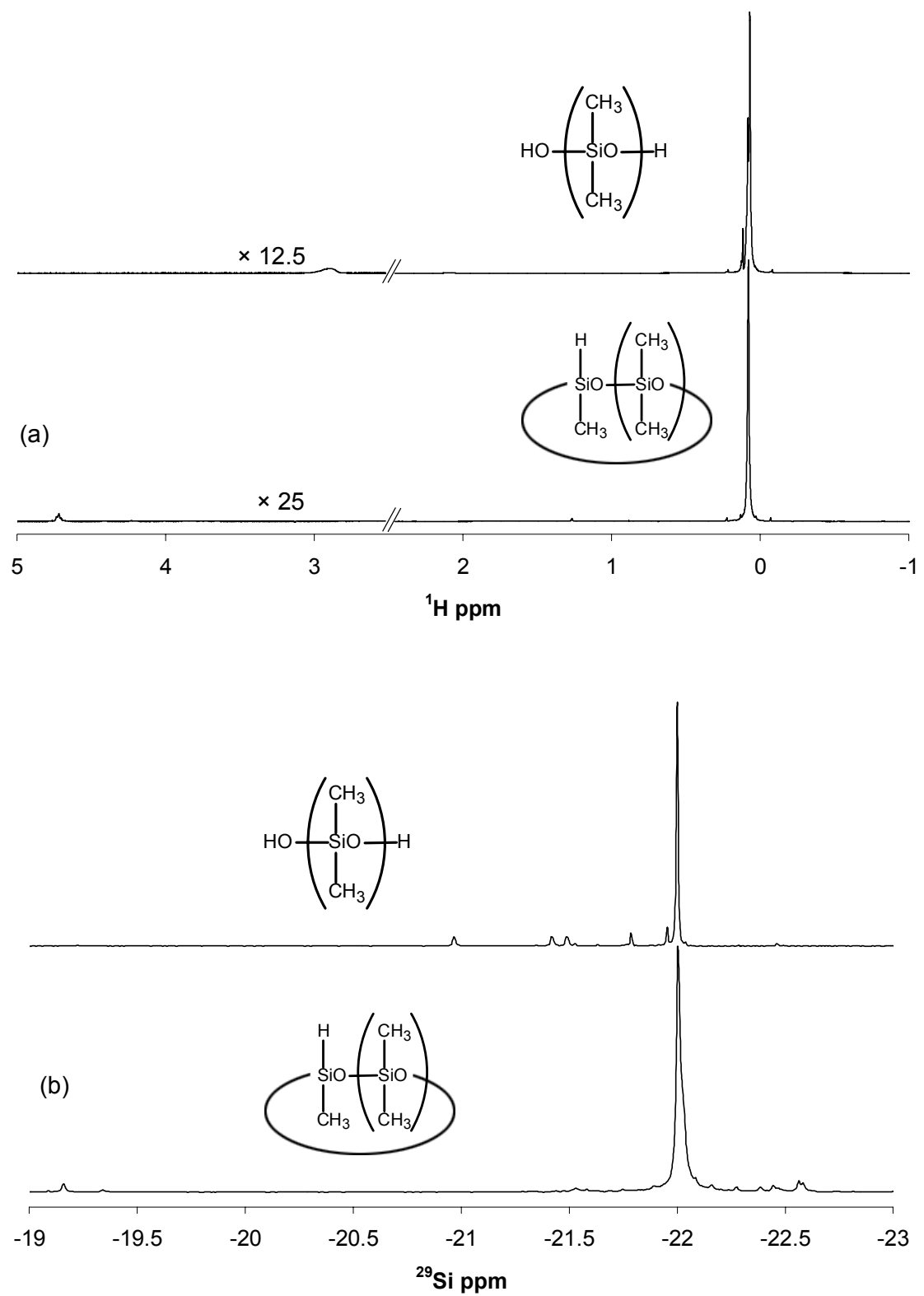
Figure 2.4 – ^{1}H (a) and ^{29}Si (b) NMR spectra of linear and hydrosilane-functionalized cyclic PDMS in CDCl$_3$.

Although the IR and NMR spectra confirm the incorporation of the hydrosilane group into the PDMS, these spectra could also indicate that the dichloromethylhydrosilane was acting as a linking agent to chain-extend the PDMS. The GPC traces of the linear starting material and cyclic product in Figure 2.5, however, indicate that no chain extension has taken place. Instead, the trace of the cyclic PDMS has shifted to a longer retention time, which corresponds to a smaller hydrodynamic volume. At first, this behavior seems unintuitive – after all, the PDMS had an extra repeat unit added, which should result in a larger polymer. The transition from a linear to a cyclic molecule, however, reduced the degrees of freedom possible for the PDMS, resulting in a smaller size. This behavior has been well-documented for PDMS and other polymers.[8]

Matrix-assisted laser desorption/ionization time of flight mass spectrometry (MALDI-TOF MS) is a technique that offers absolute mass characterization for polymers. Unlike convention mass spectrometry, the material is not fragmented by the ionizing beam; instead, entire polymer chains are excited and their mass analyzed by correlating the flight time to polymer size. Since many polymers do not ionize easily, cations are added to the polymer sample to promote desorption.[61]

A comparison of the full linear and cyclic spectrograms can be seen in Figure 2.6(a). The cyclic PDMS is a single distribution, with no higher molecular weight species to be seen. A detailed look at the traces in Figure 2.6(b) provides further evidence for cyclization: Major peaks for silver-cationized linear PDMS can be seen at 1384, 1458, and 1532 amu, all separated by 74 amu, the mass of a dimethylsiloxane repeat unit. The smaller peaks in the linear trace at 1373, 1447, and 1521 amu stem from sodium ion contaminants ionizing the PDMS. The cyclic PDMS trace shows silver-cationized peaks

at 1426, 1500, and 1574 amu – an increase of 42 amu from the starting material, caused by the addition of a methylhydrosilyl unit (+44 amu) and the loss of the silanol protons on the endgroups (-2 amu). Sodium impurities have cationized peaks at 1415, 1489, and 1563 amu, also a 42 amu increase from their linear counterparts.
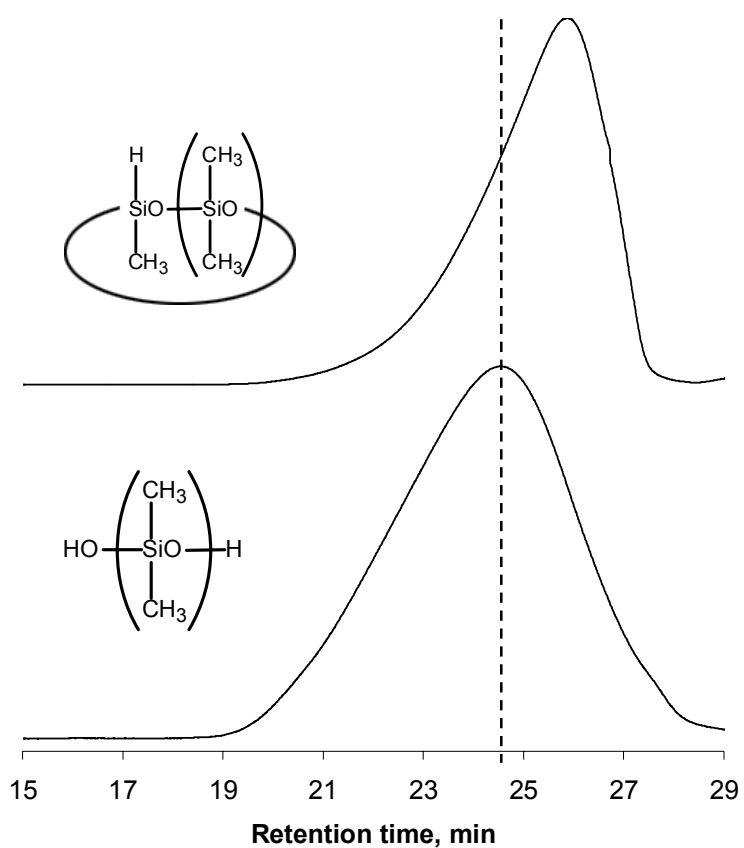
Figure 2.5 – GPC traces of linear and hydrosilane-functionalized cyclic PDMS.
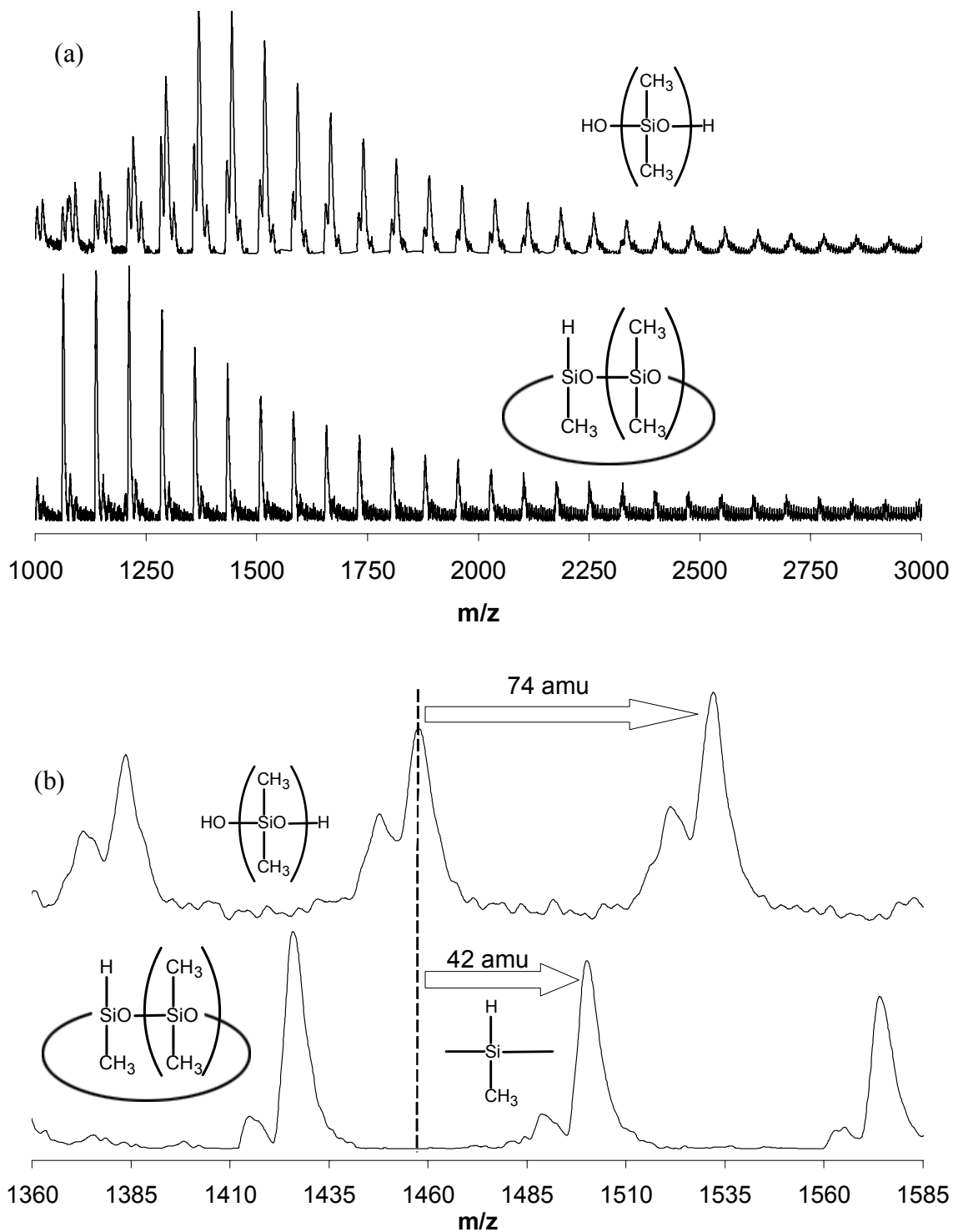
Figure 2.6 – MALDI-TOF spectrograms of linear and hydrosilane-functionalized cyclic PDMS (a). Detail of MALDI-TOF traces of linear and hydrosilane-functionalized cyclic PDMS (b).

Each peak on the mass spectrogram corresponds to the combined mass of a polymer molecule and the sodium or silver cation. To assign the peak to a particular topology, the number of repeat units of PDMS is calculated by subtracting the ion mass and the masses of other features (like endgroups or a methylhydrosilane linker) from the mass of the peak to leave only the mass of the PDMS repeat units in the polymer. This number is divided by the mass of a PDMS repeat unit, and the result should be a whole number. Every possible permutation in polymer structure – linear PDMS, chain extended PDMS, cyclic PDMS, hydrosilane-functionalized cyclic PDMS, etc. – is considered in these calculations, but the only structure that resulted in PDMS repeat units with whole numbers was hydrosilane-functionalized cyclic PDMS, cationized with silver or sodium. Sample calculations for peaks in Figure 2.6(b) are shown below in Equations 2.1 and 2.2:

23 amu (Na, ambient) + 60 amu (methylhydrosilane linker) + x * 74 amu (2.1)
(PDMS repeat unit) = 1,415 amu

x = 18 PS repeat units

108 amu (Ag, ambient) + 60 amu (methyhydrosilane linker) + x * 74 amu (2.2)
(PDMS repeat unit) = 1,500 amu

x = 18 PS repeat units

2.3.2. Vinylsilane-functionalized Cyclic PDMS

The reaction of PDMS and dichloromethylvinylsilane was conducted in a similar fashion to the reaction detailed above and was monitored by ^{1}H NMR and GPC. Unlike the previous experiment, however, the NMR of the product in Figure 2.7 showed that

side reactions had occurred across the double bond of the vinylsilane. The methyl group of PDMS is seen at δ_H 0.1 ppm, and intact vinyl groups at 5.7-6.1. Residual water is present at 2.5 ppm, as well as residual THF from the reaction at 3.6 and 1.7, but the rest of the peaks in the NMR spectrum are the result of side reactions.

As illustrated in Figure 2.8, the vinyl group is susceptible to nucleophilic attack by a silanolate, resulting in a carbanion. The carbanion then can substitute for a chlorine atom on a chlorosilane or cleave a PDMS chain by nucleophilic attack on a silicon atom, generating another silanolate ion. These secondary reactions significantly decreased the utility of this scheme compared to cyclization with dichloromethylhydrosilane.
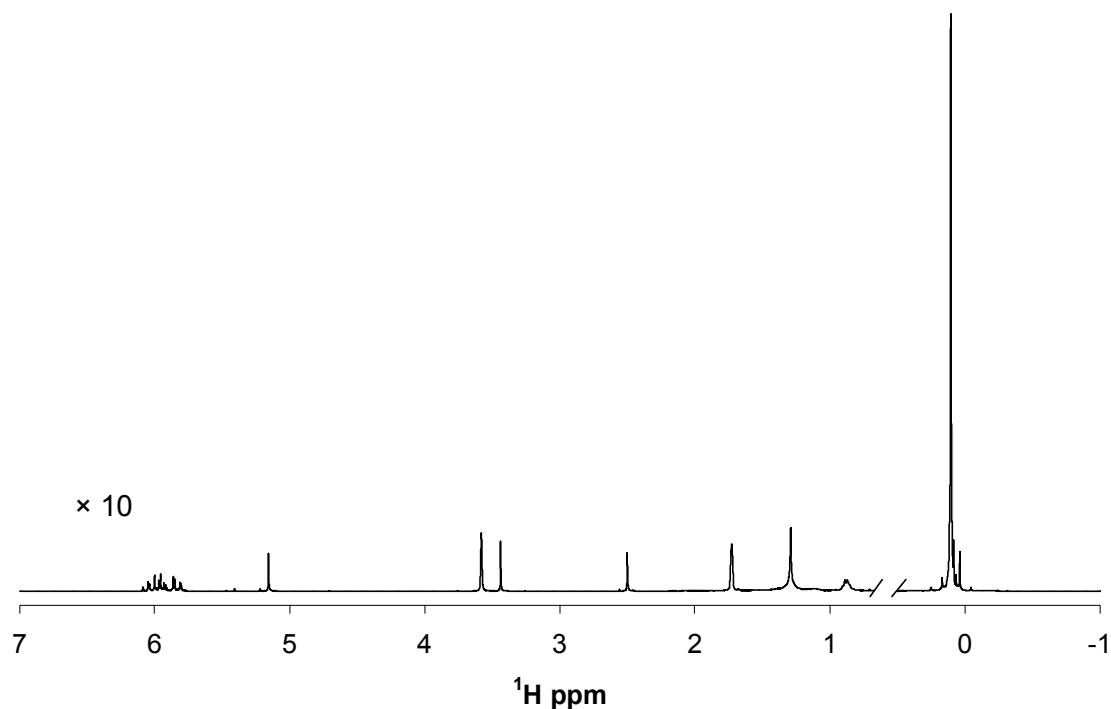
Figure 2.7 – ^{1}H NMR spectrum of the product from reacting α,ω-dihydroxy PDMS with dichloromethylvinylsilane in THF-d_g.
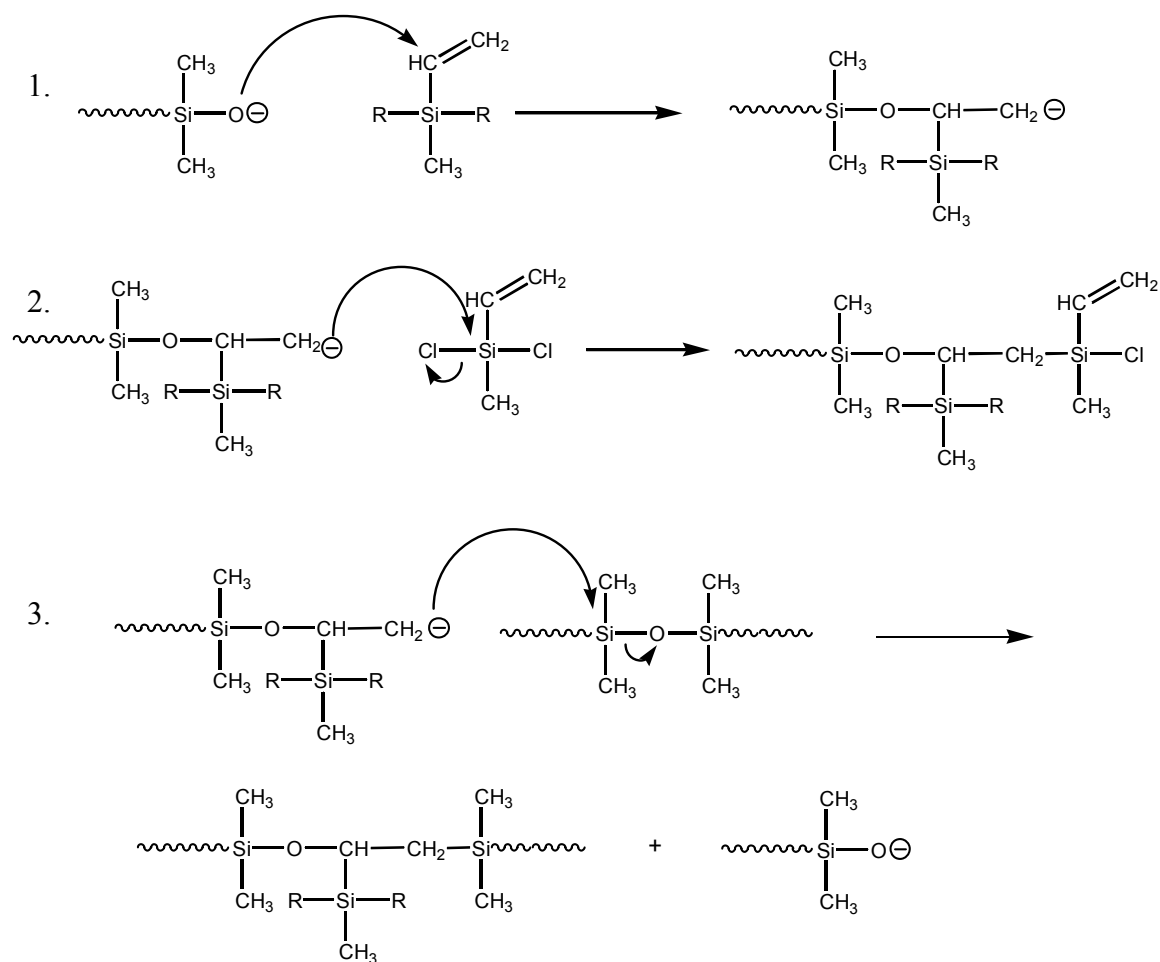
Figure 2.8 – 3 potential reactions occurring during the cyclization of PDMS with dichloromethylvinylsilane. R ≡ Cl, O-PDMS.

2.4 Conclusions

Macrocyclic polymers are prepared by one of three schemes: ring-chain equilibration, bond insertion, and ring closure. The final method was chosen to synthesize functionalized cyclic PDMS by reacting it with either dichloromethylhydrosilane or dichloromethylvinylsilane, although side reactions across the vinyl bond made the former reagent a better choice for later chemistry. To ensure the product was free of linear species, an ion-exchange resin was added to the product mixture in order to remove any

linear PDMS from solution. Hydrosilane-functionalized cyclic PDMS was recovered in 76.7% yield.

2.5 References

(1)   Iatrou, H.; Hadjicristidis, N.; Meier, G.; Frielinghous, H.; Monkenbusch, M. *Macromolecules* **2002**, *35*, 5426.

(2)   Cates, M. E.; Deutsch, J. M. *J. Phys.* **1986**, *47*, 2121.

(3)   Faust, A. B.; Sremcich, P. S.; Gilmer, J. W.; Mays, J. W. *Macromolecules* **1989**, *22*, 1250.

(4)   Santore, M. M.; Han, C. C.; McKenna, G. B. *Macromolecules* **1992**, *25*, 3416.

(5)   Nachlis, W. L.; Bendler, J. T.; Kambour, R. P.; MacKnight, W. J. *Macromolecules* **1995**, *28*, 7869.

(6)   Khokhlov, A. R.; Nechaev, S. K. *J. Phys.* **1996**, *6*, 1547.

(7)   Lecommandoux, S.; Borsali, R.; Schapacher, M.; Deffieux, A.; Narayanan, T.; Rochas, C. *Macromolecules* **2004**, *37*, 1843.

(8)   Semlyen, J. A. *Cyclic Polymers*; Elsevier: New York, 1986.

(9)   Spivack, J.; Dorn, S. B. *Environ. Sci. Technol.* **1994**, *28*, 2345.

(10)   Seyferth, D.; Prud'homme, C.; Wiseman, G. H. *Inorg. Chem.* **1983**, *22*, 2163.

(11)   Grubb, W. T.; Osthoff, R. C. *J. Am. Chem. Soc.* **1955**, *77*, 1405.

(12)   Clarkson, S. J.; Semlyen, J. A.; Horska, J.; Septo, R. F. T. *Polymer* **1986**, *27*, 31.

(13)   Shea, K. J.; Lee, S. Y.; Busch, B. B. *J. Org. Chem.* **1998**, *63*, 5746.

(14)   Wagner, C. E.; Kim, J. S.; Shea, K. J. *J. Am. Chem. Soc.* **2003**, *125*, 12179.

(15)   Goddard, J.-P.; Lixon, P.; Le Gall, T.; Mioskowski, C. *J. Am. Chem. Soc.* **2003**, *125*, 9242.

(16)   Beilawski, C. W.; Benitez, D.; Grubbs, R. H. *Science* **2002**, *297*, 2041.

(17)   He, T.; Zheng, G.-H.; Pan, C. *Macromolecules* **2003**, *36*, 5960.

(18)   Finkel'shtein, E. S.; Ushakov, N. V.; Portnykh, E. B. *J. Molec. Catal.* **1992**, *76*, 133.

(19)   Chatgilialoglu, C. *Chem. Rev.* **1995**, *95*, 1229.

(20)   Curtice, J.; Gilman, H.; Hammond, G. S. *J. Am. Chem. Soc.* **1957**, *79*, 4754.

(21)   Yan, Z. G.; Yang, Z.; Price, C.; Booth, C. *Makromol. Chem., Rapid Commun.* **1993**, *14*, 725.

(22)   Yu, G. E.; Sinnathamby, P.; Price, C.; Booth, C. *Chem. Commun.,* **1996**, *1*, 31.

(23)   Sun, T.; Yu, G. E.; Price, C.; Booth, C.; Cooke, J.; Ryan, A. J. *Polymer* **1995**, *36*, 3775.

(24)   Singla, S.; Zhao, T.; Beckham, H. *Macromolecules* **2003**, *36*, 6945.

(25)   Roovers, J.; Toporowski, P. M. *Macromolecules* **1983**, *16*, 843.

(26)   Lepoittevin, B.; Dourges, M. A.; Masure, M.; Hemery, P.; Baran, K.; Cramail, H. *Macromolecules* **2000**, *33*, 8218.

(27)   Ohtani, H.; Kotsuji, H.; Momose, H.; Matsushita, Y.; Noda, I.; Tsuge, S. *Macromolecules* **1999**, *32*, 6541.

(28)   Cho, D.; Park, S.; Kwon, K.; Chang, T.; Roovers, J. *Macromolecules* **2001**, *34*, 7570.

(29)   White, B. M.; Watson, W. P.; Barthelme, E. E.; Beckham, H. W. *Macromolecules* **2002**, *35*, 5345.

(30)   White, B. M. *Rotaxanated Polymers: I. Synthesis and Purification of Cyclic Polydimethylsiloxane. II. Synthesis of Poly[octene-pseudorotaxa-(alpha-Cyclodextrin)]*. School of Chemistry and Biochemistry, Georgia Institute of Technology, 2004.

(31)   Coqueret, X.; Wegner, G. *Makromol. Chem.* **1992**, *193*, 2929.

(32)   Chênevert, R.; D'Astous, L. *J. Heterocyclic Chem.* **1986**, *23*, 1785.

(33)   Hoss, R.; Vögtle, F. *Angew. Chem. Int. Ed. Engl.* **1994**, *33*, 375.

(34)   Bühner, M.; Geuder, W.; Gries, W.-K.; Hünig, S.; Koch, M.; Poll, T. *Angew. Chem. Int. Ed.* **1988**, *100*, 1611.

(35) Tezuka, Y.; Mori, K.; Oike, H. *Macromolecules* **2002**, *35*, 5707.

(36) Oike, H.; Hamada, M.; Eguchi, S.; Danda, Y.; Tezuka, Y. *Macromolecules* **2001**, *34*, 2776.

(37) Tezuka, Y.; Oike, H. *Prog. Polym. Sci.* **2002**, *27*, 1069.

(38) Oike, H.; Washizuka, M.; Tezuka, Y. *Macromol. Rapid Commun.* **2001**, *22*, 1128.

(39) Oike, H.; Mouri, T.; Tezuka, Y. *Macromolecules* **2001**, *34*, 6592.

(40) Schwab, P.; Grubbs, R. H.; Ziller, J. W. *J. Am. Chem. Soc.* **1996**, *118*, 100.

(41) Miller, S. J.; Blackwell, H. E.; Grubbs, R. H. *J. Am. Chem. Soc.* **1996**, *118*, 9606.

(42) Grubbs, R. H. *Tetrahedron* **2004**, *60*, 7117.

(43) Dodgson, K.; Semlyen, J. A. *Polymer* **1977**, *18*, 1265.

(44) Oike, H.; Imaizumi, H.; Mouri, T.; Yoshioka, Y.; Uchibori, A.; Tezuka, Y. *J. Am. Chem. Soc.* **2000**, *122*, 9592.

(45) Lesec, J. *J. Liq. Chromatogr.* **1985**, *8*, 875.

(46) Dodgson, K.; Sympson, D.; Semlyen, J. A. *Polymer* **1978**, *19*, 1285.

(47) Lee, H. C.; Lee, H.; Lee, W.; Chang, T.; Roovers, J. *Macromolecules* **2000**, *33*, 8119.

(48) Pasch, H.; Deffieux, A.; Henze, I.; Schapacher, M.; Rique-Lurbet, L. *Macromolecules* **1996**, *29*, 8776.

(49) Harada, A. *Coordination Chemistry Reviews* **1996**, *148*, 115.

(50) Harada, A.; Kamachi, M. *Macromolecules* **1990**, *23*, 2821.

(51) Harada, A. *Acc. Chem. Res.* **2001**, *34*, 456.

(52) Harada, A.; Nishiyama, T.; Kawaguchi, Y.; Okada, M.; Kamachi, M. *Macromolecules* **1997**, *30*, 7115.

(53) Harada, A.; Nishiyama, T.; Kawaguchi, Y.; Okada, M.; Kamachi, M. *Macromolecules* **2000**, *33*, 4472.

(54) Okumura, H.; Kawaguchi, Y.; Harada, A. *Macromolecules* **2001**, *33*, 4472.

(55)   Huang, L.; Tonelli, A. E. *Polymer* **1998**, *39*, 4857.

(56)   Huang, L.; Tonelli, A. E. *Polymer* **1998**, *40*, 3211.

(57)   Porbeni, F. E.; Edeki, E.; Shin, I. D.; Tonelli, A. E. *Polymer* **2001**, *42*, 6907.

(58)   Wenz, G.; Keller, B. *Angew. Chem. Int. Ed. Engl.* **1992**, *31*, 783.

(59)   Rusa, C. C.; Tonelli, A. E. *Macromolecules* **2000**, *33*, 1813.

(60)   Shuai, X.; Porbeni, F. E.; Wei, M.; Bullions, T.; Tonelli, A. E. *Macromolecules* **2002**, *35*, 3775.

(61)   Nielen, M. W. *Mass Spectrometry Reviews* **1999**, *18*, 309.

CHAPTER III

AMPHIPHILIC TADPOLES FROM SILICONE RINGS WITH OXYETHYLENE TAILS

3.1. **Introduction**

Hybrid macrocycles are variations of conventional homocycles that incorporate unusual architectures or chemical compositions to create new topological systems.[1] Living ionic and controlled radical polymerizations have made it possible to exercise control over polymer microstructure, allowing the creation of elaborately designed block copolymers with telechelic groups for subsequent chemical reactions. When coupled with advances in polymer cyclization and purification methods, shapes such as knots, bridged macrocycles, cycles, branched cycles, theta macrocycles, and other shapes are now possible.

Because many of these new shapes defy classification by standard IUPAC methodologies, a new system for nonlinear architectures has been proposed.[2,3] Cycles are given a Roman numeral according to the number of rings present – monocyclic systems are designated I, bicyclic systems II, and so on. Next, the Roman numeral is assigned a subscript for the smallest number of points that could constitute the molecule. Finally, the number of junctions and termini are listed in parentheses. Thus, for the tadpole molecule discussed in this chapter, the classification would be $I_4(1,1)$ – a monocycle whose shape could be approximated by 4 points, with one junction and one terminus, as depicted below in Figure 3.1.
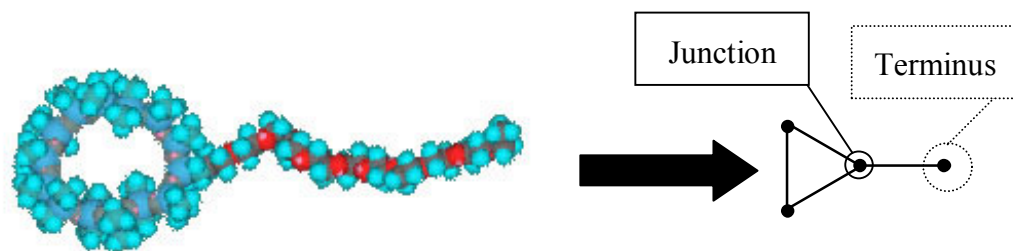
Figure 3.1 – Anatomy of a I$_4$(1,1) hybrid macrocycle. This monocycle can be approximated by a 4-point structure consisting of a cyclopropane with a methyl tail, possessing 1 junction and 1 terminus.

Already many of these shapes have been prepared by the self-assembly and covalent fixation scheme developed by Tezuka and Oike.[2-20] By this method, linear or branched polymers are prepared via ionic polymerization and the endgroups are functionalized to produce quaternized amine salts. These polymers self-assemble with linking moieties containing 2 or more carboxylate groups, then are heated to convert the ionic bonds to covalent linkages. Although these shapes have only been prepared as homopolymers, one can envision block copolymer versions just a step away. Furthermore, Tezuka has created a class known as *kyklo*-telechelics: macrocycles containing functional groups such as hydroxyl and vinyl groups that can be utilized in subsequent chemical reactions.[16,20]

To date, several hybrid macrocycles have been prepared by methods other than the one listed above. Some have begun with cyclic species like cyclodextrins,[21] calixarenes,[22] and silsesquioxanes,[23,24] adding hydrophilic or lipophilic groups to the reactive sites on the rings. Others have made supramolecular cycles by self-assembling components as ligands around a metallic core.[25] Hogen-Esch has prepared a

poly(styrene)-poly(dimethylsiloxane) (PS-PDMS) diblock macrocycle by anionically polymerizing styrene with a difunctional initiator for the first block, then adding the PDMS block by opening eight-membered PDMS rings, and finally conducting a ring-closure step under dilute conditions.[26] "Click chemistry,"[27] a design motif involving modular high-yield reactions, has resulted in a poly(oxyethylene)-poly(ethylene) (POE-PE) diblock macrocycle with amides linking the blocks.[28]

An alternative method has been used to synthesize a tadpole with a poly(styrene) tail and poly(hydroxyethyl vinyl ether) (PHVE) head by first preparing a PS-PHVE linear diblock polymer, then getting the PHVE block to backbite and form a ring.[29] Pugh et al. have synthesized a tadpole by first preparing a crown ether containing a phenyl ring and then attaching an alkyl tail by electrophilic aromatic substitution.[30,31] Similarly, Höger et al. have created multiarmed cycles with a rigid π-conjugated ring of phenyls and alkyne bonds, with a variety of branched substituents arising from the phenyls.[32-36]

For the PDMS-POE tadpole prepared herein, the synthetic plan involved joining a functionalized cyclic "head" with a linear "tail" in such a modular fashion such that this scheme could work with a variety of linear polymers using a hydrosilylation reaction, like in Figure 3.2.[23,37-40] The hydrosilane group is nonreactive during the PDMS cycle formation, and any linear polymer only needs to possess a vinyl functional group in order to be joined. The resultant silicon-carbon bond is stable to a wide variety of conditions, and the reaction typically results in high yields. When radicals[41] are used to catalyze the process instead of transition metals, the option of growing the tail as a comb polymer is added, further increasing the utility of the scheme.
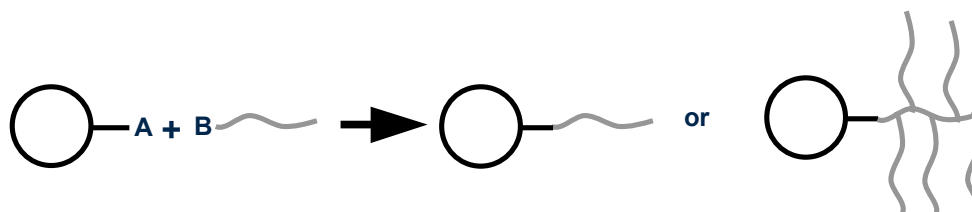
Figure 3.2 – Synthetic route for joining linear and cyclic polymer species to make a "tadpole" hybrid macrocycle. "A" represents a hydrosilane group and "B" a vinyl group.

When the hybrid macrocycle consists of chemically different polymers, the blocks have a tendency to phase separate.[26] This can occur in the solid state if the system T_g is sufficiently high, or in solution.[42] In either state, the molecules can behave like liquid crystals, forming domains or micelles in the shape of spheres, cylinders, lamellae, and gyroids,[43] and the shape formed depends on both the relative concentrations of the hybrid components and solution concentration.

The main difference between linear block copolymers and hybrid macrocycles, however, is that the unique topologies of the macrocycles force certain constraints. For example, Kellermann's amphiphilic dendro-calixarene hybrid macrocycle forms structurally persistant micelles in aqueous solution,[22] instead of rapidly disassembling and reassembling. Höger's rigid macrocycles with multiple branches act as if they have "molecular reversible coats,"[36] with the branches either outside the ring, shielding it from the solvent, or inside the ring, hiding from the solvent.

In addition to providing additional systems with which to study the process of phase separation,[3,26] hybrid macrocycles have many other uses. Tailoring the topology to restrict self-assembly into certain shapes increases control over designing new liquid crystals[44] and core-shell nanoparticles,[45] hydrogels,[43] and nanoreactors.[46]   Adding

amphiphilic characteristics with biocompatible polymers like PDMS and POE allows for biomedical applications such as artificial cell membranes[44] and bone scaffolds, as well as drug delivery systems.[46] Finally, it has been postulated that using hybrid macrocycles would be a way to form rotaxanes by emulsion polymerization, allowing a new route to supramolecular topologies.[31]

3.2. **Experimental Section**

3.2.1. Materials

All reagents were used without further purification unless otherwise specified. Di-*tert*-butyl peroxide (DTBP, 98%), sodium hydride (dry, 95%), platinum(0)-1,3-divinyl-1,1,3,3-tetramethyldisiloxane complex [platinum(divinylsilane), 3 wt.% in xylenes], platinum(II)chloride (98%), chloroplatinic acid (99.9%), α-methoxy,ω-hydroxy poly(oxyethylene) (POE, M_n 660 g/mol, PDI 1.1 as determined by MALDI-TOF MS), and allyl bromide (99%) were purchased from Aldrich Chemical Co. Also obtained from Aldrich were the solvents tetrahydrofuran (THF, anhydrous, 99.9%, inhibitor-free), methyl ethyl ketone (MEK, HPLC grade, 99.5%), dimethylsulfoxide-d_6 (DMSO-d_6, 99.9 atom % D), and chloroform-d (99.8 atom % D). Macroporous ion-exchange resin AG MP-1M (1 mequiv/mL, 0.7 g/mL, 100-200 mesh, chloride form) was purchased from Bio-Rad Laboratories and dried for 16 hours at a pressure of 500 mTorr before use. Toluene (anhydrous, 99%), ethyl acetate (reagent grade), hexanes (reagent grade), toluene (HPLC grade), methanol (histological grade), and THF (HPLC, inhibitor-free), were obtained from Fisher Scientific. Linear α,ω-dihydrosilyl PDMS (M_n 550 g/mol, PDI 2.13 as determined by MALDI-TOF MS) was purchased from Gelest.

3.2.2.   Instrumentation

GPC was conducted in THF (1 mL/min) at 303 K on three Waters Styragel columns (5 μm beads: HR 1, 100 Å; HR 3, 1000 Å; HR 4, 10000 Å) that were connected to a Waters 2690 separations module and Waters 2410 refractive index detector. Injections of 100 – 200 μL were made from 5 – 10 wt% solutions.

NMR spectra were measured on a Bruker AMX 400 in chloroform-d and DMSO-d_6. Concentrations of approximately 1 wt% were used for ^{1}H NMR, and 10 wt% for ^{13}C and ^{29}Si NMR.

Differential scanning calorimetry was performed on a Seiko Instruments DSC 220C under nitrogen purge with samples weighing 10 – 15 mg sealed in aluminum pans and heated at a rate of 10 °C/min. The power and temperature scales of the calorimeter were calibrated against the enthalpies of fusion and melting temperatures of pure indium and tin.

Surface tension measurements were performed on a Fisher Scientific Surface Tensiomat Model 21 at 25 °C in MEK and toluene.

Dynamic light scattering in MEK and toluene was conducted with a Wyatt Technologies DAWN EOS light scattering detector equipped with a quasielastic light scattering autocorrelator.

A Jouan MR23i was used to centrifuge samples at 5000 RPM for 10 minutes at 20 °C.

3.2.3. Synthesis of α-methoxy,ω-allyl POE

A 50-mL oven-dried and inert-gas-purged round bottom flask with gas inlet and stir bar was charged with 25 mL of THF using a purged gastight syringe. Under positive nitrogen flow, α-methoxy,ω-hydroxy POE (10.4 g, 15.8 mmol) that previously had been dried for 16 hours *in vacuo*, and NaH (0.439 g, 17.4 mmol) was added. After 2 hours, 15.0 mL (21.0 g, 174 mmol) allyl bromide was injected dropwise. 16 hours later the solution was quenched with the ion-exchange resin (10 g) and stirred for 4 hours, then filtered through a 0.45 μm membrane. The solvent and excess allyl bromide were removed by rotary evaporation, and 9.624 g of a waxy, faintly yellow polymer was recovered (87.0%) with M_n 700 g/mol and PDI 1.1. ^{1}H NMR (DMSO-d_6, ppm): 3.3 (OCH$_3$), 3.6 (CH$_2$CH$_2$O), 4.0 (CH$_2$), 5.3 (=CH$_2$), 5.9 (CH=). ^{13}C NMR (DMSO-d_6, ppm): 58 (OCH$_3$), 69 (CH$_2$CH$_2$O), 115 (=CH$_2$), 137 (CH=).

3.2.4. Synthesis of Tadpole via Platinum-catalyzed Hydrosilylation

The α-methoxy,ω-allyl POE (1.275 g, 1.82 mmol) was added to a 50-mL oven-dried and inert-gas-purged round bottom flask with gas inlet and stir bar. The system was held at a pressure of 500 mTorr and a temperature of 85 °C for 2 hours to dry the POE, then backfilled with nitrogen gas. Next, the flask was charged with 1 mL of anhydrous toluene using a purged gastight syringe, and a solution of platinum(divinylsilane) (0.10 mL) was added with a microliter syringe. Finally, the hydrosilane-functionalized cyclic PDMS (2.0 mL, 1.5 mmol) was added using a purged gastight syringe. The reaction was allowed to proceed for 3 hours, and then the solvent was removed by rotary evaporation.

This reaction was also repeated using chloroplatinic acid and platinum(distyrene) in place of platinum(divinylsilane).

3.2.5. Synthesis of Linear PDMS-POE Block Copolymer via Platinum-catalyzed Hydrosilylation

The α-methoxy,ω-allyl POE (2.49 g, 3.56 mmol) was added to a 50-mL oven-dried and inert gas-purged round bottom flask with gas inlet and stir bar. The system was held at a pressure of 500 mTorr and a temperature of 85 °C for 2 hours to dry the POE, then backfilled with nitrogen gas. Next, the flask was charged with 10 mL of anhydrous toluene using a purged gastight syringe, and a solution of platinum(divinylsilane) (0.10 mL) was added with a microliter syringe. Finally, α,ω-dihydrosilyl PDMS (1.0 mL, 1.78 mmol) was added using a purged gastight syringe. The reaction was allowed to proceed for 3 hours, and then the solvent was removed by rotary evaporation. Using GPC with polystyrene standards, the polymer was determined to have an M_n of 2,270 g/mol and PDI of 2.14. This reaction was repeated using chloroplatinic acid in place of platinum(divinylsilane) to yield similar results.

3.2.6. Synthesis of Tadpole via Radical-catalyzed Hydrosilylation

A 50-mL oven-dried and purged round bottom flask with gas inlet and stir bar was charged with 11.14 g (8.57 mmol) of the hydrosilane-functionalized PDMS macrocycles via gastight syringe, and the flask was heated to 120 °C while N_2 was flushed through the system. Next, 50 μL (40 mg, 0.27 mmol) di-*tert*-butyl peroxide (DTBP) was added with a syringe and the contents were allowed to stir for 15 minutes. 1.00 g (1.43 mmol) of α-

methoxy,ω-allyl POE that had been previously dried under vacuum overnight was dissolved in 10 mL anhydrous toluene in a 25-mL oven-dried and purged flask and added at a rate of 1.45 mL/hr with a syringe pump and gastight syringe. After 2 hours, an additional 10 mL anhydrous toluene was added via gastight syringe to replace the solvent that had already evaporated, and the contents were allowed to react for an additional 4 hours. Because this procedure occurred at temperatures well above the flash point of toluene (66 °C), extreme care was taken with the organic solvent.

Since the radical hydrosilylation required a large excess of PDMS for adequate chain transfer, cleanup began by removing the extra PDMS by dissolution in ethyl acetate (20 mL) and precipitation into hexanes (3 × 200 mL). The precipitant was collected each time by centrifugation for 10 minutes at 5000 rpm at 20 °C. The product was further purified by dissolution in toluene (20 mL) and fractionation with hexane to remove nonpolar species, and dissolution in methyl ethyl ketone (20 mL) followed by the addition of methanol to remove polar species. The recovered product was soft and cream-colored with M_n of 2,000 g/mol and weighing 1.57 g, a 54.9% yield. ^{1}H NMR (CDCl$_3$, ppm): 0.3 (Si-CH$_3$), 3.4 (OCH$_3$), 3.6 (CH$_2$CH$_2$O). ^{13}C NMR (CDCl$_3$, ppm): 1 (Si-CH$_3$), 30 (Si-CH$_2$), 69 (CH$_2$CH$_2$O). ^{29}Si NMR (CDCl$_3$, ppm): -22.00 (Si-CH$_3$), -22.06 (Si-CH$_2$). DSC: T$_m$ 24 °C.

3.2.7.   Surface Tension Measurements of Tadpole

Solutions of the amphiphilic tadpole were prepared by dissolving 115.0 mg in toluene or MEK. 5 measurements were recorded at each concentration to provide a sample average and standard deviation, and then the solution was diluted by the addition of 2 mL

of the solvent. The solution was gently stirred, and the process was repeated. The CMC was calculated by finding the point of inflection between the dilute and concentrated regions. The tadpole formed micelles in MEK at 5.06 mg/mL and inverse micelles in toluene at 6.76 mg/mL.

3.2.8. Dynamic Light Scattering Measurements of Tadpole

Quasielastic light scattering (QELS) measurements were conducted in HPLC-grade MEK and toluene in glass scintillation vials. Before use, the vials were washed with soap and water, then rinsed with filtered acetone, wiped with Kimwipes, and dried in an oven at 120 °C. Solutions were prepared by dissolving the tadpole macrocycle in solvent filtered through a 0.1-μm membrane. The data were processed with Wyatt's QELSBatch package, using an algorithm derived from CONTIN called DYNALS that sorts the data into size distributions and calculates the average hydrodynamic radius and standard deviation for each distribution. To increase the signal-to-noise ratio for measurements below the CMC, the QELS detector was moved from its standard position at 108° to a new position at 44°. This had the effect of now detecting a larger scattering volume, increasing the sensitivity of the measurements. The data are summarized in Table 3.1 for MEK solutions and Table 3.2 for toluene solutions.

3.3. Results and Discussion

3.3.1. α-methoxy,ω-allyl POE

Following an established procedure,[38] the α-methoxy,ω-hydroxy POE was activated by deprotonation with sodium hydride and subsequently reacted with allyl bromide to

prepare it for hydrosilylation, as shown in Figure 3.3. As with the PDMS, unfunctionalized POE was removed with the ion-exchange resin, resulting in pure vinyl-functionalized POE.
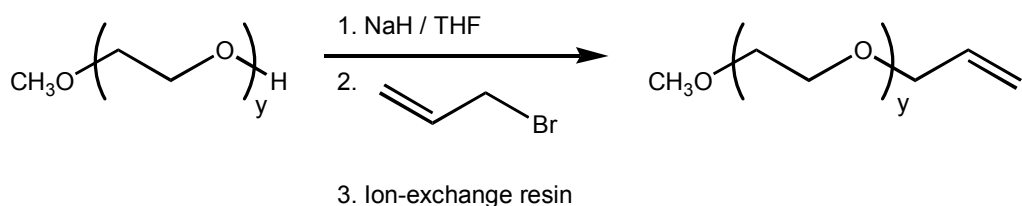
Figure 3.3 – Preparation of α-methoxy,ω-allyl POE from α-methoxy,ω-hydroxy POE.

The ^{1}H and ^{13}C NMR spectra in Figure 3.4 for the starting material and product indicate the loss of the hydroxyl proton (δ_H = 4.6 ppm and δ_C = 65 ppm for the proximal carbon) and replacement with the allyl group (δ_H = 3.7 - 6.0, δ_C = 121 and 140 ppm). The NMR were collected in DMSO-d_6 to minimize any proton-deuteron exchange that would render the hydroxyl group of the POE starting material undetectable and complicate assessments of the product's purity.

(a)

(b)
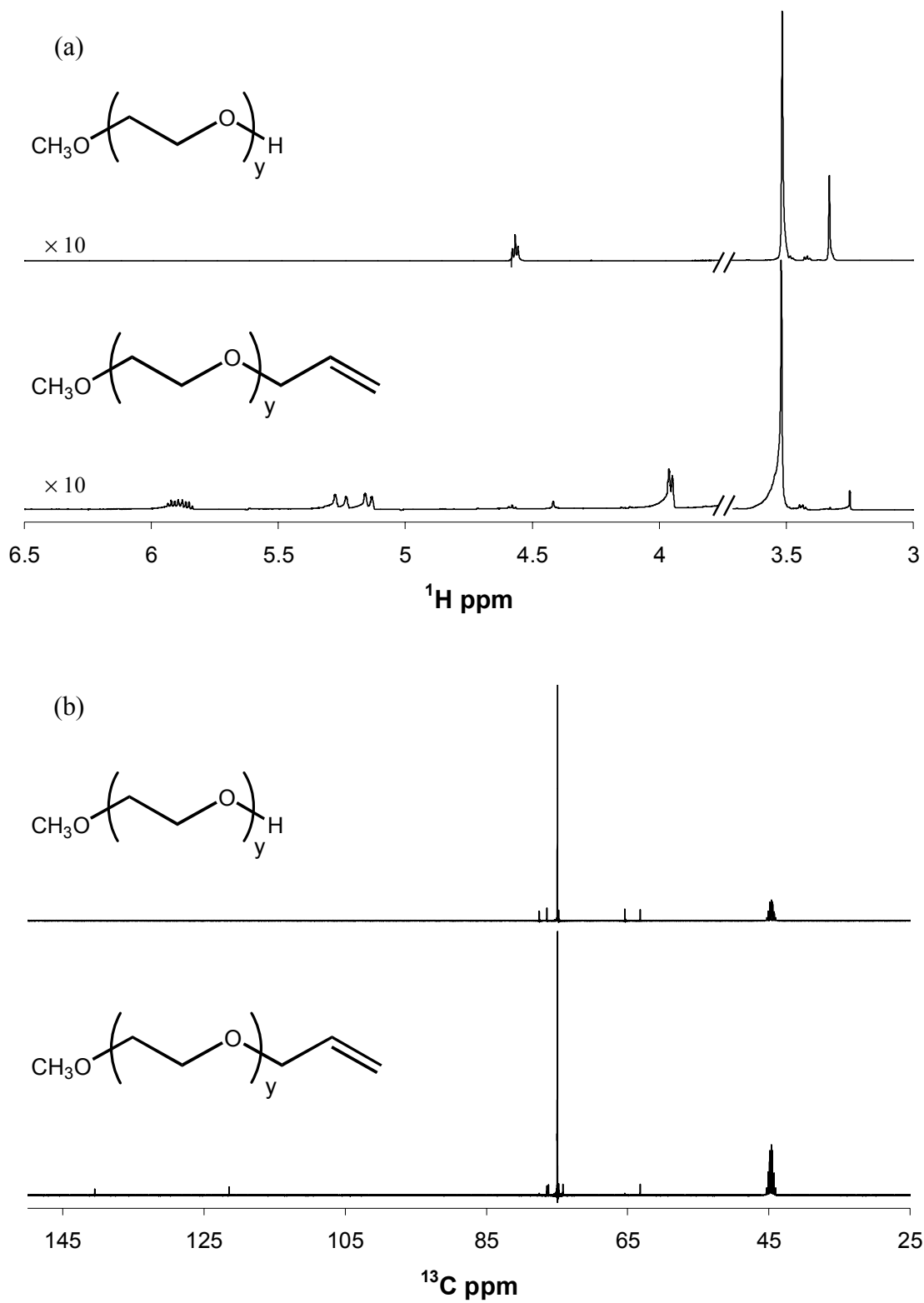
Figure 3.4 – ^{1}H (a) and ^{13}C (b) NMR spectra of α-methoxy,ω-allyl POE and its precursor in DMSO-d_6.

3.3.2.   Platinum-catalyzed Hydrosilylations

For the hydrosilylation reaction, platinum(divinylsilane) and chloroplatinic acid were chosen because they are two of the most commonly used catalysts for reactions between vinyl and hydrosilane groups.[23,38-40,47] A third catalyst, platinum(distyrene), was prepared from PtCl$_2$ according to a literature procedure.[37]   Although all three were used with varying stoichiometry in reactions like the one in Figure 3.5 to link the hydrosilane-functionalized PDMS macrocycle and the vinyl-functionalized POE, none were ever observed to result in a larger molecule by GPC.
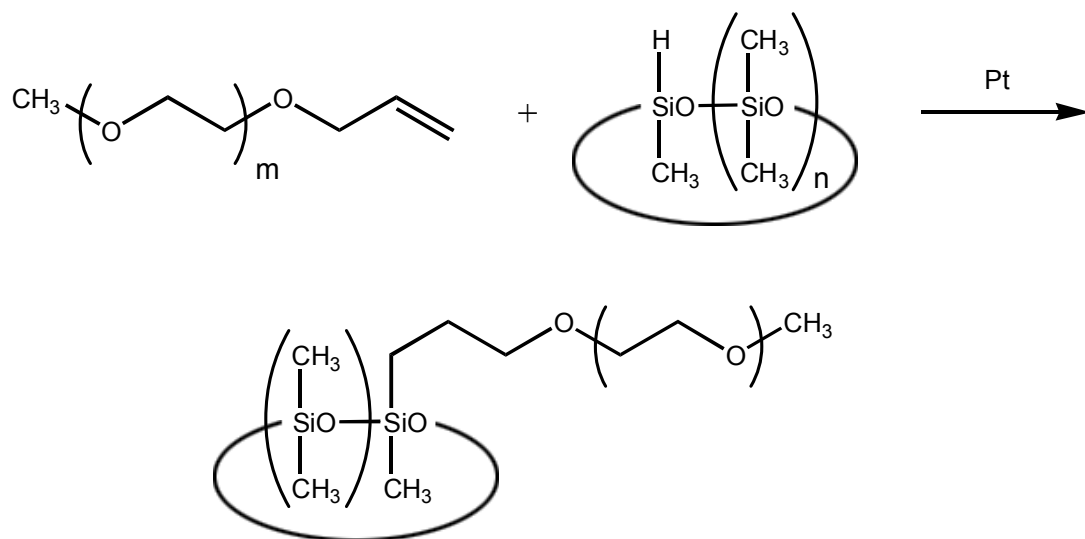
Figure 3.5 – Platinum-catalyzed reaction scheme between hydrosilane-functionalized cyclic PDMS and α-methoxy,ω-allyl POE.

The GPC plot of the platinum-catalyzed hydrosilylation reaction between hydrosilane-functionalized cyclic PDMS and α-methoxy,ω-allyl POE in Figure 3.6 shows that the product trace is identical to that of the vinyl-functionalized POE. If the product appeared at a shorter retention time, it would be a sign that a larger molecule had been synthesized, but since the retention time has not changed it can be deduced that the sample is just a mixture of the linear POE and cyclic PDMS. The reason the product mixture looks like the POE and not the sum of the cyclic PDMS and POE traces is because POE has a higher specific refractive increment than PDMS in THF, causing it to overwhelm the PDMS signal on the differential refractive index detector. Similarly, the ^{13}C NMR of the reaction product in Figure 3.7 showed that the tadpole had not been prepared. Although PDMS can be seen at $\delta_c = 1$ ppm, the vinyl carbons are still present at 121 and 140 ppm, indicating that the sample is just a mixture of the two species.
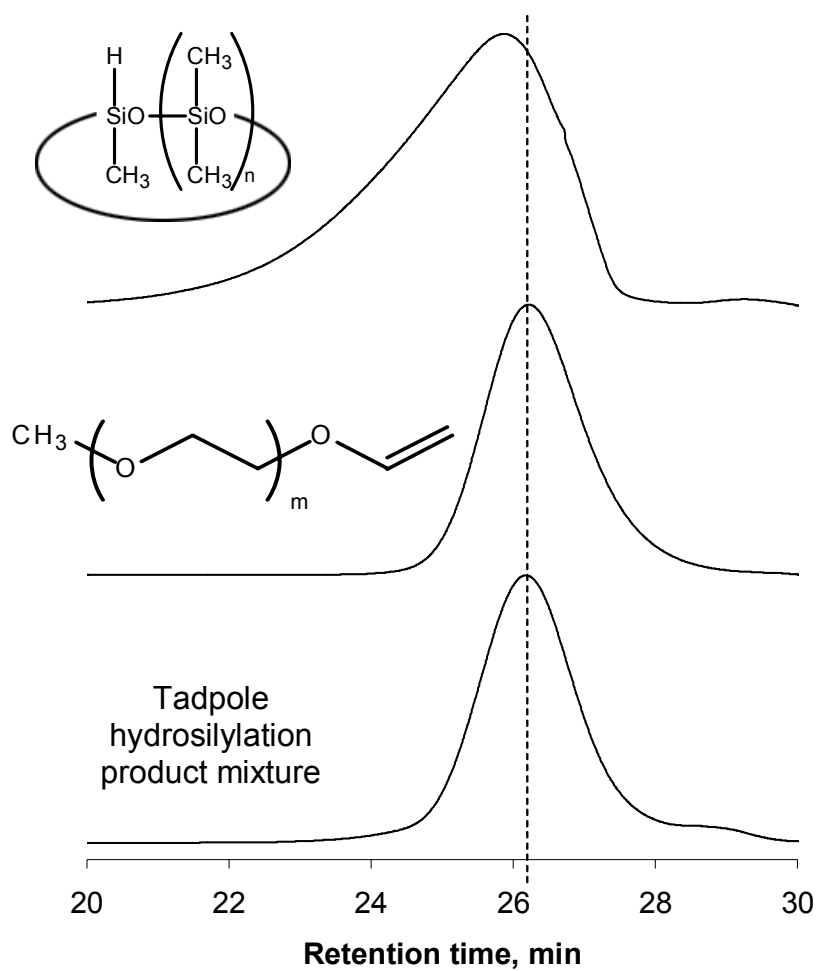
Figure 3.6 – GPC traces of hydrosilane-functionalized cyclic PDMS (top), α-methoxy,ω-allyl POE (middle), and the product of the platinum-catalyzed tadpole hydrosilylation reaction (bottom).
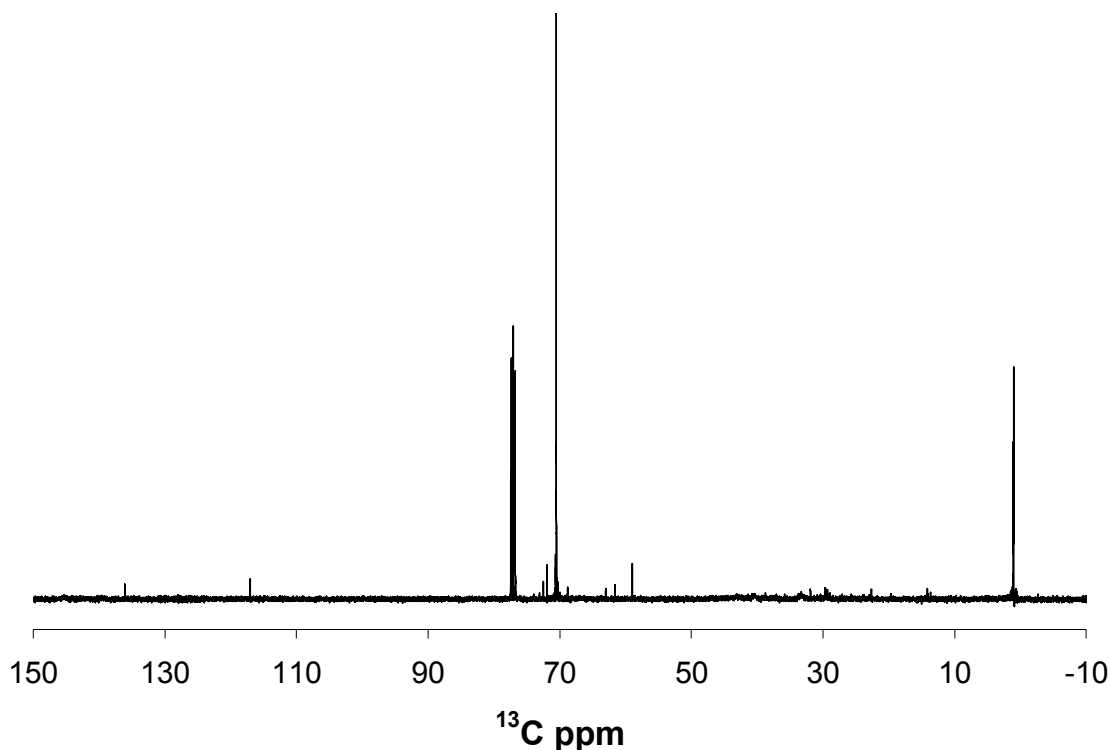
Figure 3.7 – ^{13}C NMR spectrum of the platinum-catalyzed hydrosilylation product in CDCl$_3$, which is actually a mixture of α-methoxy,ω-allyl POE and hydrosilane-functionalized cyclic PDMS.

When no reaction was observed using cyclic PDMS and vinyl-functionalized POE, a model reaction shown in Figure 3.8 employing linear α,ω-dihydrosilyl PDMS instead of the cyclic PDMS was used to elucidate any problems with the platinum catalyzed reaction. With the linear PDMS, the hydrosilane groups were found to react with the POE and form higher molecular weight block polymers, as shown by the GPC in Figure 3.9. The formation of the triblock polymers were confirmed by ^{1}H NMR in Figure 3.10, which shows that the allylic protons from $\delta_H = 4.1$-6.0 ppm have disappeared.
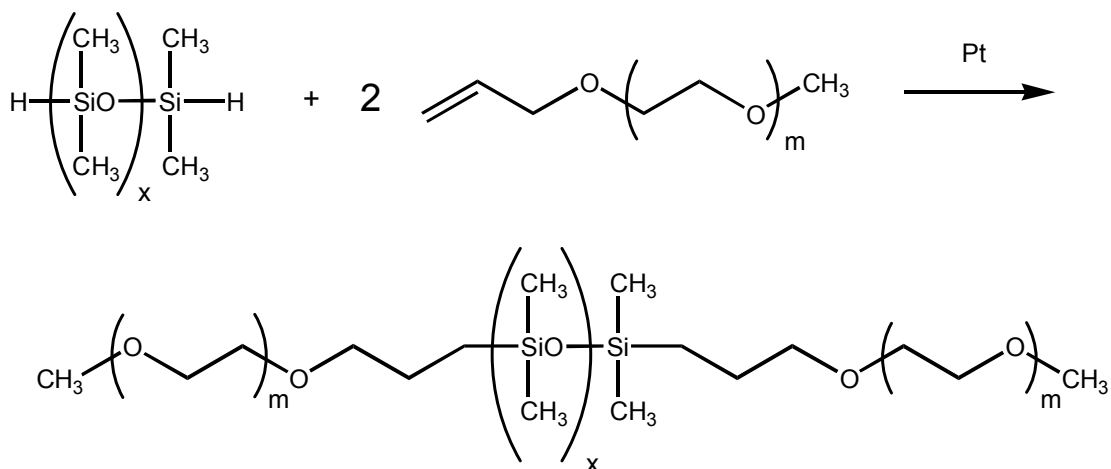
Figure 3.8 – The platinum-catalyzed reaction scheme between α,ω-dihydrosilyl PDMS and α-methoxy,ω-allyl POE.

Since the only difference between the two sets of reactions were linear versus cyclic PDMS, it was speculated that the hydrosilane endgroups on the linear PDMS were much more accessible to the platinum catalysts, while the dimethylsiloxane groups surrounding the lone hydrosilane group in the macrocycle proved too sterically bulky for the catalyst to insert itself between the hydrogen and silicon atoms in the hydrosilane bond and initiate the reaction.[40]
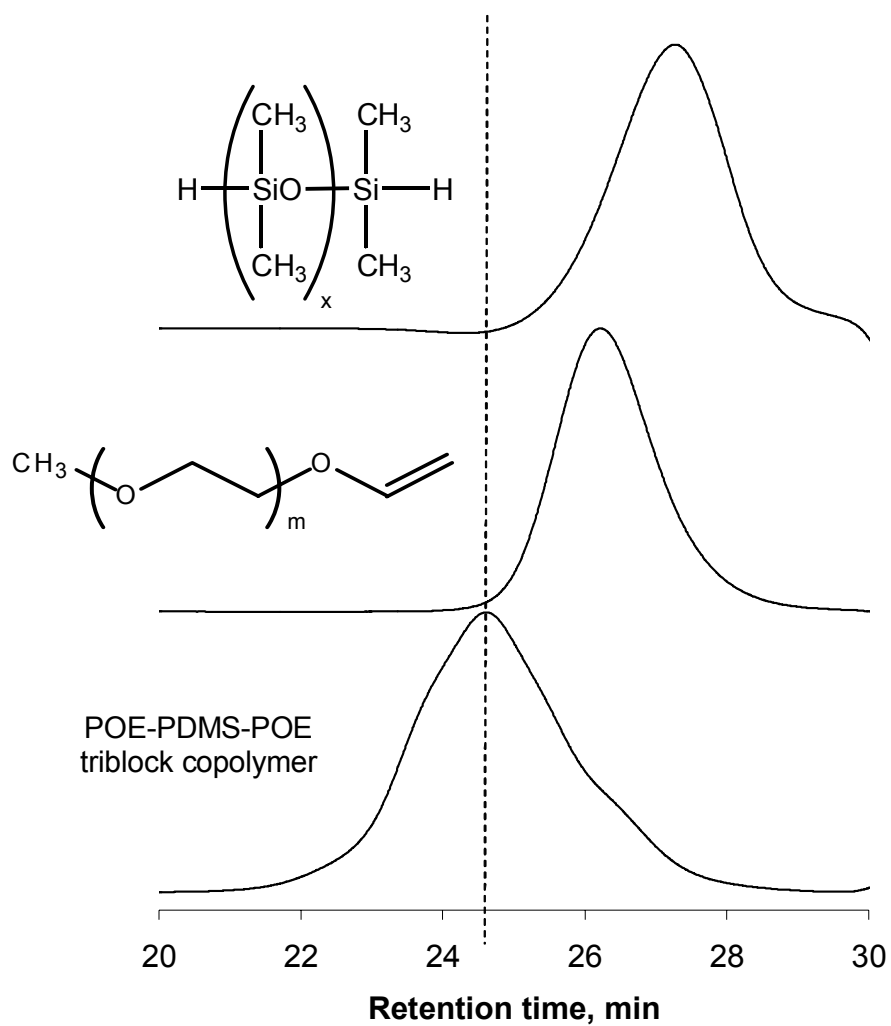
Figure 3.9 – GPC traces from the platinum-catalyzed hydrosilylation reaction of α,ω-dihydrosilyl PDMS and α-methoxy,ω-allyl POE to produce a triblock POE-PDMS-POE copolymer.
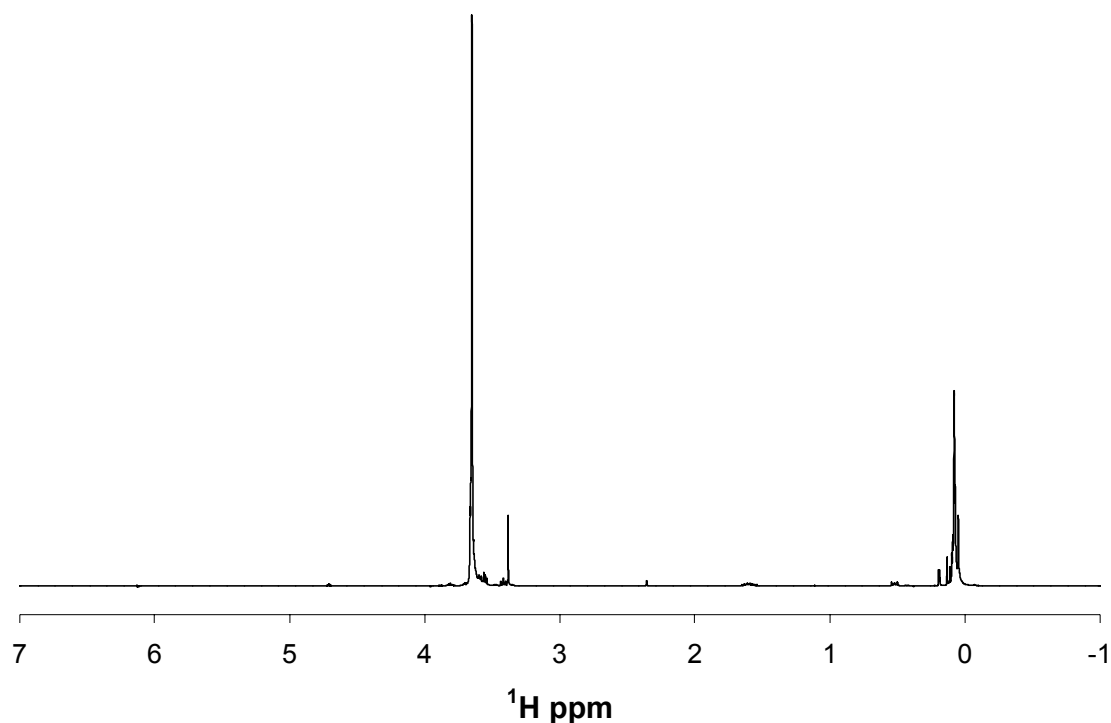
Figure 3.10 – ^{1}H NMR spectrum of the POE-PDMS-POE triblock copolymer in CDCl$_3$.

3.3.3. Radical-catalyzed Hydrosilylation

Since conventional reaction pathways were insufficient, the tadpole was synthesized by a free-radical hydrosilylation as shown in Figure 3.11, exploiting the high chain transfer constant of the hydrosilane group.[48,49] The initiator DTBP was selected as catalyst because it generates electronegative butoxy radicals upon decomposition at 120 °C. These electronegative radicals quickly react with the hydrosilane groups to generate electropositive silyl radicals.[41] The resulting silyl radicals now can react across the POE double bond, generating an electropositive carbon radical, and the transition state is small enough that sterics do not hinder the reaction. The carbon radical then can restart the catalytic cycle by transferring to a new hydrosilane, or chain-extend by reacting with additional allyl-terminated POE.

The main difficulty with this reaction scheme is ensuring that the catalytic cycle restarts by reacting the carbon radical with a hydrosilane group to produce a new hydrosilyl radical. Radical transfer from an electronegative species, like an oxygen radical, to an electropositive species, like a silyl radical, is thermodynamically favored and occurs readily. Transferring from a silyl radical to a carbon radical, another electropositive species, is much less thermodynamically favorable than reacting across more vinyl groups to result in a chain-extended product.[41]

By increasing the relative concentration of hydrosilane groups to approximately 40 times that of the radical species, the statistical likelihood that the carbon radical will collide with and react with a hydrosilane group instead of a vinyl group is much higher. This was accomplished by using a 6-fold stoichiometric excess of PDMS to POE, and then adding a 10 wt% solution of the linear POE dropwise over the course of 7 hours. In this way, the yield of the kinetic product (tadpole) dominates the yield of the thermodynamic product (chain-extended "comb" tadpole). This competition can be advantageous, however, if a comblike product is desired – merely reduce the amount of hydrosilane groups and chain transfer will decrease, resulting in comblike tails.
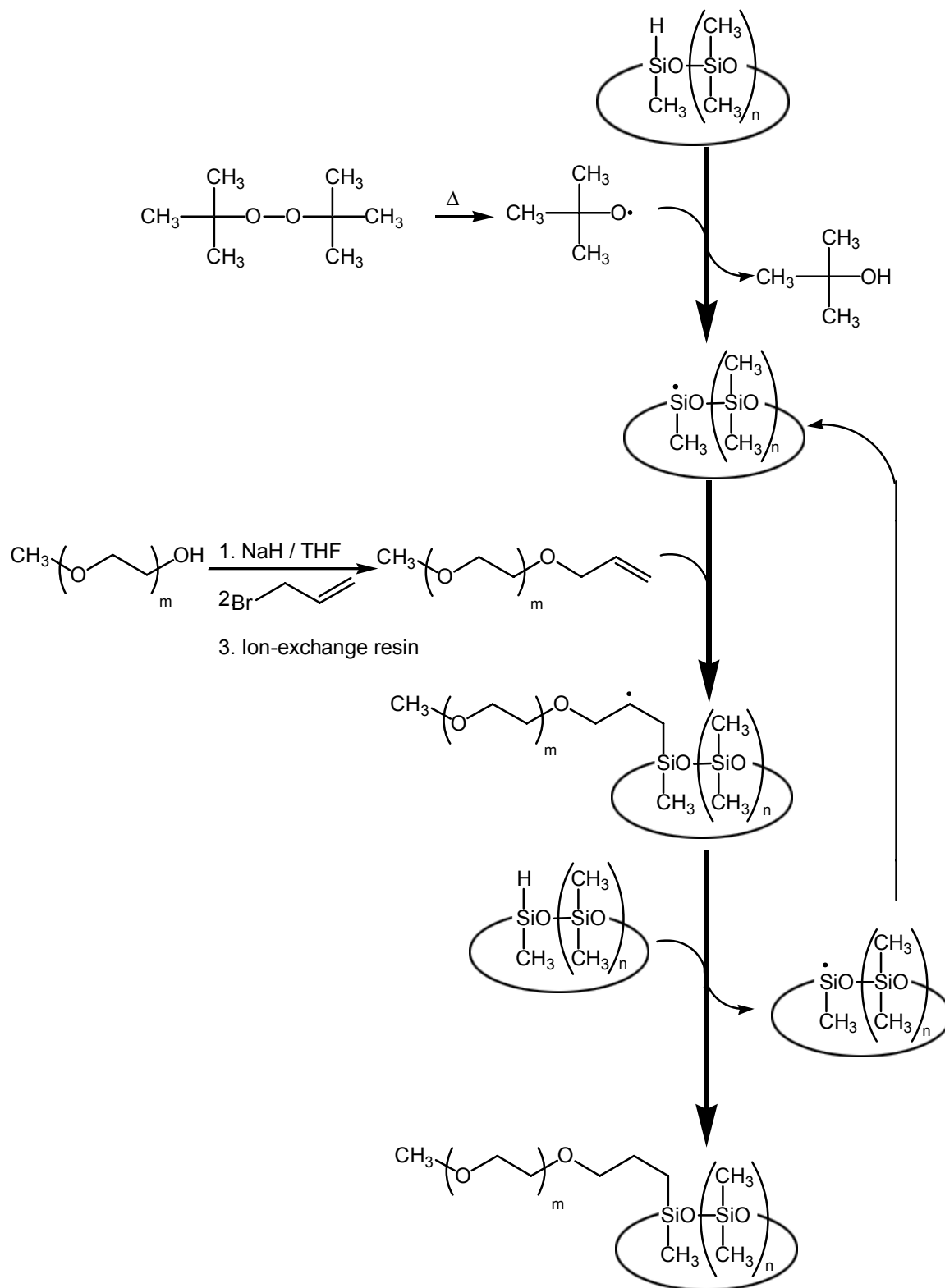
Figure 3.11 – Synthetic scheme for free-radical hydrosilylation to produce a PDMS-POE tadpole.

After the reaction ends, the excess hydrosilane-functionalized cyclic PDMS, tadpole, and any chain-extended byproducts are the only species present in the system. These species were separated by precipitation followed by careful fractionation, both monitored by ^{1}H NMR. Initially, the reaction products were dissolved in ethyl acetate and precipitated into a beaker of hexanes, after which the container was chilled overnight in a freezer to further the separation process. Finer separations were then accomplished by dissolving the precipitant in methyl ethyl ketone and fractionating with methanol to remove the last of the unreacted PDMS, and then dissolving in toluene and fractionating with hexanes to precipitate any chain-extended polar species. As the comparison of GPC traces in Figure 3.12 shows, the radical hydrosilylation product has increased in size relative to the starting materials, but the peak is narrow and unimodal. This discrete increase in size indicates that only 1 POE tail was added to the macrocycle, instead of an uncontrolled addition which would have lead to a comblike POE tail.
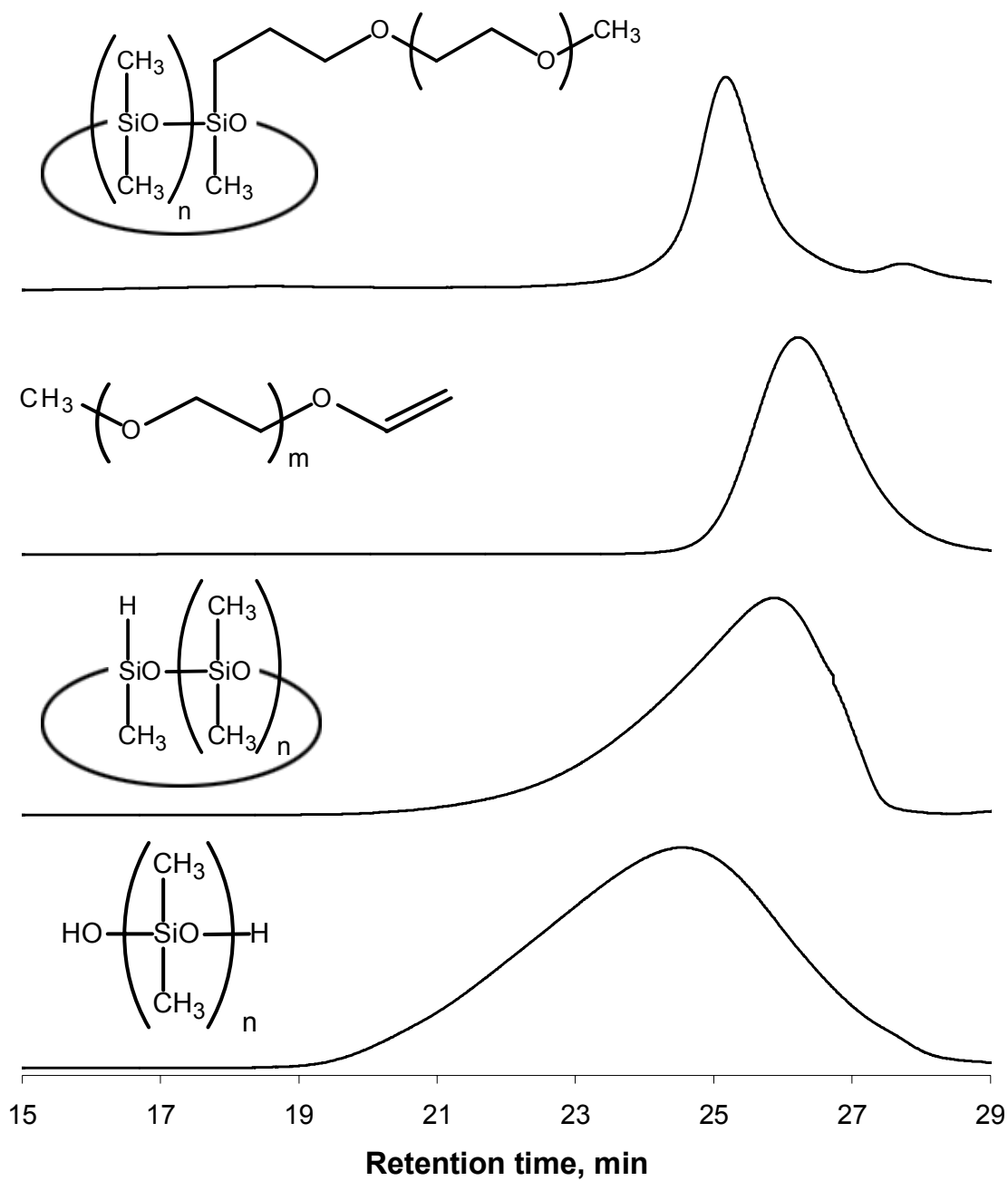
Figure 3.12 – GPC traces of starting materials, intermediates, and radical hydrosilylation product.

Multinuclear NMR analysis of the purified tadpole was conducted, with results shown below in Figure 3.13 and 3.14. In the ^{1}H NMR spectrum presented in Figure 3.13, the ratio of the POE methylene peak (δ_H = 3.6 ppm) to the methyl PDMS peak (δ_H = 0.3 ppm) is 1.0:1.7, which is as expected for a 700 g/mol POE attached to a 1,330 g/mol PDMS molecule. Also present are the methoxy group from the end of the POE tail (3.4 ppm) and a peak for methanol (3.3 ppm). The ^{13}C and ^{29}Si spectra in Figure 3.14(a) and 3.14(b) show a peak for the linking carbon and silicon atoms at δ_C = 30 and δ_{Si} = -22.06 ppm. Also of note is the absence of the hydrosilane silicon at δ_{Si} = -19.16 ppm, another indication of tadpole formation.
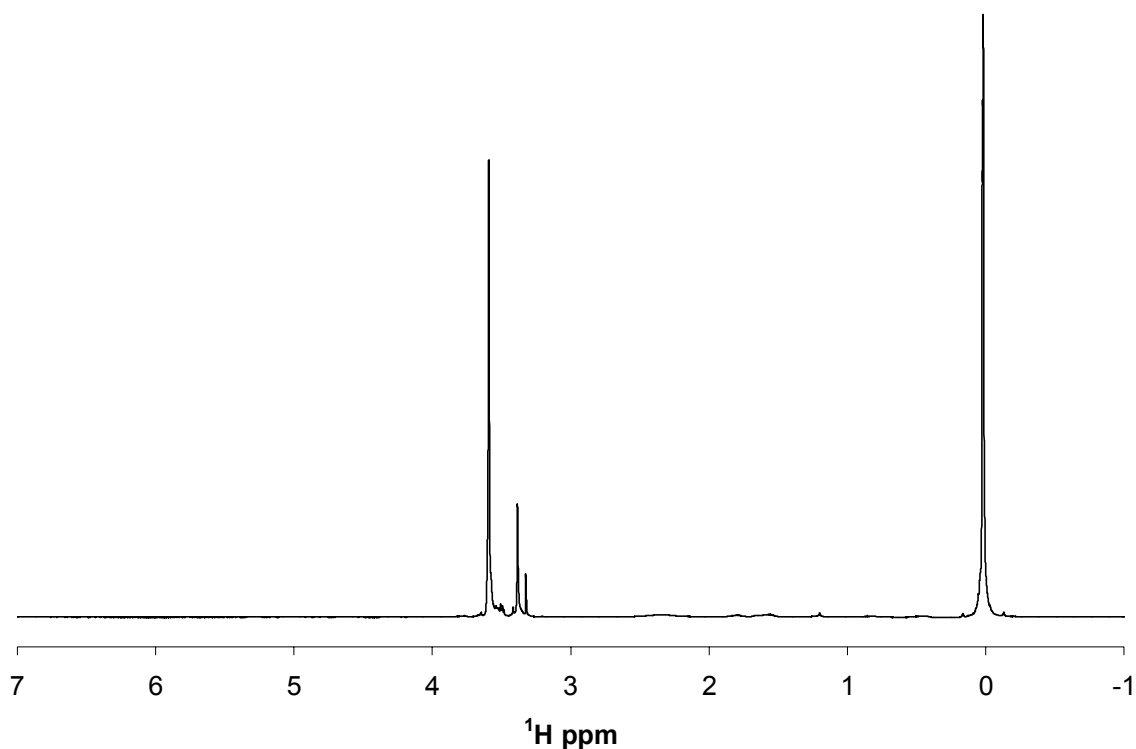
Figure 3.13 – ^{1}H NMR spectrum of the PDMS-POE tadpole in CDCl$_3$.
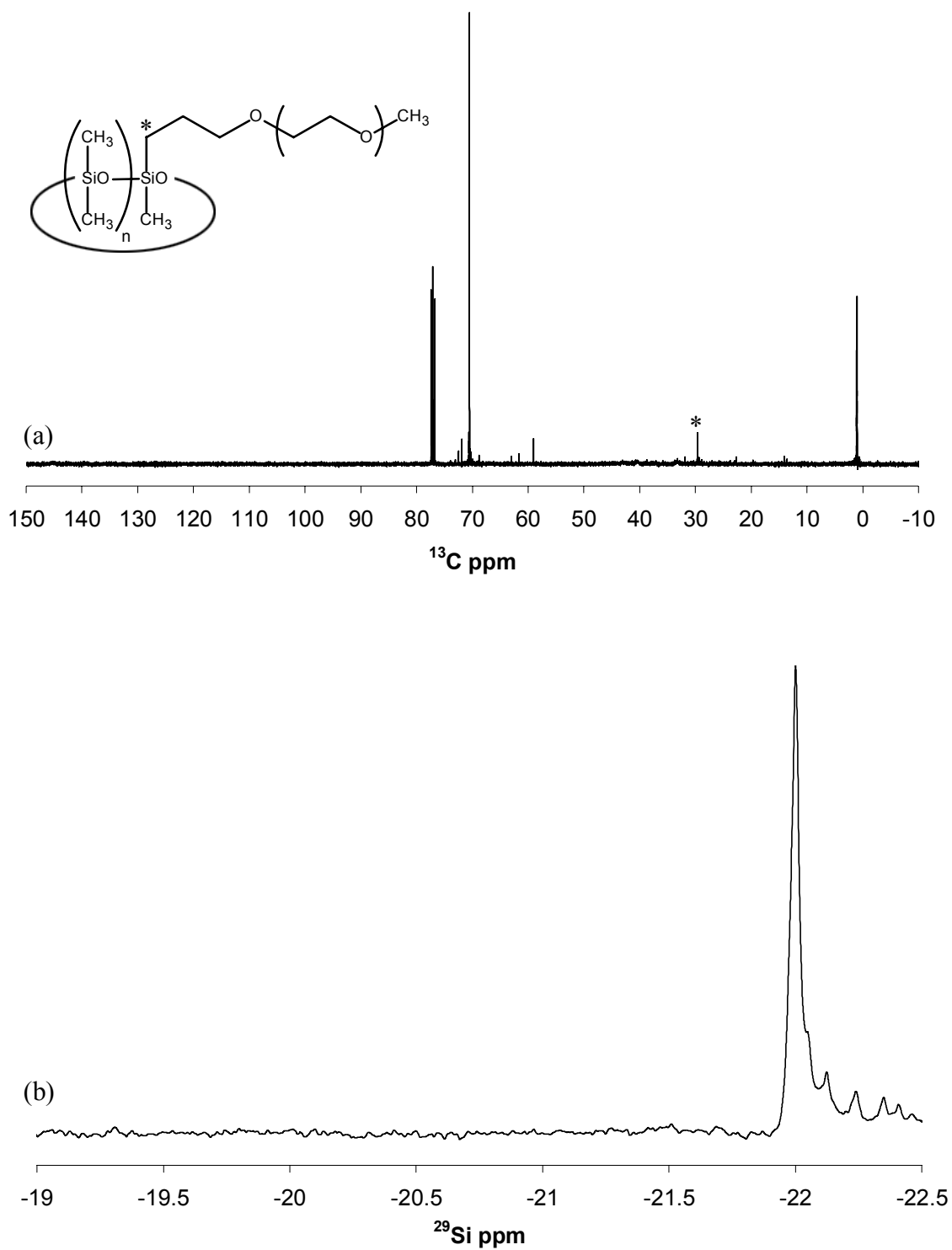
Figure 3.14 – ¹³C (a) and ²⁹Si (b) NMR spectra of the PDMS-POE tadpole in CDCl₃. An asterisk (*) is used to designate the carbon atom that links the cyclic and linear portions of the tadpole in (a).

3.3.4.   Thermal Analysis of Tadpole

Thermal analysis was performed on the PDMS-POE tadpole to determine if the PDMS and POE would behave similarly to linear diblock polymers and phase separate in the solid state. The starting materials have vastly different thermal characteristics: The linear POE shows a melting endotherm at 33 °C, and is so highly crystalline that its glass transition temperature (T_g) is not evident. The hydrosilane-functionalized cyclic PDMS, conversely, does not show any thermal transitions from -150 to 150 °C, most likely because the material's T_g was below -150 °C, the lowest temperature attainable by the DSC.

   As illustrated in Figure 3.15, the tadpole shows a melting endotherm at 24 °C, and no T_g over a range of -150 to 150 °C. The presence of the melting endotherm indicates that the tadpole has undergone microphase separation in the solid state, and that the POE tails have a sufficiently uniform structure to crystallize. The presence of comblike tails would disrupt crystallization, so the melting point observed in the DSC confirms the purity of the hybrid macrocycle. Furthermore, it is hypothesized that the melting temperature (T_m) is depressed due to the effect of the bulky cyclic heads on the packing of the POE tails, leading to smaller crystals with a lower T_m, although wide-angle x-ray diffraction would need to be performed for verification.
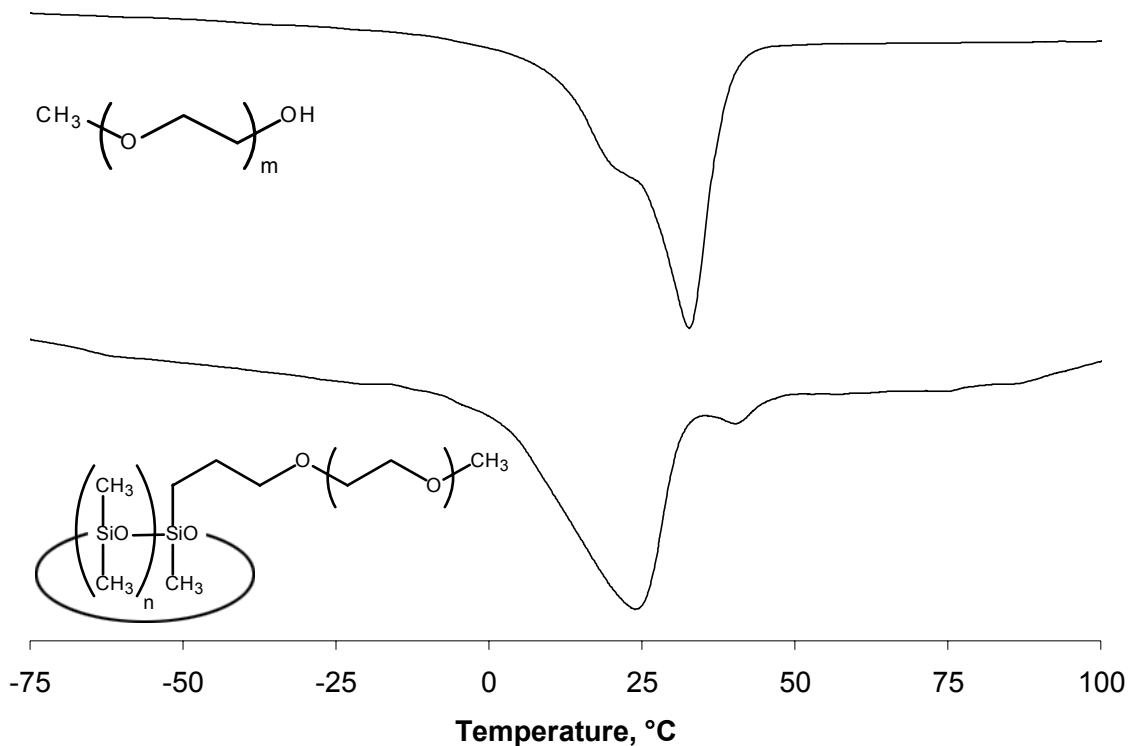
Figure 3.15 – DSC thermograms (second heating, 10 °C/min) of α-methoxy,ω-hydroxy POE (top) and the PDMS-POE tadpole (bottom).

3.3.5.   Surface Active Properties of Tadpole

Whereas POE is soluble in polar to moderately nonpolar solvents, and PDMS soluble in moderately polar to nonpolar solvents, the tadpole is only soluble in moderately polar and moderately nonpolar solvents. The high ratio of PDMS to POE repeat units causes it to immediately form micelles in solvents like water, methanol, and acetone at all concentrations, giving it a lower critical micelle concentration (CMC) in water than commercial surfactants.[50] Similarly, it forms micelles in all concentrations in hexanes, petroleum ether, and similarly nonpolar media.   The poorest solvents at each end of the polarity scale are now MEK and toluene, in which micelles will still form if the polymer concentration is sufficiently high enough.

Surface tensiometry was used to measure the change in surface tension as a function of concentration, as shown in Figure 3.16 for MEK and 3.17 for toluene. The critical micelle concentration is located at the point where the surface tension of the system stops decreasing. In toluene, the CMC was determined to be 6.76 mg/mL, and in MEK the CMC was calculated to be 5.06 mg/mL.
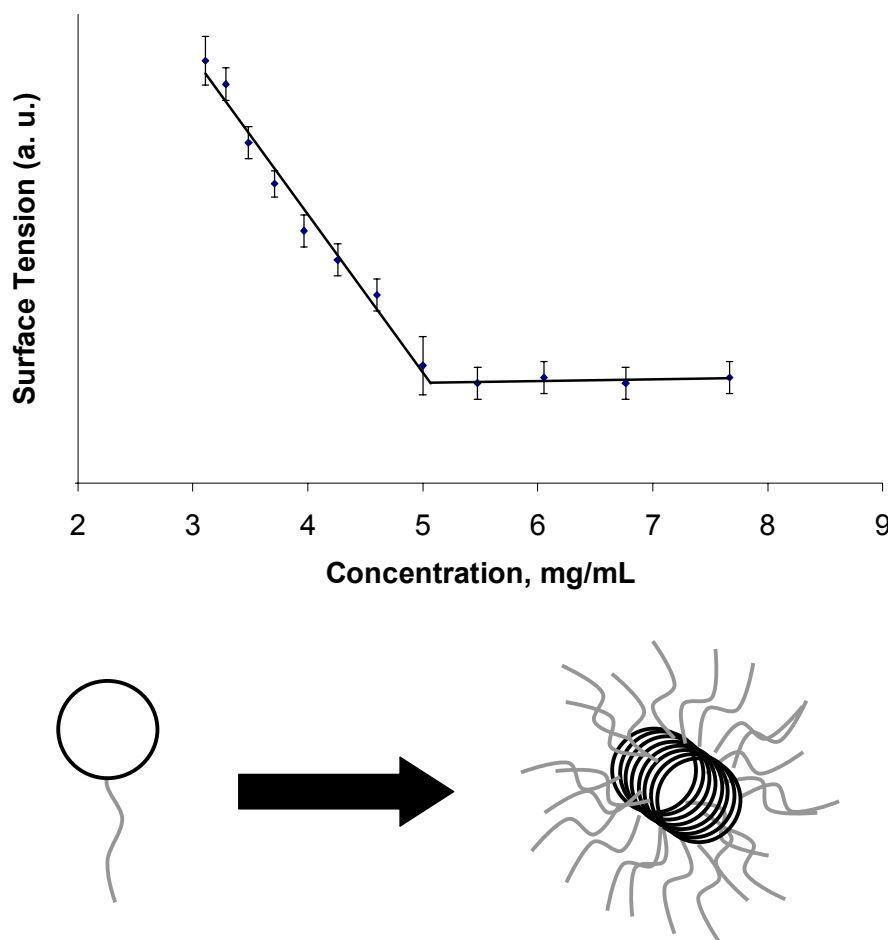
Figure 3.16 – Surface tensiometry plot and diagram of micellar structure of the tadpole macrocycle in MEK.
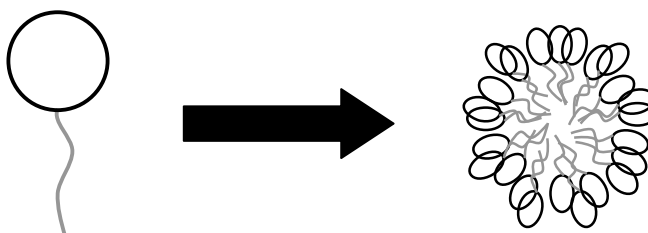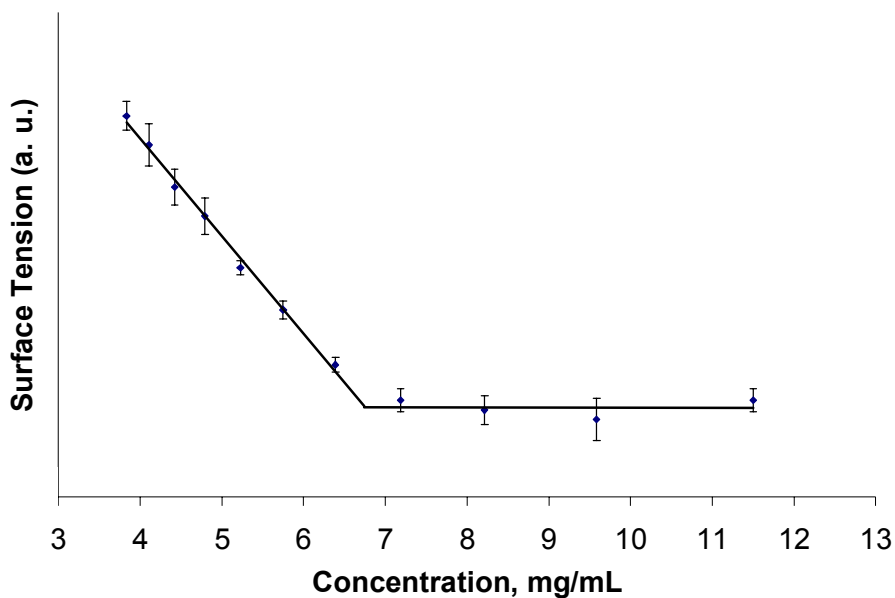
Figure 3.17 – Surface tensiometry plot and diagram of inverse micellar structure of the tadpole macrocycle in toluene.

After the CMC was determined, DLS measurements above and below the CMC were conducted to observe changes in particle size due to micelle formation. The results illustrate not only the effects of solvent quality, but also the tadpole shape on the micelle. MEK is a poorer solvent for the tadpole than toluene, which is one reason why the micelle size increases much more rapidly for it than for toluene. The other reason is that the tadpoles are most likely forced to adopt different shapes in polar and nonpolar

solutions, leading to different micellar architectures.[30,36] These two factors combine to cause large micelles in MEK, so that at a concentration of 15 mg/mL the solution is cloudy to the naked eye. The QELS results are summarized in Table 3.1 for MEK and 3.2 for toluene. Aggregation numbers were calculated by dividing the hydrodynamic radius of the micelle by the hydrodynamic radius of a single tadpole macrocycle.

Table 3.1 – Hydrodynamic radius of PDMS-POE tadpole in MEK solutions.

Concentration, mg/mL	R_h, nm	Standard Deviation, nm	Aggregation Number
1.0	1.19	0.702	N/a
10.0	8,670	1,220	7,290

Table 3.2 – Hydrodynamic radius of PDMS-POE tadpole in toluene solutions.

Concentration, mg/mL	R_h, nm	Standard Deviation, nm	Aggregation Number
1.0	2.39	0.369	N/a
10.0	366	31.9	153
15.0	768	75.9	321

Amphiphiles consisting of either a tadpole or multiarmed rings have been prepared previously,[30,36] although their aqueous solution properties have not been fully explored. Both systems, however, have been shown to form micelles in which the macrocycles stack in a columnar fashion. Also, studies have been performed on a number of linear and comblike PDMS-POE surfactants in aqueous solutions,[50,51] finding that the CMC depends not only on the PDMS:POE ratio, but also the topology of the silicone at the air-water interface: the denser the silicones can pack at the surface of the fluid, the lower the

surface energy. Furthermore, the more tightly the hydrophobic groups can pack in the interior of the micelle, the better the solubilizing ability of the surfactant. From these studies, it is expected that the PDMS-POE tadpole may be a more effective surfactant under nonpolar conditions than under polar conditions.

3.4. **Conclusions**

An amphiphilic tadpole consisting of a macrocyclic PDMS head and a linear POE tail was prepared via radical-catalyzed hydrosilylation. The resultant hybrid macrocycle was purified by fractionation and analyzed by GPC, and ^{1}H, ^{13}C, and ^{29}Si NMR. Critical micelle concentrations were measured with surface tensiometry, and determined to be 6.76 mg/mL in toluene and 5.06 mg/mL in MEK. Quasielastic light scattering showed that the tadpole structure led to micelles that were larger by an order of magnitude in polar than in nonpolar solution. Thermal analysis showed that the POE and PDMS blocks had undergone microphase separation in the solid state, allowing the POE to show a melting endotherm at 24 °C, 9 °C lower than the T_m of the POE starting material.

3.5. **References**

(1)   Frisch, H. L.; Wasserman, E. *J. Am. Chem. Soc.* **1961**, *83*, 3789.

(2)   Tezuka, Y.; Oike, H. *J. Am. Chem. Soc.* **2001**, *123*, 11570.

(3)   Tezuka, Y.; Oike, H. *Prog. Polym. Sci.* **2002**, *27*, 1069.

(4)   Tezuka, Y.; Iwase, T.; Shiomi, T. *Macromolecules* **1997**, *30*, 5220.

(5)   Oike, H.; Imamura, H.; Tezuka, Y. *Macromolecules* **1999**, *32*, 8816.

(6)   Oike, H.; Imamura, H.; Tezuka, Y. *Macromolecules* **1999**, *32*, 8666.

(7)   Oike, H.; Imamura, H.; Imaizumi, H.; Tezuka, Y. *Macromolecules* **1999**, *32*, 4819.

(8)   Oike, H.; Kobayashi, F.; Tezuka, Y.; Hashimoto, S.; Shiomi, T. *Macromolecules* **1999**, *32*, 2876.

(9)   Oike, H.; Imaizumi, H.; Mouri, T.; Yoshioka, Y.; Uchibori, A.; Tezuka, Y. *J. Am. Chem. Soc.* **2000**, *122*, 9592.

(10)   Oike, H.; Kobayashi, S.; Tezuka, Y.; Goethals, E. J. *Macromolecules* **2000**, *33*, 8898.

(11)   Oike, H.; Imaizumi, H.; Mouri, T.; Yoshioka, Y.; Uchibori, A.; Tezuka, Y. *J. Am. Chem. Soc.* **2000**, *122*, 9592.

(12)   Oike, H.; Mouri, T.; Tezuka, Y. *Macromolecules* **2001**, *34*, 6229.

(13)   Oike, H.; Washizuka, M.; Tezuka, Y. *Macromol. Rapid Commun.* **2001**, *22*, 1128.

(14)   Oike, H.; Mouri, T.; Tezuka, Y. *Macromolecules* **2001**, *34*, 6592.

(15)   Oike, H.; Hamada, M.; Eguchi, S.; Danda, Y.; Tezuka, Y. *Macromolecules* **2001**, *34*, 2776.

(16)   Oike, H.; Kobayashi, S.; Mouri, T.; Tezuka, Y. *Macromolecules* **2001**, *34*, 2742.

(17)   Tezuka, Y. *Macromolecules* **2001**, *34*, 2776.

(18)   Tezuka, Y.; Mori, K.; Oike, H. *Macromolecules* **2002**, *35*, 5707.

(19)   Tezuka, Y.; Tsuchitani, A.; Yoshioka, Y.; Oike, H. *Macromolecules* **2003**, *36*, 65.

(20)   Oike, H.; Uchibori, A.; Tsuchitani, A.; Kim, H.-K.; Tezuka, Y. *Macromolecules* **2004**, *37*, 7595.

(21)   Lombardo, D.; Longo, A.; Darcy, R.; Mazzaglia, A. *Langmuir* **2004**, *20*, 1057.

(22)   Kellermann, M.; Bauer, W.; Hirsch, A.; Schade, B.; Ludwig, K.; Böttcher, C. *Angew. Chem. Int. Ed.* **2004**, *43*, 2959.

(23)   Zhang, C.; Laine, R. M. *J. Am. Chem. Soc.* **2000**, *122*, 6979.

(24)   Bassindale, A. R.; Gentle, T. E. *J. Mater. Chem.* **1993**, *3*, 1319.

(25)   Gohy, J.-F.; Hofmeier, H.; Alexsev, A.; Schubert, U. S. *Macromol. Chem. Phys.* **2003**, *204*, 1524.

(26)   Yin, R.; Hogen-Esch, T. E. *Macromolecules* **1993**, *26*, 6952.

(27)   Kolb, H. C.; Finn, M. G.; Sharpless, K. B. *Angew. Chem. Int. Ed.* **2001**, *40*, 2004.

(28)   Matthews, S. E.; Pouton, C. W.; Threadgill, M. D. *Tetrahedron Lett.* **2001**, *42*, 1355.

(29)   Beinat, S.; Schappacher, M.; Deffieux, A. *Macromolecules* **1996**, *29*, 6737.

(30)   Brandys, F. A.; Pugh, C. *Macromolecules* **1997**, *30*, 8153.

(31)   Pugh, C.; Bae, J.-Y.; Scott, J. R.; Wilkins, C. L. *Macromolecules* **1997**, *30*, 8139.

(32)   Höger, S.; Meckenstock, A.-D.; Müller, S. *Chem. Eur. J.* **1998**, *4*, 2423.

(33)   Höger, S. *J. Polym. Sci., Part A: Polym. Chem.* **1999**, *37*, 2685.

(34)   Höger, S.; Bonrad, K.; Mourran, A.; Beginn, U.; Möller, M. *J. Am. Chem. Soc.* **2001**, *123*, 5651.

(35)   Rosselli, S.; Ramminger, A.-D.; Wagner, T.; Silier, B.; Wiegand, S.; Häußler, W.; Lieser, G.; Scheumann, V.; Höger, S. *Angew. Chem. Int. Ed.* **2001**, *40*, 3138.

(36)   Höger, S.; Morrison, D. L.; Enkelmann, V. *J. Am. Chem. Soc.* **2002**, *124*, 6734.

(37)   Caseri, W. R.; Pregosin, P. S. *Organometallics* **1988**, *7*, 1373.

(38)   Lestel, L.; Cheradame, H.; Boileau, S. *Polymer* **1990**, *31*, 1154.

(39)   Roy, A. K.; Taylor, R. B. *J. Am. Chem. Soc.* **2002**, *124*, 9512.

(40)   Stein, J.; Lewis, L. N.; Gao, Y.; Scott, R. A. *J. Am. Chem. Soc.* **1999**, *121*, 3693.

(41)   El-Durini, N. M. K.; Jackson, R. A. *J. Organomet. Chem.* **1982**, *232*, 117.

(42)   Minatti, E.; Borsali, R.; Schappacher, M.; Deffieux, A.; Soldi, V.; Narayanan, T.; Putaux, J.-L. *Macromol. Rapid Commun.* **2002**, *23*, 978.

(43)   Khandpur, A. K.; Farster, J. S.; Bates, F. S.; Hamley, I. W.; Ryan, A. J.; Brass, W.; Almdal, K.; Mortensen, K. *Macromolecules* **1995**, *28*, 8796.

(44)   Kickelbick, G. B., J.; Husing, N.; Andersson, M.; Palmqvist, A. *Langmuir* **2003**.

(45)   Knischka, R.; Hanselmann, R.; Frey, H.; Lutz, P. J. *Langmuir* **1999**, *15*, 4752.

(46)   Luk, Y.-Y.; Abbott, N. L. *Curr. Opin. Coll. In. Sci.* **2002**, *7*, 267.

(47)   Coqueret, X.; Wegner, G. *Makromol. Chem.* **1992**, *193*, 2929.

(48)   Curtice, J.; Gilman, H.; Hammond, G. S. *J. Am. Chem. Soc.* **1957**, *79*, 4754.

(49)   Chatgilialoglu, C. *Chem. Rev.* **1995**, *95*, 1229.

(50)   Anathapadmanabhan, K. P.; Goddard, E. D.; Chandar, P. *Coll. Surf.* **1990**, *44*, 281.

(51)   Soni, S. S.; Sastry, N. V.; George, J. *J. Phys. Chem. B* **2003**, *107*, 5382.

CHAPTER IV

PREPARATION OF DIETHYLENE GLYCOL-LINKED CYCLIC POLY(STYRENE) AND SUBSEQUENT ROTAXANATION WITH LINEAR POLY(STYRENE)

4.1 Introduction

Polyrotaxanes, commonly known simply as rotaxanes, are supramolecular assemblies of polymers formed by threading macrocycles onto a linear backbone.[1-5] Named for the Latin words for wheel (*rota*) and axle (*axis*), this class of materials was first postulated to exist in 1961[6] and was first synthesized by Harrison and Harrison in 1967.[7] Nine years later, Ogata and coworkers reported their success in making a polyrotaxane,[8] and soon others followed.

As the field has grown, conventions have been established to distinguish rotaxanes according to their chemical structures, their method of assembly, and the presence or absence of blocking groups to prevent dethreading. Homorotaxanes have linear and macrocyclic species that consist of the same polymeric repeat unit, while heterorotaxanes are comprised of chemically different molecules. Macrocycles can be threaded by self-assembly if the two components have a driving force that causes them to form a complex, such as in the case of α-cyclodextrin and linear POE, where the oxyethylene repeat unit of POE is drawn into the hydrophobic interior of the cyclodextrin in aqueous solution.[9-12] Another example is the threading of cyclic POE by linear poly(urethanes), where hydrogen bonding between the two species results in the rotaxane.[13]

The other method, for systems that either have no thermodynamic driving force to complex or have a driving force to phase separate, is statistical rotaxanation.[14-16] In this method, monomer is polymerized (either step growth or chain growth kinetics) in the presence of the macrocycle, and as the polymer grows, macrocycles are trapped along its length. Le Chatelier's principle governs the probability that a cycle will be incorporated into the rotaxane: the greater the concentration of the macrocycle, the greater the probability. Another concern is the openness of the cyclic cavity, generally reflected by the number of atoms in its backbone – the larger the cavity, the greater the likelihood that the cycle will be threaded.[17] The statistical method, however, results in lower threading amounts due to its lower efficiency. These threading methodologies are illustrated in Figure 4.1.

$\Delta G < 0$

$\Delta G \geq 0$
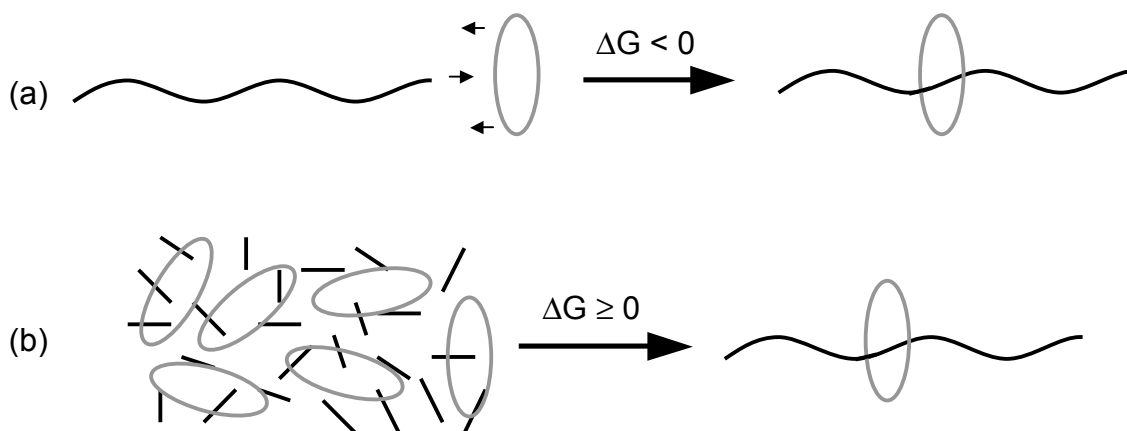
Figure 4.1 – Threading of macrocycles by self-assembly (a) and statistical (b) means.

Once the cycles are threaded, they must be kept from slipping off the linear polymer. "True rotaxanes" have sterically bulky blocking groups that prevent the macrocycles

from dethreading.[1,3,4,14,18] In the case of self-assembly, the blocking groups can be added after rotaxanation, but with some loss of threading.[12] For step-growth statistical polymerizations, a monofunctional blocking group can be added to cap the chains *in situ* and control the overall molecular weight.[19] Free radical initiators that incorporate blocking groups[20] such as the one pictured in Figure 4.2 have been developed to block at least one end of the rotaxane. These initiators work best with polymers such as poly(styrene) (PS), which terminates almost exclusively by coupling, simultaneously blocking both ends. A fourth method is available to ionic polymerizations, which is to quench the growing chain end(s) with a functionalized blocking group.[21] Without blocking groups, the assembly is known as a polypseudorotaxane, or simply a pseudorotaxane, and is subject to dethreading.[22] It has been postulated, although not proven, that a polymer with a large enough contour length could mitigate this thermodynamically unstable condition and stay threaded for an appreciable amount of time,[14,23] and the controlled diffusion of cycles from the linear polymer would be useful in certain applications, such as drug delivery.
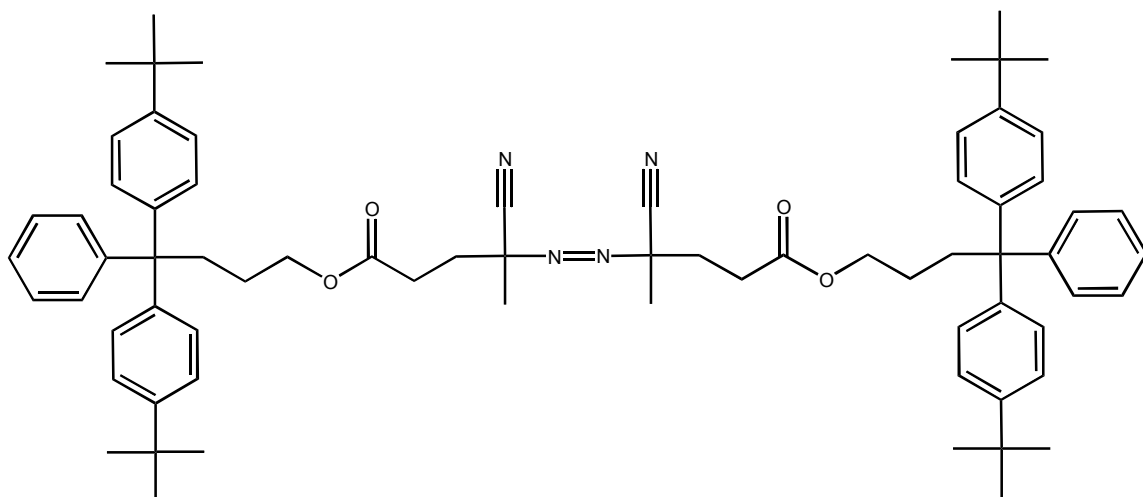
Figure 4.2 – Structure of *meso*-4,4-bis(*p-tert*-butylphenyl)-4-phenylbutyl 4,4'-azobis[4-cyanopentanoate], a blocking group/free radical initiator for use in statistical rotaxanations.[20]

Although many have used rotaxanes as merely an example of the expanding horizons of designer molecular topology, these modular assemblies also have the potential for unique physical and chemical properties. Nanomachines like molecular pistons[24] have been designed from pseudorotaxanes, and the binary threaded/unthreaded states could become the core of a molecular computer.[25] Harada has produced a "molecular abacus" in which the rings of the polyrotaxane move along the linear polymer as they alternately repel and attract each other.[26] Finally, rotaxane films can have "smart surfaces," with threaded macrocycles coming to the surface under favorable environmental conditions and then diffusing below the surface when exposed to an unfavorable environment.[27,28]

The macrocycle is a crucial part of the rotaxane topology. The primary criterion is that it has to be big enough to be threaded – 22 backbone atoms provide a large enough opening for poly(ethylene), which has an effective cross-sectional area of 4.5 Å.[7] The maximum size of the cycle depends on the hydrodynamic radius of the blocking group,

but the blocking group in Figure 4.2 has been shown to work with POE cycles with up to 42 backbone atoms.[18] The final requirement of the cycle is that it must be able to be threaded without reacting with the polymer, ensuring that the assembly is noncovalent in structure.

The chemical composition of the macrocycle is the second consideration in design. If the linear polymer can interact with the macrocycle[13,29,30] through hydrogen bonds, dipolar interactions, π-stacking, or hydrophobic interactions, the system can self-assemble to some extent and increase the threading level. For statistical threading, one of the dominant factors is the miscibility of the macrocycle and the resulting rotaxane with the monomer and homopolymer matrix. If the macrocycle is not miscible with the monomer, a cosolvent can be added to bring everything into the same phase, but reducing the concentration of macrocycles can lower threading levels. Furthermore, if the macrocycle is immiscible with the polymer, the rotaxane will eventually precipitate from the system, also limiting the threading level.

Unfortunately, many potentially interesting properties arise from systems where the linear and cyclic species are chemically different. Threading cyclic POE onto PS, for example, produces an amphiphilic molecule. Unlike a blend of POE and PS, however, the system cannot phase separate to a great degree, because the components are mechanically joined, making rotaxanes good candidates to compatibilize immiscible polymer blends. Furthermore, not all phase separation is problematic – in some cases, it is even desired. The PS-*rotaxa*-POE mentioned above could undergo microphase separation if the fraction of POE is high enough, and the POE phase then can be brought to the surface by annealing in a humid environment, increasing the hydrophilicity and

biocompatibility of the system. In a blend, however, POE can leach from the surface into the surrounding environment, reducing the benefits of blending over time. A rotaxane would not suffer this problem, because threading would keep it bound to the surface of the film.

The use of hybrid macrocycles instead of homocycles is one way to balance the need for chemically different species without making the thermodynamics of mixing prohibitively unfavorable. By incorporating a block of polymer in the macrocycle that resembles the linear polymer in the rotaxanes, unfavorable thermodynamics can be reduced and result in yields approaching those of homorotaxanes while preserving a heterogeneous threaded system.

The determination of threading levels is the crux of rotaxane characterization. When threading macrocycles cause or experience changes in local electronic structure, spectroscopic techniques such as ^{1}H NMR can be used to quantitate the extent of rotaxanation.[17,31-36] When the electronic perturbations are not present, as is frequently the case with statistically rotaxanated systems, spectroscopy was used to quantitate the amount of cycles left after a purification cycle (e.g. precipitation or washing). If the macrocycle concentration stabilized after several such cycles, it was assumed that it was trapped by rotaxanation. Mass spectrometry was also used, but suffers from one drawback – the relative intensities of each species depend not only on the concentration, but also on the ionization potential of each species. If the linear and cyclic moieties have a large difference in ionization potentials, the differences will complicate determining the number of rotaxanes present versus the number of unthreaded linear and cyclic molecules.

Furthermore, the effect of rotaxanation on ionization potential is only beginning to be explored.[21,37]

Another technique, 2-dimensional diffusion-ordered NMR spectroscopy (DOSY) has been successfully applied to rotaxanes[12,38] to quantify threading levels by providing the diffusion coefficient as a function of proton chemical shift, alleviating any ambiguities associated with the alternative analyses. The pulse program is designed to begin by magnetically exciting protons with a 90° pulse, similar to a standard ^{1}H NMR. Next, as shown in Figure 4.3(a), a gradient pulse is applied, spatially encoding the molecules. Time is provided for the molecules to diffuse, and then a second gradient with equal strength and duration but opposite sign as the first is then used to refocus the magnetic fields and spatially decode the molecules. The resultant signal is read, and if no molecules diffused the maximum signal is returned, as seen in Figure 4.3 (b). Otherwise, a weaker signal results, and is processed to obtain the diffusion coefficients.
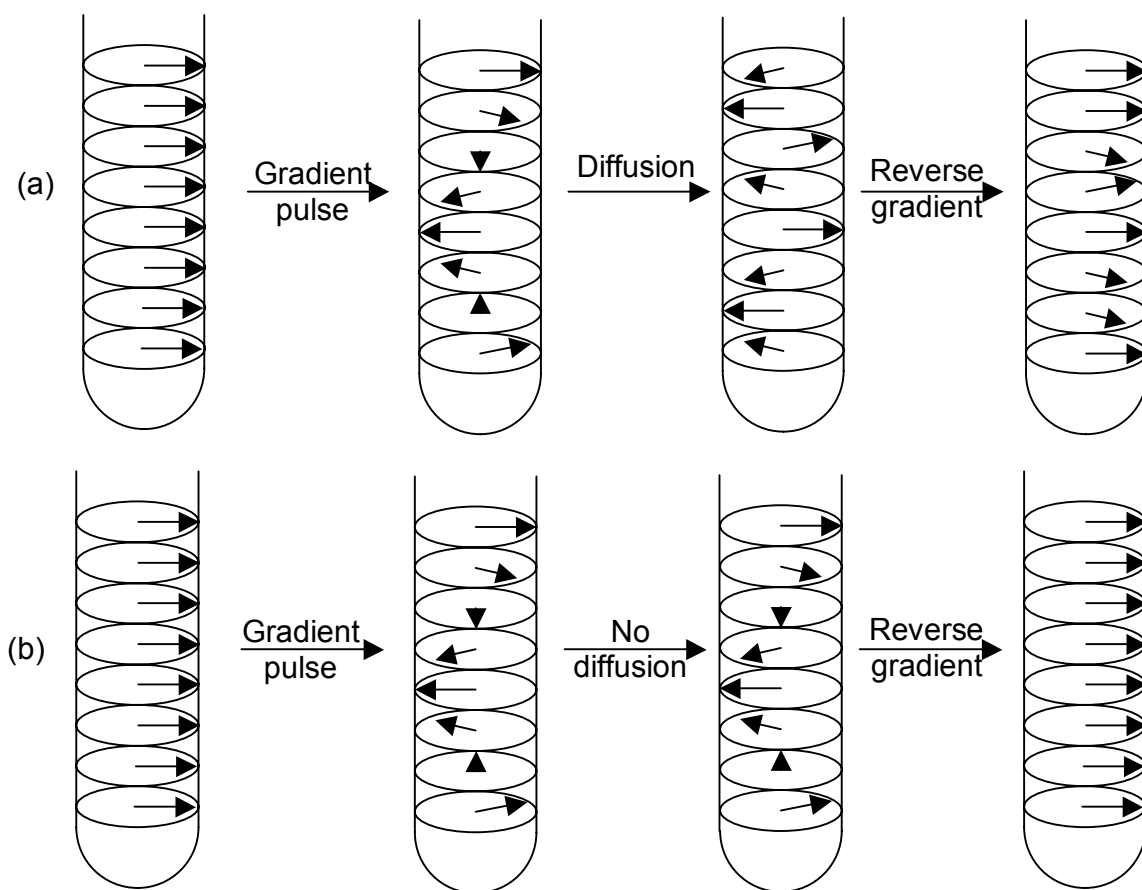
Figure 4.3 – Examples of how the DOSY pulse program spatially encodes and then decodes molecules in an NMR tube. Each small arrow in the tube represents the magnetic moment of a molecule located along the Z axis of the NMR tube. A gradient pulse is applied along the Z axis, and then the system can either undergo diffusion (a) or not diffuse (b). A second gradient is then applied to refocus the magnetic moments, and the resultant signal is used to calculate the diffusion coefficient.[39]

As shown in Figure 4.4, a mixture of the small cyclic and large linear polymer would result in 2 different diffusion coefficients, while a rotaxane would show the chemical shifts for both moieties diffusing at the same rate, confirming the supramolecular structure. This experiment can also be used to determine if different blocks of a hybrid

macrocycle have been combined, assuming the precursors have sufficiently different diffusion coefficients.
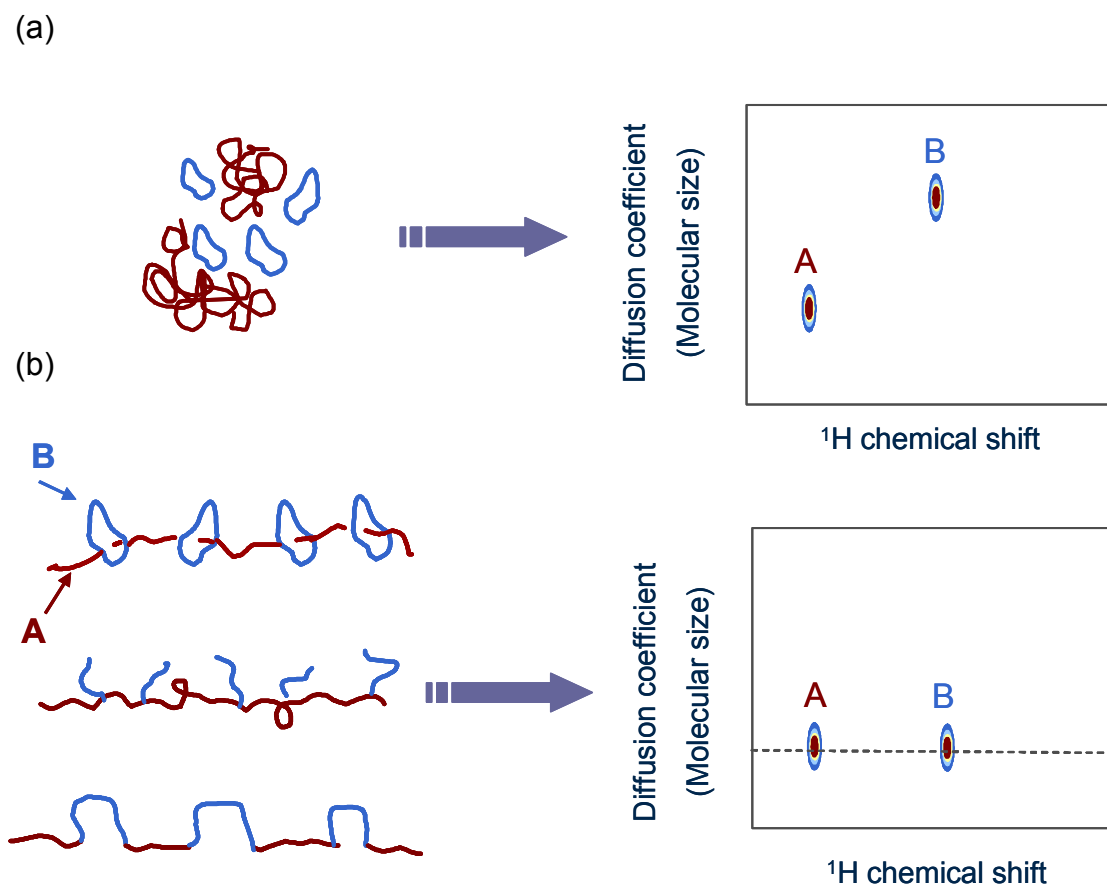
Figure 4.4 –   Schematic of information obtained by 2D diffusion-ordered NMR spectroscopy (DOSY).   In the case of a physical blend of large linear polymer A and small cyclic polymer B, the 2 moieties would appear at their usual chemical shifts but moving with different diffusion coefficients (a).   If A and B are mechanically or chemically linked, their chemical shifts would be observed at the same diffusion coefficient (b).[40]

4.2 Experimental Section

4.2.1. Materials

All reagents were used without further purification unless otherwise specified. Styrene (99%, inhibited with 10-15 ppm-*tert*-butylcatechol), *tert*-butylcatechol inhibitor remover, calcium hydride (95%), α,α'-dibromo-*p*-xylene (97%), copper(I)bromide (98%), and 2,2'-bipyridine (bipy, 99+%), sodium hydride (95%), diethylene glycol di-*p*-tosylate (DEG ditosylate, 98%), quinuclidine (97%), tetrabutylammonium hydroxide (1.0 M solution in methanol), α,ω-dicarboxymethyl poly(oxyethylene) (M_n 600 g/mol, PDI 1.4), heptane (anhydrous, 99%), and silica gel (70-270 mesh, 60 Å) were purchased from Aldrich. The deuterated solvents chloroform-*d* (CDCl$_3$, 99.8 atom % D), dimethylsulfoxide-*d$_6$* (DMSO-*d$_6$*, 99.9 atom % D), and tetrahydrofuran-*d$_8$* (THF-*d$_8$*, 99.5 atom % D) were also obtained from Aldrich. Potassium hydroxide (90+%), toluene (anhydrous, 99.8%), hydrochloric acid, chloroform, dichloromethane, acetone, acetic acid (glacial), methanol (histological), petroleum ethers, and tetrahydrofuran (THF, inhibitor-free, anhydrous, 99.9%) were obtained from Fisher Scientific. Macroporous ion-exchange resin AG MP-1M (1 mequiv/mL, 0.7 g/mL, 100-200 mesh, chloride form) was purchased from Bio-Rad Laboratories and dried under a vacuum of 500 mTorr at room temperature for 16 hours before use.

4.2.2. Instrumentation

GPC was conducted in THF (1 mL/min) at 303 K on three Waters Styragel columns (5 μm beads: HR 1, 100 Å; HR 3, 1000 Å; HR 4, 10000 Å) that were connected

to a Waters 2690 separations module and a Waters 2410 refractive index detector. Injections of 100 – 200 μL were made from 0.5-5 wt% solutions.

MALDI-TOF mass spectrometry was carried out on a Micromass TofSpec 2E with dithranol serving as the matrix and silver trifluoroacetate used for ionization. Solutions of the polymer (10 mg/mL), matrix (10 mg/mL), and silver trifluoroacetate (2 mg/mL) were mixed in the order listed in volume ratios of 1:1:1, 1:10:1, and 1:100:1. Aliquots of 1 – 2 μL were withdrawn and used to collect mass spectrograms, and the ones with the highest signal/noise ratio were reported.

^{1}H and DOSY NMR spectra were collected with a Bruker DRX 500 in chloroform-d, DMSO-d_6, and THF-d_8. The DOSY experiments were conducted using the bipolar pulse pair and longitudinal eddy current delay (BPP-LED) pulse sequence. Field gradient calibration was accomplished using the self-diffusion coefficient of pure water at 25 °C (2.299×10^{-9} m^{2}s^{-1}). The gradients were applied for 2 ms and the diffusion time was 80 ms. Gradient settling times were 500 μs and the eddy current elimination duration was 5 ms. Homospoil gradients were applied for 1 ms during diffusion and eddy current settling durations. The gradients were incremented 16 times from 1.7 G/cm to 63.0 G/cm, resulting in attenuation of the polystyrene resonances to approximately 2% of their original intensities. A total of 32 free induction decays containing 8K complex data points were collected at each gradient. The recycle delay was 10 s and 8 dummy scans were applied before the first data were collected. ^{13}C NMR spectra were measured on a Bruker AMX 400 in chloroform-d, DMSO-d_6, and tetrahydrofuran-d_8. Concentrations of approximately 1 wt% were used for ^{1}H and DOSY NMR, and 10 wt% for ^{13}C NMR.

Differential scanning calorimetry was performed on a Seiko Instruments DSC 220C under nitrogen purge with samples weighing $10 - 15$ mg sealed in aluminum pans heated at a rate of 10 °C/min. The power and temperature scales of the calorimeter were calibrated against the enthalpies of fusion and melting temperatures of pure indium and tin.

A Jouan MR23i was used for centrifugation, spinning at 5000 rpm at 20 °C for 10 minutes.

4.2.3. Synthesis of α,ω-dibromo PS

This scheme was used to prepare functionalized PS ranging in size from M_n 3,320 g/mol and PDI 1.77 to 1,870 g/mol and PDI 1.12. The procedure described here is for M_n 1,990 and PDI 1.13. Prior to the reaction, styrene was de-inhibited by passing it 3 times through a column packed with *tert*-butylcatechol remover. Next, it was dried over CaH, distilled into a round bottom flask, and stored under a nitrogen atmosphere. The α,α'-dibromo-*p*-xylene initiator was recrystallized from chloroform and dried under vacuum.[41] Copper(I) bromide was purified by placing it on a 0.45-μm filter and washing it with 25 mL of glacial acetic acid, followed by 25 mL methanol and 25 mL acetone, then dried under vacuum.[42]

A 250-mL round bottom flask, inert gas inlet, and magnetic stir bar were dried overnight at 120 °C, then evacuated and purged with nitrogen 3 times. The α,α'-dibromo-*p*-xylene (1.20 g, 4.55 mmol), CuBr (2.91 g, 20.3 mmol), and bipy (6.33 g, 40.5 mmol) were added under positive nitrogen flow. A gastight syringe was purged 3 times with nitrogen and used to inject 7.0 mL styrene (6.4 g, 61 mmol), and a cannula was used

to transfer 100 mL anhydrous toluene to the flask. The solution was heated to reflux over the course of an hour, and allowed to react for 16 hours.

The product mixture was filtered through a 0.45-μm membrane to remove most of the α,α'-dibromo-*p*-xylene, CuBr, and bipy catalysts, and then the solution was rotovapped to give a green-tinged solid. The polymer was then dissolved in dichloromethane (10 mL) and passed through a silica gel column with dichloromethane as mobile phase to remove any remaining ATRP catalysts.[43] The materials causing the green tint were trapped in the column, only eluting when water was passed through. The dichloromethane solution was rotovapped to give 6.19 g of the hard, off-white polymer α,ω-dibromo PS (82.3% yield). The M_n calculated from GPC with polystyrene standards was 1,990 g/mol with a PDI of 1.13. ^{1}H NMR (THF-d_8, ppm): 1.0-2.3 (CH_2), 2.3-3.0 (Ar-CH), 4.5-4.7 (CH-CH_2-CH-Br, CH-CH_2-CH-CH_2-CH-Br), 5.0 (CH-Br), 6.3-7.4 (aryl H). ^{13}C NMR (THF-d_8, ppm): 32 (CH_2-Ar-CH_2), 39-45 (CH_2), 48 (CH-Br), 49-53 (Ar-CH), 125-130 (aryl C).

4.2.4. Synthesis of α,ω-dihydroxy PS

This scheme was used to prepare hydroxyl-terminated PS with M_n 1,860 g/mol and PDI 1.13 and 2,730 g/mol and PDI 1.35. The procedure described here is for M_n 1,860 and PDI 1.13. A 250-mL Erlenmeyer flask was filled with THF (150 mL) and the α,ω-dibromo PS (2.34 g, 1.18 mmol) was dissolved in it. Finely-ground KOH (0.221 g, 3.54 mmol) was added to the solution and allowed to react with the PS for 3 hours. The reaction was quenched with the addition of HCl (0.3 mL, 3.9 mmol). The solids were removed by filtration through a 0.45 μm membrane, and the solvents were rotovapped.

The mass of the resulting hard, off-white polymer α,ω-dihydroxy PS collected was 2.16 g (98.5% yield), with a M_n of 1,860 g/mol and PDI of 1.13. ^{1}H NMR (THF-d_8, ppm): 1.0-2.3 (CH$_2$), 2.3-3.0 (Ar-CH), 4.1 (OH), 4.5-4.7 (CH-OH, CH-CH$_2$-CH-OH, CH-CH$_2$-CH-CH$_2$-CH-OH), 6.3-7.4 (aryl H). ^{13}C NMR (THF-d_8, ppm): 32 (CH$_2$-Ar-CH$_2$), 39-45 (CH$_2$), 49-53 (Ar-CH), 68 (Ar-CH-OH), 125-130 (aryl C). DOSY [CDCl$_3$, log(m^2/s)]: -8.98 and T_g 51 °C for the 1,860 g/mol PS.

4.2.5. Synthesis of α,ω-ditosyl PS

A 250-mL round bottom flask, inert gas inlet, and magnetic stir bar were dried overnight at 120 °C, then evacuated and purged with nitrogen 3 times. Anhydrous toluene (100 mL) was charged to the flask via cannula, and then α,ω-dihydroxy PS (M_n 2,730 g/mol, 6.73 g, 2.47 mmol) was added under positive N$_2$ flow and allowed to dissolve. Next, NaH (0.129 g, 5.11 mmol) was added under positive N$_2$ flow and the system was given 2 hours to deprotonate. Afterward, tosyl chloride (1.88 g, 9.86 mmol) that had been dried overnight *in vacuo* was added under positive N$_2$ flow. The system was allowed to react for 2 more hours, at which time the toluene was removed by rotary evaporation. The product mixture was then redissolved in 15 mL THF and precipitated into 250 mL methanol. The ditosylate-functionalized PS precipitant was collected by filtration through a 0.45-μm membrane, and then the precipitation cycle was repeated 2 more times. The PS was dried under vacuum to give 6.93 g of the hard, off-white polymer α,ω-ditosyl PS (92.3 % yield), with M_n 3,040 and PDI 1.35. ^{1}H NMR (THF-d_8, ppm): 1.0-2.3 (CH$_2$), 2.3 (Ar-CH$_3$), 2.3-3.0 (Ar-CH), 4.6 (CH-O), 6.3-7.4 (aryl H).

4.2.6. Synthesis of quinuclidine-functionalized PS

A 250-mL round bottom flask, inert gas inlet, and magnetic stir bar were dried overnight at 120 °C, then evacuated and purged with nitrogen 3 times. Anhydrous toluene (100 mL) was charged to the flask via cannula, and then α,ω-ditosyl PS (2.72 g, 0.895 mmol) was added under positive N_2 flow, followed by quinuclidine (0.298 g, 2.69 mmol). The system was heated to 90 °C and allowed to react for 16 hours, after which time the toluene was removed by rotary evaporation. The product mixture was redissolved in 25 mL toluene and precipitated into 500 mL petroleum ethers, then filtered through a 0.45-μm membrane to collect the quinuclidine-functionalized PS. Two more precipitation cycles were performed, and then the polymer was dried under vacuum to give 2.42 g of the hard, off-white polymer (82.9 % yield), with M_n of 3,260 g/mol and PDI of 1.35. ^{1}H NMR (THF-d_8, ppm): 1.2 (N-CH$_2$CH$_2$), 1.3-2.3 (CH$_2$N-CH$_2$CH$_2$CH), 2.3 (Ar-CH$_3$), 2.3-3.0 (Ar-CH), 3.7 (N-CH$_2$), 6.3-7.4 (aryl H). DOSY [CDCl$_3$, log(m^2/s)]: -9.16.

4.2.7. Preparation of tetrabutylammonium POE dicarboxylate

A 125-mL Erlenmeyer flask was partially filled with distilled water (50 mL), and then α,ω-dicarboxymethyl POE (15 mL, 31.5 mmol) was dissolved in it. Next, the solution of tetrabutylammonium hydroxide in methanol was added (65 mL, 65 mmol). The reaction was allowed to proceed for 3 hours, and then the solvents and excess tetrabutylammonium hydroxide were removed by rotary evaporation and the POE was dried under vacuum to result in 34.1 g of a clear viscous liquid with M_n 1,080 g/mol and PDI 1.4. ^{1}H NMR CDCl$_3$, ppm): 0.65 (N-CH$_2$-CH$_2$-CH$_2$-CH$_3$), 1.1 (N-CH$_2$-CH$_2$-CH$_2$),

1.3 (N-CH$_2$-CH$_2$), 2.9 (N-CH$_2$), 3.6 (CH$_2$CH$_2$O), 3.8 (CH$_2$-CO$_2^-$).   DOSY [CDCl$_3$, log(m^2/s)]: -8.81.

4.2.8. Self-assembly of Quinuclidine-functionalized PS and Tetrabutylammonium POE Dicarboxylate

The functionalized PS (0.94 g, 0.29 mmol) was dissolved in THF (10 mL) and the functionalized POE (34.1 g, 31.5 mmol) was dissolved in acetone (200 mL) in a 250-mL round bottomed flask.   The PS solution was added dropwise to the POE solution, immediately precipitating and turning the solution cloudy.   The mouth of the flask was covered with aluminum foil and the mixture was stirred for 3 hours to ensure that the reagents had ample opportunity to ion-exchange, and then the flask was sealed with a rubber septum and cooled in a freezer for 16 hours.   Next, the precipitant was collected by centrifugation for 10 minutes at 5000 rpm at 20 °C and dried under vacuum. 0.8144 g of the self-assembled product, a soft and waxy off-white polymer, was collected.

4.2.9. Covalent Fixation of Self-assembled Quinuclidine-functionalized PS and Tetrabutylammonium POE Dicarboxylate

A 1000-mL round bottom flask, inert gas inlet, condenser, and magnetic stir bar were dried overnight at 120 °C, then evacuated and purged with nitrogen 3 times and charged with 700 mL anhydrous toluene via cannula**.** The self-assembled product (0.4072 g) was dissolved in anhydrous toluene (20 mL) and then transferred to the reaction flask with a purged gastight syringe. The system was heated to reflux and reacted for 30 hours, at which time the solvent was removed by rotary evaporation and the polymer was dried under vacuum.   The crude polymer mixture recovered weighed 0.3981 g. ^{1}H NMR

(CDCl$_3$, ppm): 0.65 (N-CH$_2$-CH$_2$-CH$_2$-CH$_3$), 1.1 (N-CH$_2$-CH$_2$-CH$_2$), 1.2 (N-CH$_2$CH$_2$), 1.3-2.3 (N-CH$_2$-CH$_2$, CH$_2$), 2.3 (Ar-CH$_3$), 2.3-3.0 (Ar-CH, N-CH$_2$), 3.6 (CH$_2$CH$_2$O), 3.7 (N-CH$_2$), 6.3-7.4 (aryl H). DOSY [CDCl$_3$, log(m^2/s)]: -9.32.

4.2.10. Synthesis of PS-*block*-DEG Macrocycle

A 3000-mL round bottom flask, inert gas inlet, and magnetic stir bar were dried overnight at 120 °C, then evacuated and purged with nitrogen 3 times. The α,ω-dihydroxy PS (M$_n$ 1,860 g/mol, 1.82 g, 0.978 mmol) was added under positive nitrogen flow. Next, anhydrous THF (1300 mL) and anhydrous heptane (700 mL) were added via cannula. Finally, NaH (0.0495 g, 1.96 mmol) was added under positive nitrogen flow and allowed to react with the PS for 9 hours. Afterwards, diethylene glycol (DEG) ditosylate (0.415 g, 1.00 mmol) was added under positive nitrogen flow and the solution was stirred for 24 hours. Finally, the reaction was quenched by the addition of 2.97 g of vacuum-dried ion-exchange resin that was added under positive nitrogen flow.

The contents of the flask were filtered through a 0.45-μm membrane to eliminate the resin, and then the solvents were removed with a rotovap. The resultant brown solid was dissolved in THF (10 mL) and precipitated dropwise into methanol (150 mL). The precipitant was trapped by filteration and redissolved in THF (50 mL), producing a cloudy solution. The THF solution was filtered to remove the brown contaminant and then rotovapped, giving 1.49 g of an off-white waxy polymer (78.7% yield), with M$_n$ 1,930 g/mol and PDI 1.13. ^{1}H NMR (CDCl$_3$, ppm): 1.0-2.3 (CH$_2$), 2.3-3.0 (Ar-CH), 3.6 (CH$_2$O), 4.4-4.7 (CH-O-DEG, CH-CH2CH-O-DEG), 6.3-7.4 (aryl H). ^{13}C NMR (CDCl$_3$, ppm): 32 (CH$_2$-Ar-CH$_2$), 39-45 (CH$_2$), 49-53 (Ar-CH), 69 (CH$_2$CH$_2$O), 125-130 (aryl C). DOSY [CDCl$_3$, log(m^2/s)]: -8.97. T$_g$ 24 °C.

4.2.11. Synthesis of PS-*rotaxa*-cyclo(PS-*block*-DEG)

A glass test tube (25 mm × 150 mm) and stir bar were dried overnight at 120 °C and the PS-DEG macrocycle (1.40 g, 0.725 mmol) was added. The tube was sealed with a rubber septum, then evacuated and purged with nitrogen 3 times. Dried and deinhibited styrene (3.0 mL, 26 mmol) was charged with a purged gastight syringe, and the system was stirred until the macrocycle was dissolved in the monomer. Finally, the septum was momentarily removed in order to add the blocking group/initiator *meso*-4,4-bis(*p-tert*-butylphenyl)-4-phenylbutyl 4,4'-azobis[4-cyanopentanoate][20] (10.2 mg, 9.51 × 10^{-3} mmol). 3 freeze-pump-thaw cycles were performed to degas the system, and then the test tube was backfilled with nitrogen and heated to 90 °C. The polymerization was allowed to proceed for 16 hours, upon which point a hard white solid was obtained. The product was dissolved in 10 mL acetone and fractionated with methanol to precipitate threaded and unthreaded PS from any unthreaded macrocycles. The precipitants were collected by centrifugation at 20 °C and 5000 rpm for 10 minutes. ^{1}H (CDCl$_3$, ppm): 1.2 (*t*-Bu CH$_3$), 1.3 (NC-C-CH$_3$), 1.4-2.4 (CH$_2$), 2.5-3.0 (Ar-CH), 3.6 (O-CH$_2$CH$_2$-O), 4.0 (CO$_2$-CH$_2$-CH$_2$), 6.3-7.8 (Ar-H). ^{13}C (CDCl$_3$, ppm): 21 (Ar$_3$-C-CH$_2$), 23 (NC-C-CH$_3$), 25 (CO$_2$-CH$_2$), 29 (CO-CH$_2$), 31 (*t*-Bu CH$_3$), 34-43 (CH$_2$), 44 (NC-C), 51-53 (Ar-CH), 58 (Ar$_3$-C), 66 (CO$_2$-CH$_2$-CH$_2$), 70 (O-CH$_2$CH$_2$-O), 125-150 (Ar-C), 173 (C=O). DOSY [CDCl$_3$, log(m^2/s)]: -9.73. T$_g$ 79 °C. M$_n$ 9,630 g/mol, PDI 1.53.

4.3 Results and Discussion

4.3.1. Preparation of α,ω-dihydroxy PS

The design of the rotaxane herein was influenced by several factors, the foremost of which is the necessity for blocking groups on the linear polymer. Initiation using the moiety in Figure 4.2 has been studied exhaustively, and PS terminates by coupling an overwhelming majority of the time, facilitating the preparation of a true rotaxane. Next, a difunctional PS oligomer must be synthesized for the diblock. Living anionic polymerizations offer exceptional control of polymer size and distribution, and have been successfully used to make cyclic PS[44-46] and PS-PDMS[47] diblock macrocycles, but a controlled radical polymerization (CRP)[48-52] scheme was chosen instead because it still offered a great degree of control over polymer size and distribution while being more resistant to the presence of moisture. The remaining steps involved merely picking lengths of oxyethylene repeats to stay below 42 total backbone atoms and then using them as a linker to cyclize the macromolecule.

Atom transfer radical polymerization (ATRP) has become an important CRP technique, has been thoroughly investigated in the polymerization of PS, and all the reagents used in the reaction are commercially available.[42,51-55] The organohalide groups of the dibromo-*p*-xylene homolytically cleave at high temperatures, initiating the reaction shown in Figure 4.5.
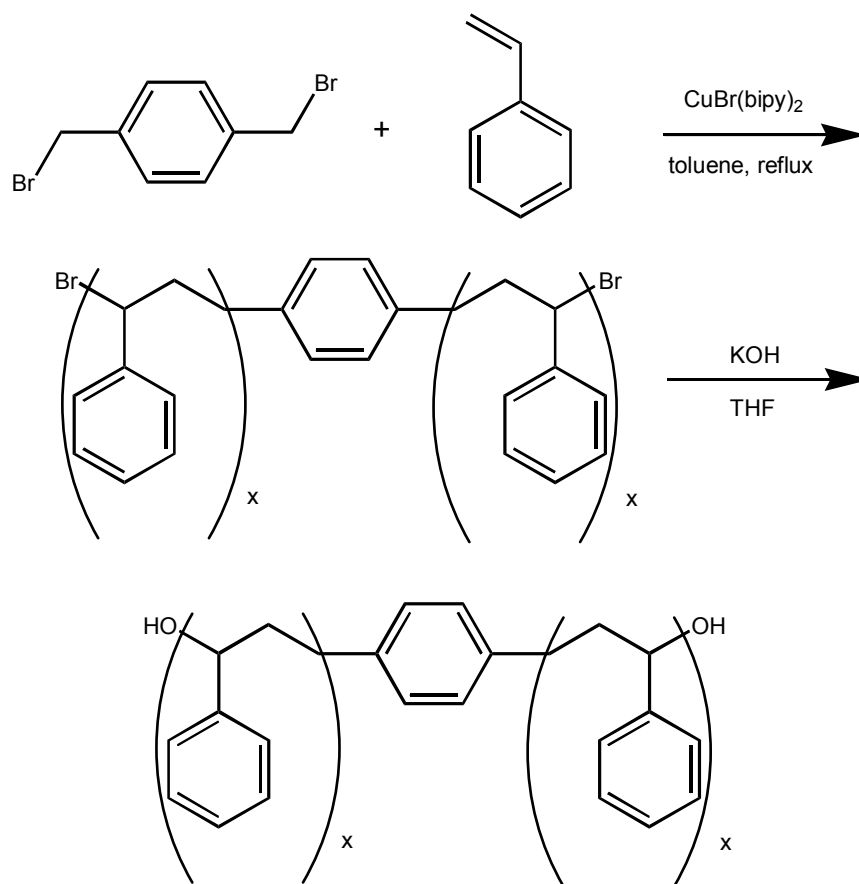
Figure 4.5 – Synthesis of α,ω-dibromo PS by atom transfer radical polymerization, followed by reaction with KOH to produce α,ω-dihydroxy PS.

Meanwhile, the CuBr(bipy)$_2$ complex rapidly deactivates and reactivates the radicals, slowing the rate of propagation and preventing termination by coupling, allowing a low-molecular weight PS to be obtained with bromine endgroups which was subsequently reacted with KOH to give α,ω-dihydroxy PS. The ^{1}H NMR spectra of the dibromo and dihydroxy PS can be seen in Figure 4.6. In both spectra, residual peaks from the THF solvent can be seen at δ_H = 1.7 and 3.6 ppm, and water at 2.5 ppm. Protons located on the phenyls can be seen from δ_H = 6.3-7.5 ppm, those along the backbone of the polymer are present at 1.0-3.0 ppm, and located around 4.6 ppm is a broad peak for the backbone C-

H protons near the endgroups. The main difference lies in the presence of a peak for the proton immediately next to the bromine endgroup at 5.0 ppm in the α,ω-dibromo PS, and a peak at 4.1 ppm in the α,ω-dihydroxy PS for the hydroxyl proton.

Similarly in Figure 4.7, the aromatic carbons are at δ_C = 125-130 ppm, the backbone CH_2 carbons from 32-45 ppm, and the backbone CH carbons from 49 to 53 ppm. For α,ω-dibromo PS, the carbon next to the bromine endgroup is located at 48 ppm, and the carbon next to the hydroxyl group in α,ω-dihydroxy PS is at 68 ppm. THF residual peaks are located at 25 and 67 ppm. The GPC trace for α,ω-dihydroxy PS is shown in Figure 4.14.

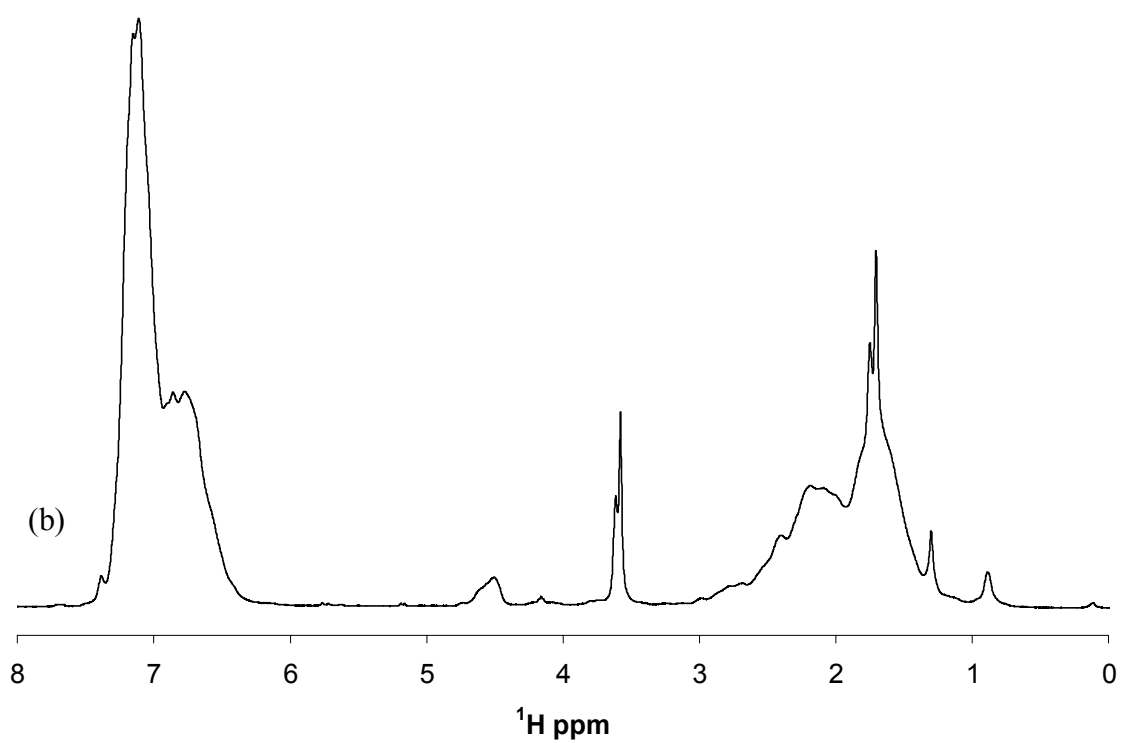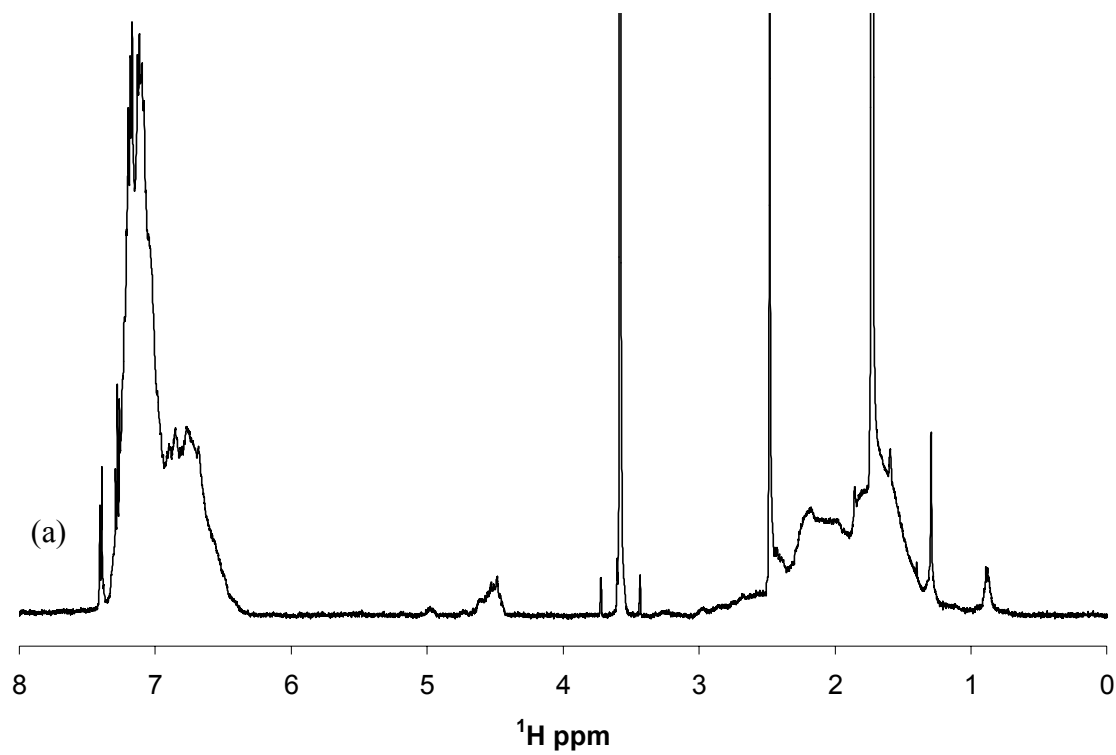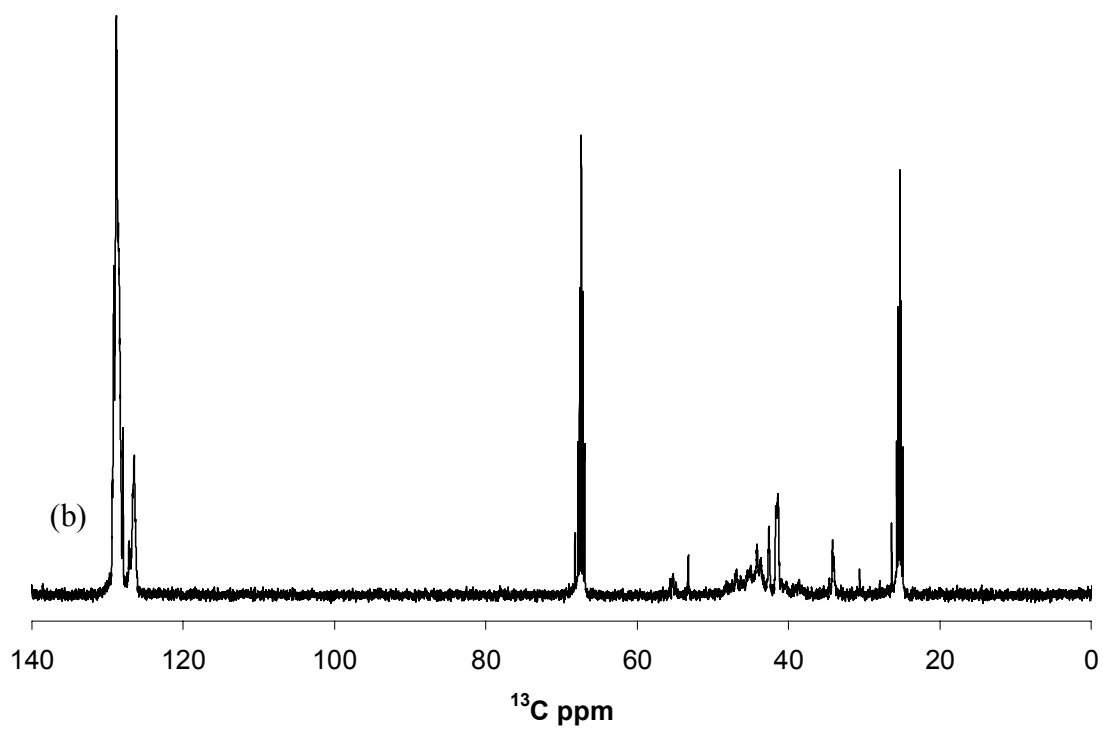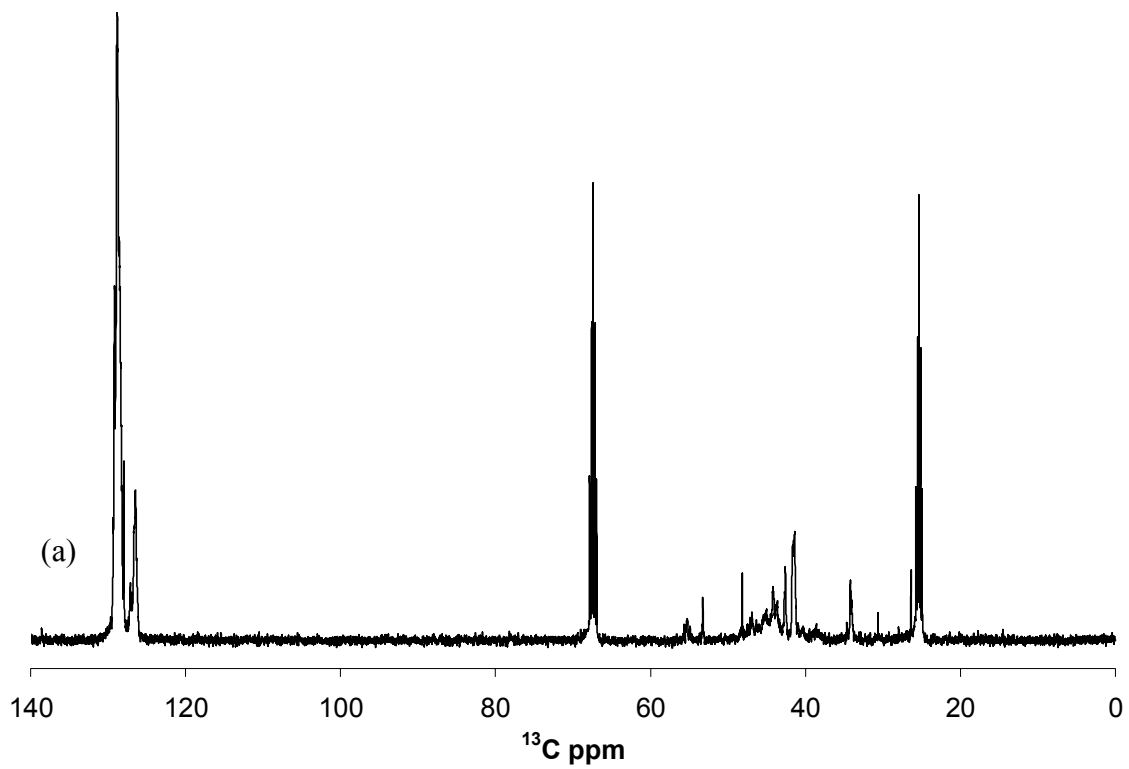**Figure 4.6 –** ¹H NMR spectrum of α,ω-dibromo PS (a) and α,ω-dihydroxy PS (b) in THF-d_8.

Figure 4.7 – ¹³C NMR spectrum of α,ω-dibromo PS (a) and α,ω-dihydroxy PS (b) in THF-d_8.

4.3.2. Self-assembly and covalent fixation of PS and POE

Tezuka and Oike's self-assembly and covalent fixation scheme[56-58] was the first method attempted for building a hybrid macrocycle consisting of styrene and oxyethylene blocks. This path was chosen because the cyclization step results in nearly a 100% cyclic yield, so separating the cycles from any linear species is not an issue. Since the presence of moisture reduces the effectiveness of the ion-exchange resin, the hygroscopic nature of PEG was a concern in using White's method.[59] Using cyclodextrins, in a similar fashion to the separation of linear and cyclic POE,[60] was another option. The high PS content of the proposed macrocycles would limit their solubility in water, however, and filtering to remove any cyclodextrin-complexed linear species would surely trap the PS-POE macrocycle as well.

Tezuka's method begins with functionalizing one of the linear polymer precursors with tosyl chloride to result in a ditosylate-functionalized macromolecule. The tosyl groups can be displaced by weak nucleophiles, such as the lone pair of electrons on the nitrogen atom in the reaction with quinuclidine in Figure 4.8(a), giving a quaternized amine salt with tosylate counterion at each end of the PS.

The second precursor for self-assembly must have carboxylate endgroups, so-called "soft" anions that will be able to exchange with the PS ionic endgroups when the two species are combined. POE with carboxymethyl endgroups can be commercially obtained in several sizes, and easily reacted with a base to provide the proper carboxylate functionality. Originally, POE was reacted with KOH, but the resulting polymer proved to be only minimally soluble in organic solvents. By reacting the POE with

tetrabutylammonium hydroxide as in Figure 4.8(b), the tetrabutylammonium counterions were able to provide increased solubility in organic solvents.

Once both precursors have been prepared, the self-assembly step in Figure 4.9 can commence. The carboxylate-containing species is dissolved in an aprotic solvent that is good for the carboxylate but poor for the quinuclidine-containing polymer – in this case, acetone was chosen. The PS was then dissolved in THF, which was a good solvent for it and also miscible with acetone. As the two polymers collide in solution, the carboxylate groups displace the tosylate counterions, and the solution was stirred at room temperature for 3 hours to ensure that the components had ample opportunity to react. Finally, the system was cooled in a freezer to precipitate the PS-containing self-assembled product.
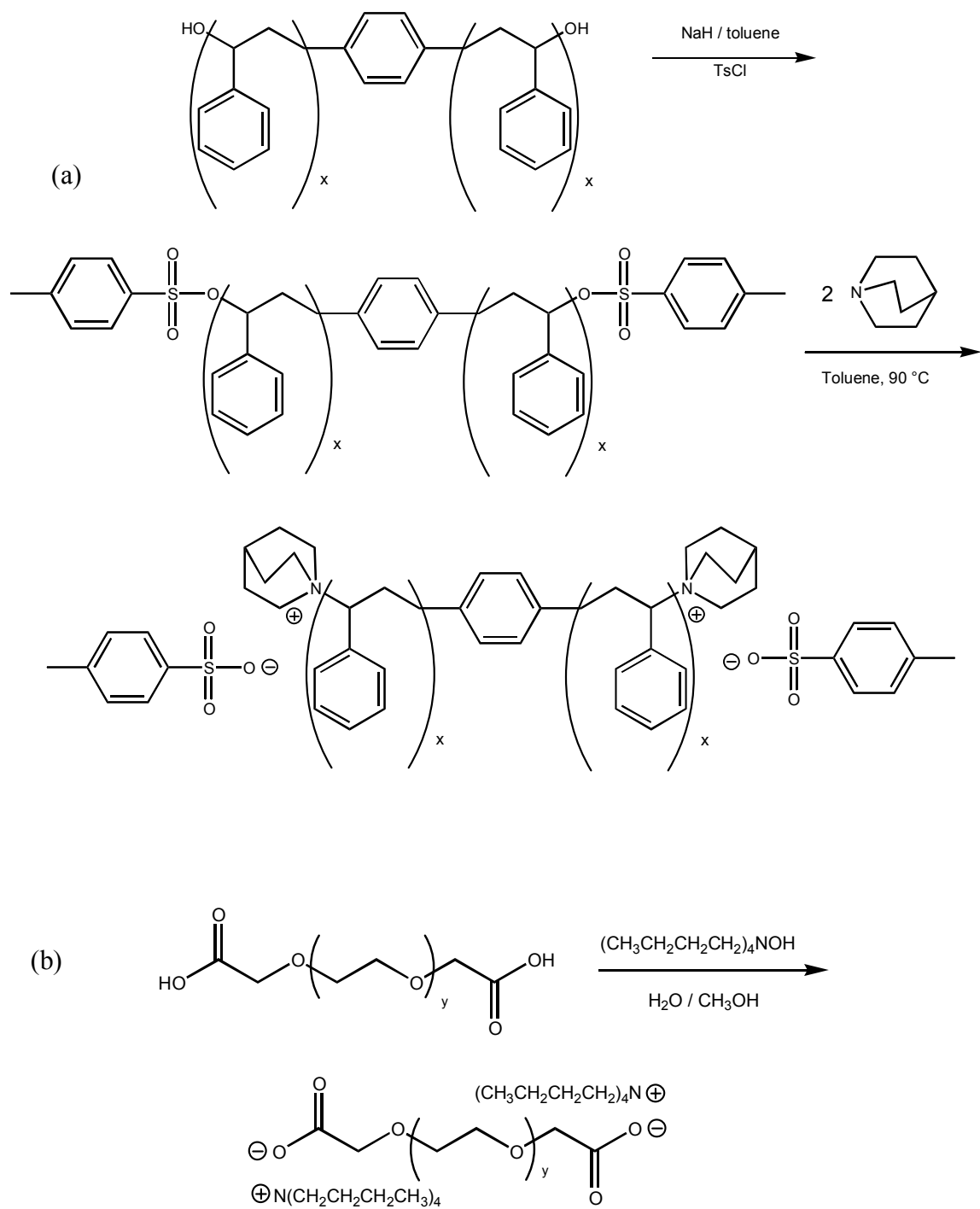
Figure 4.8 – Preparation of quinuclidine-functionalized PS from α,ω-dihydroxy PS (a) and tetrabutylammonium carboxylate-functionalized POE (b).

The precipitant was dried to remove any traces of moisture, and then dissolved in toluene under very dilute conditions. The self-assembled product begins as a dense cluster of ions in the organic solvent, but high dilution causes the ions to disperse and balance the charges.[61] If the polymer solution is too concentrated, however, chain extension can still result. Upon heating, a carbon adjacent to the nitrogen in quinuclidine is attacked by a carboxylate group, causing one of the rings in the bicyclic molecule to open and form an ester linkage, as well as turning the quaternized amine salt into a more stable tertiary amine, as depicted in Figure 4.9. While elimination of one of the groups attached to the amine was a possible unfavorable side-reaction for some quaternized amine salts, the bicyclic structure of quinuclidine ensures that ring-opening is the only way the ionic charges are converted into a covalent bonds.[58]

The ^{1}H NMR spectra of the precursors for self-assembly can be observed in Figure 4.10. The protons from quinuclidine overlap somewhat with the broad peaks from the protons along the PS backbone, but they are still visible at $\delta_H = 1.2$ and 3.7 ppm. The final proton from the quinuclidine is at 2.0 ppm, and its signal is mingled with those from the protons along the PS backbone. Another note is that peaks from the tosylate counterions are also still visible at 2.3, 7.2, and 7.4 ppm, although they are also overlapped with other protons from PS. In Figure 4.10(b), the POE peak is visible at 3.6 ppm, with the methylene groups proximal to the endgroups located at 3.8 ppm. The protons from the tetrabutylammonium counterions are located at 1.0, 1.4, 1.6, and 3.2 ppm. The residual chloroform peak from the NMR solvent is at 7.3 ppm.

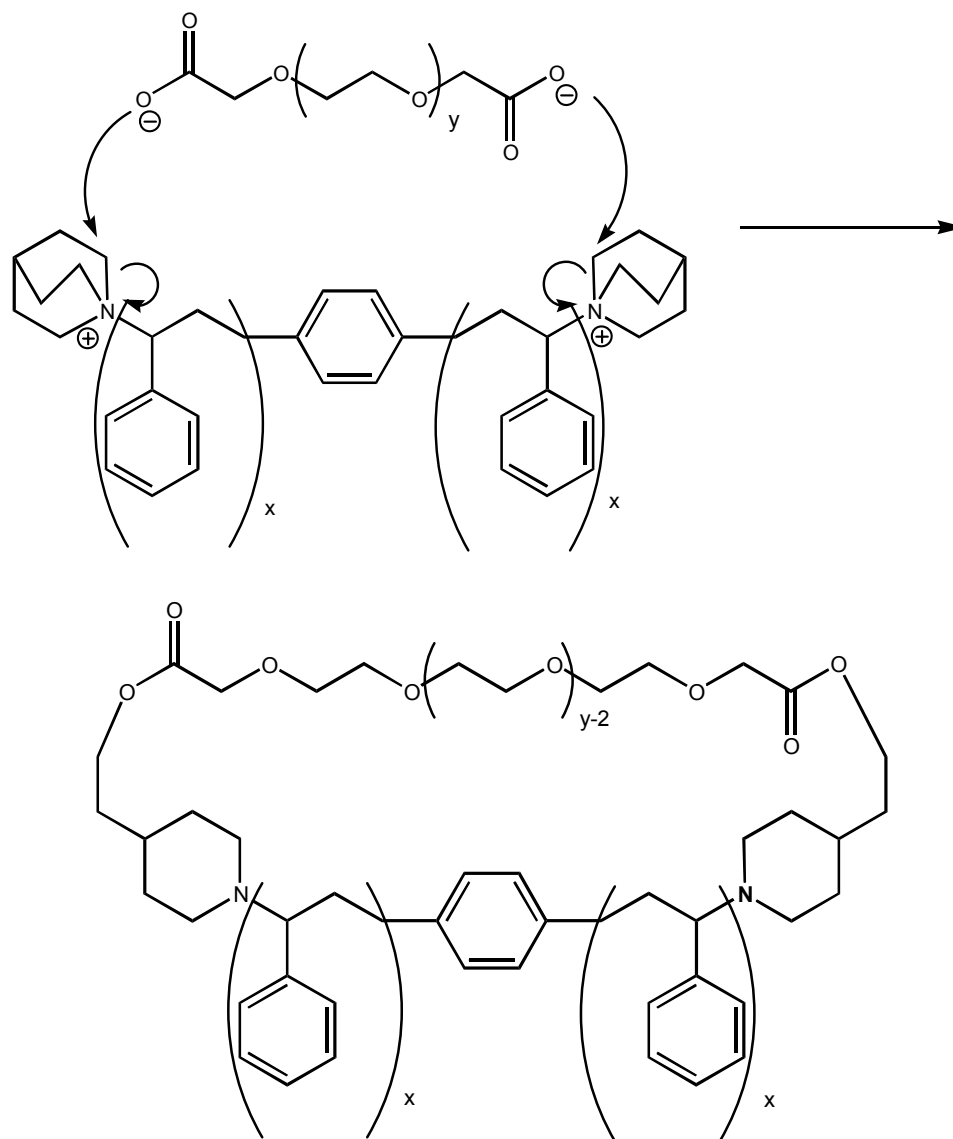**Figure 4.9 –** Covalent fixation step between carboxy-terminated POE and quinuclidine-terminated PS, showing the ring opening of quinuclidine by α,ω-dicarboxylate POE to result a PS-*block*-POE macrocycle.
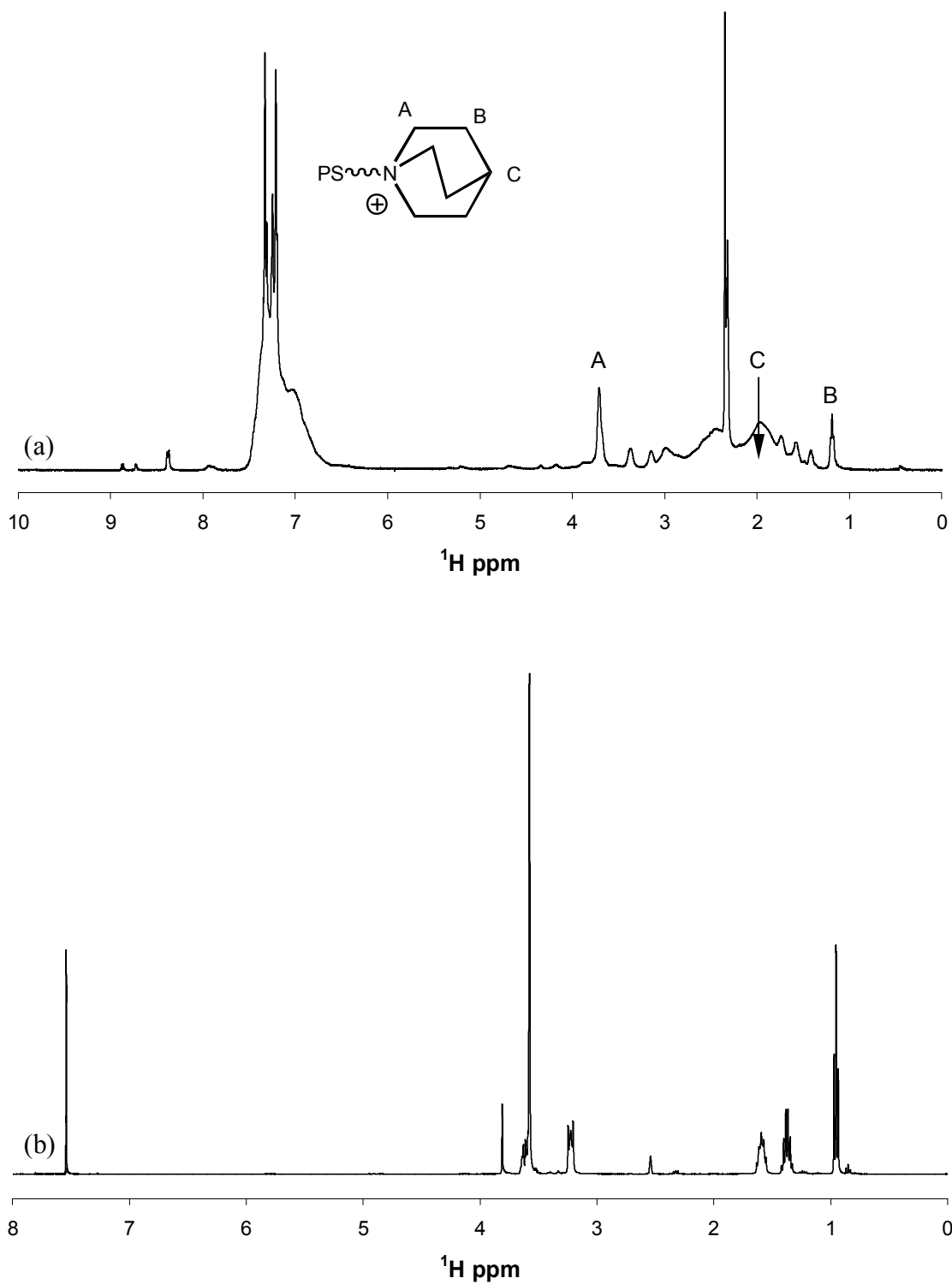
Figure 4.10 – ¹H NMR spectra of the quinuclidine-functionalized PS in THF-d_8 and detail showing a quinuclidine endgroup with peak assignments (a) and tetrabutylammonium carboxylate-functionalized POE in DMSO-d_6 (b).

The crude product from the covalent fixation step was analyzed by GPC and DOSY NMR. The GPC in Figure 4.11 shows that the retention time of the crude product has decreased relative to those of the reactants, indicating that the precursors have linked to form a larger molecule. The distribution of the product is bimodal, however, suggesting that it could contain a mixture of cyclic and chain-extended linear species. Another possible reason could be the bimodal distribution of molecular weights in the POE starting material causing a bimodal distribution when incorporated into the cyclic product. Additionally, some free POE can also be seen at a retention time of 27 minutes in the product trace, indicating that the product needs to be purified.
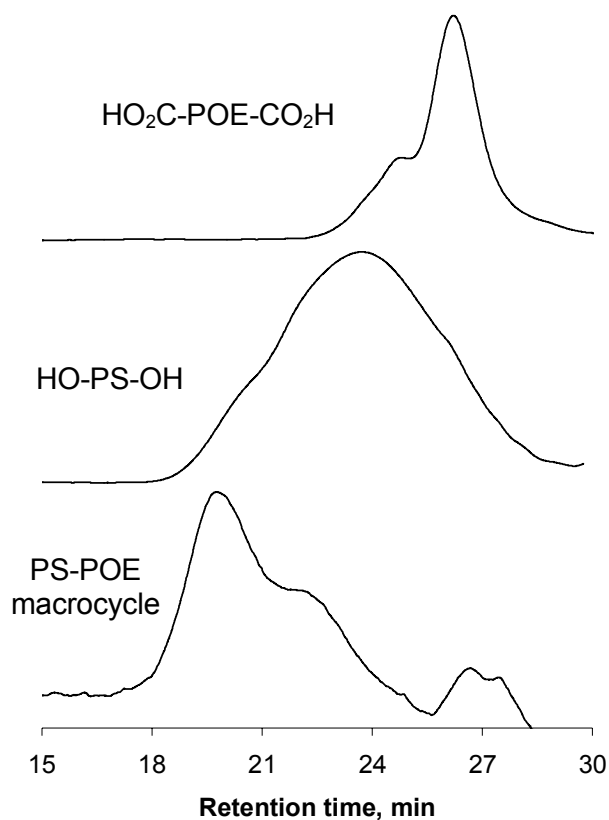
Figure 4.11 – GPC traces of α,ω-dicarboxymethyl POE (top), α,ω-dihydroxy PS (middle), and the crude PS-POE cyclization product (bottom).

Comparing the DOSY NMR spectra depicted in Figure 4.12 and 4.13 is inconclusive as well. The log of the diffusion coefficient of the product (-9.32) is lower than those of the α,ω-dicarboxymethyl POE (-8.81) and α,ω-dihydroxy PS (-9.16), although it is difficult to conclude if the increase in size is a product of cyclization, chain extension, or both. An alternative technique, such as MALDI, would be able to shed more light on that question. The DOSY does show a wide distribution for the POE, extending to faster diffusion times than the rest of the system, again pointing to some free POE in the system that needs to be removed by purification.

Figure 4.12 – 2D DOSY NMR spectrum of α,ω-dicarboxymethyl POE in CDCl$_3$.

Figure 4.13 – 2D DOSY NMR spectra of α,ω-dihydroxy PS (a), and the PS-POE self-assembly and covalent fixation product (b) in CDCl₃.

Ultimately, though, it became apparent that the best initiator for the rotaxanation experiment would only block cycles having up to 42 backbone atoms. With the ring-opened quinuclidines and ester linkages accounting for roughly 16 atoms – that is, 38% – of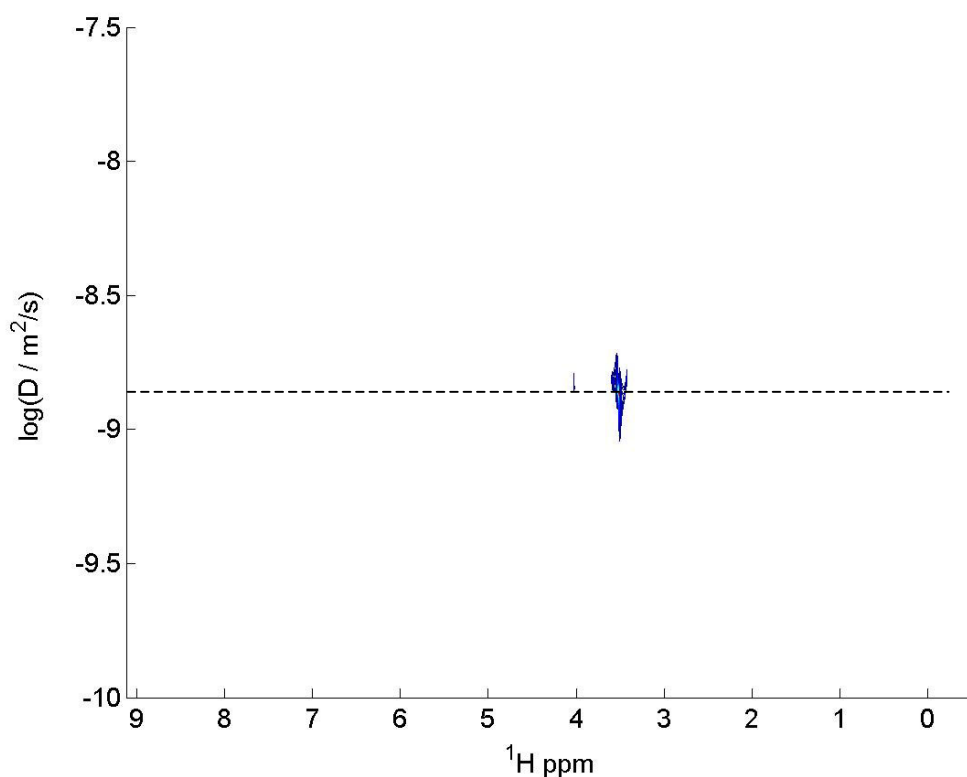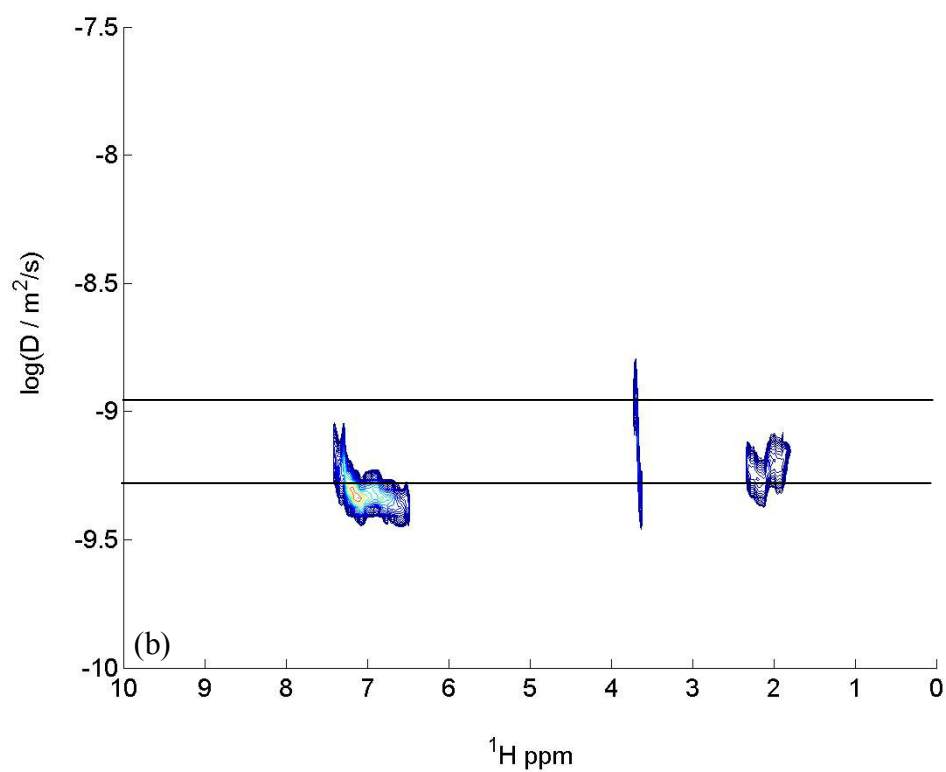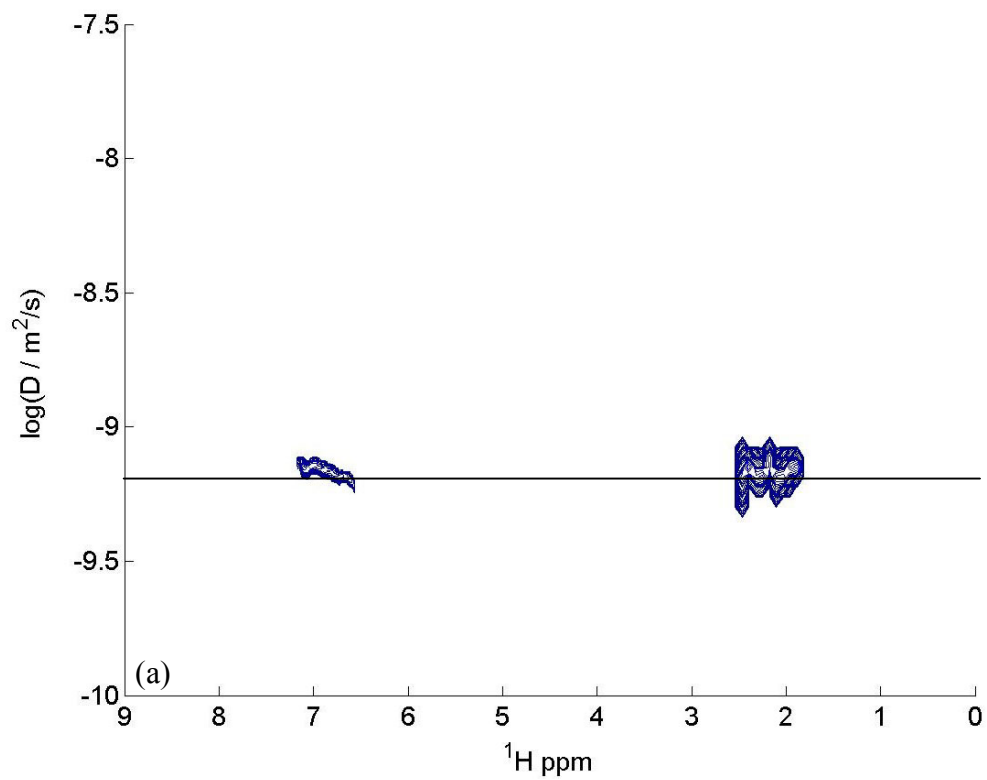 the cyclic backbone, an alternate design was conceived to maximize the presence of styrene and oxyethylene in the macrocycle.

4.3.3. PS-*block*-DEG Macrocycle

The cyclization of the PS-DEG macrocycle is very similar to the scheme for cyclizing PDMS followed in Chapter II – a linear polymer with hydroxyl endgroups is deprotonated, cyclized with a small linking molecule, and then purified by the addition of an ion-exchange resin. To ensure that cyclization would be favored over chain extension, the reaction was conducted under dilute conditions, and heptane, a nonsolvent for PS, constituted 33% of the solvent volume to reduce the distance between the PS endgroups. The ion-exchange resin was added to trap any unreacted PS species, and precipitation into methanol removed other byproducts.

Since bromines are naturally good leaving groups, no further functionalization was needed before the macromolecule could be cyclized with diethylene glycol. To provide additional spectroscopic information, however, the bromine endgroups on the PS were converted to hydroxyls by reacting them with potassium hydroxide. The newly-formed dihydroxy PS was reacted with diethylene glycol ditosylate according to Figure 4.14 so that the disappearance of the tosylate groups would be another indication of formation of the cycle.
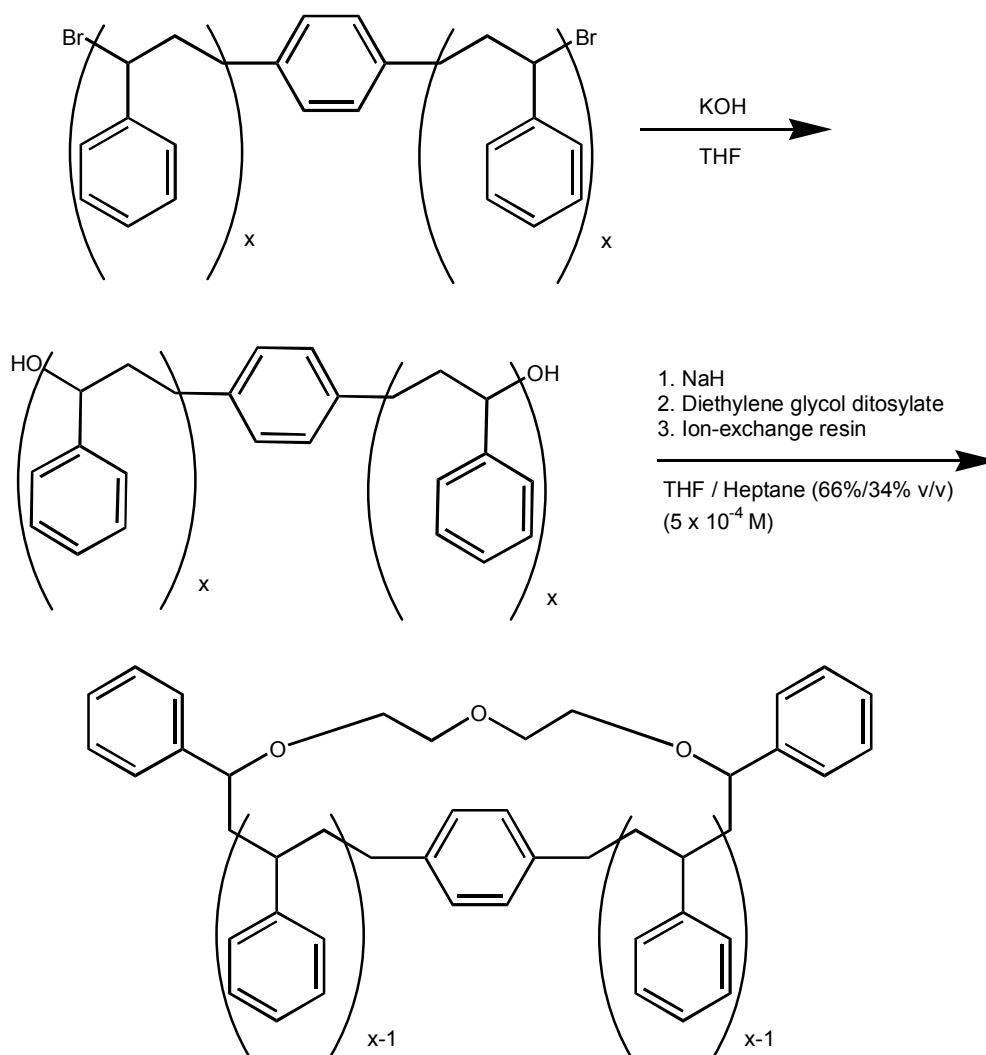
Figure 4.14 – Preparation of a hybrid PS-DEG macrocycle from α,ω-dibromo PS.

Figure 4.15 shows the almost-identical GPC traces of the dihydroxy PS and the PS-DEG cycle. Normally, the addition of 2 ethylene glycol units to such an oligomer would be sufficient to cause an increase in size and consequent decrease in the retention time of the molecule; when coupled by the well-documented decrease in hydrodynamic volume caused by cyclization, however, the molecule reverts to approximately its original size.

106
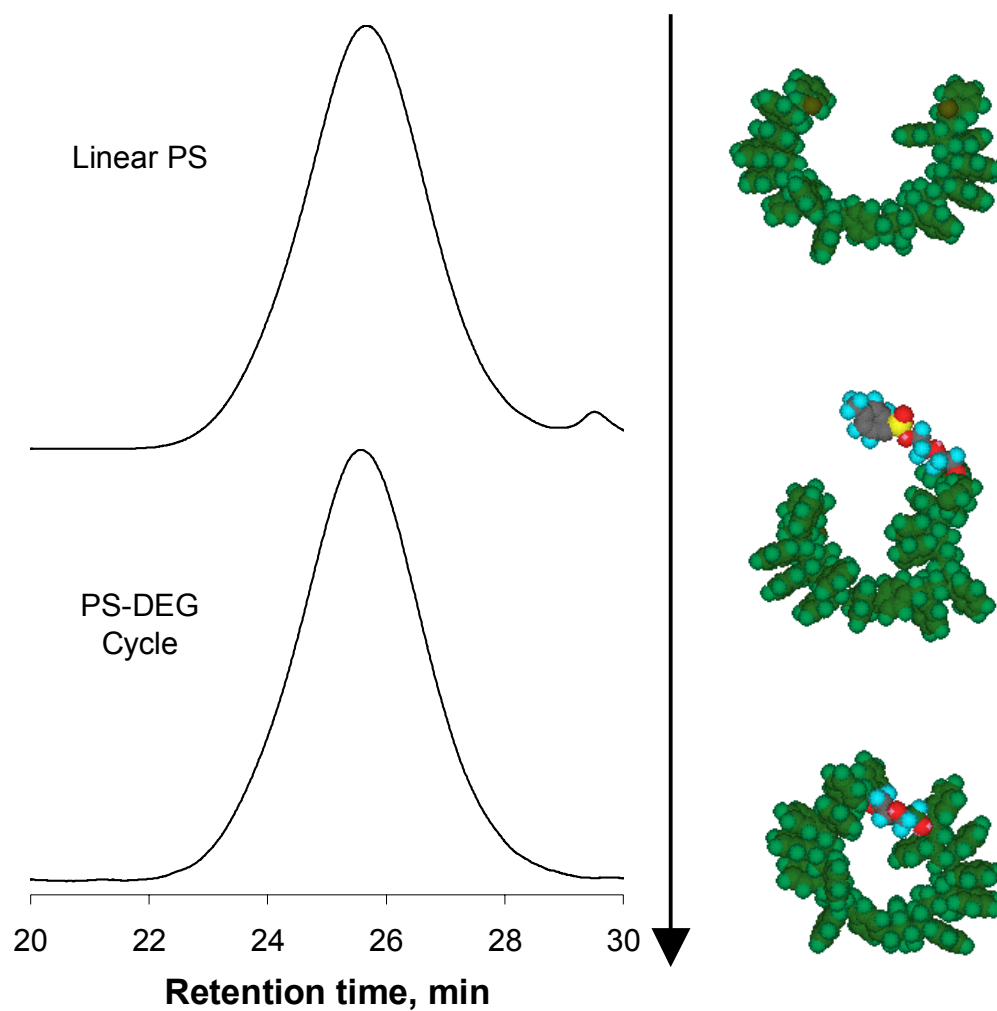
Figure 4.15 – GPC traces of linear PS and the PS-DEG macrocycle compared with three-dimensional space filling models of the linear PS (top), the linear PS-DEG intermediate (middle), and the PS-DEG macrocycle (bottom). The PS repeat units have been tinted to distinguish them from diethylene glycol ditosylate.

The MALDI-TOF mass spectrogram in Figure 4.16 provides better evidence that the reaction proceeded correctly. All the main peaks in the plot represent the mass of a PS-DEG cycle cationized with silver ions from silver trifluoroacetate. The secondary and tertiary peaks also correspond to the macrocycle, but cationized by sodium impurities from the reagent sodium hydride and potassium impurities from the potassium hydroxide solution used to clean glassware in the laboratory. None of the peaks correspond to linear species.
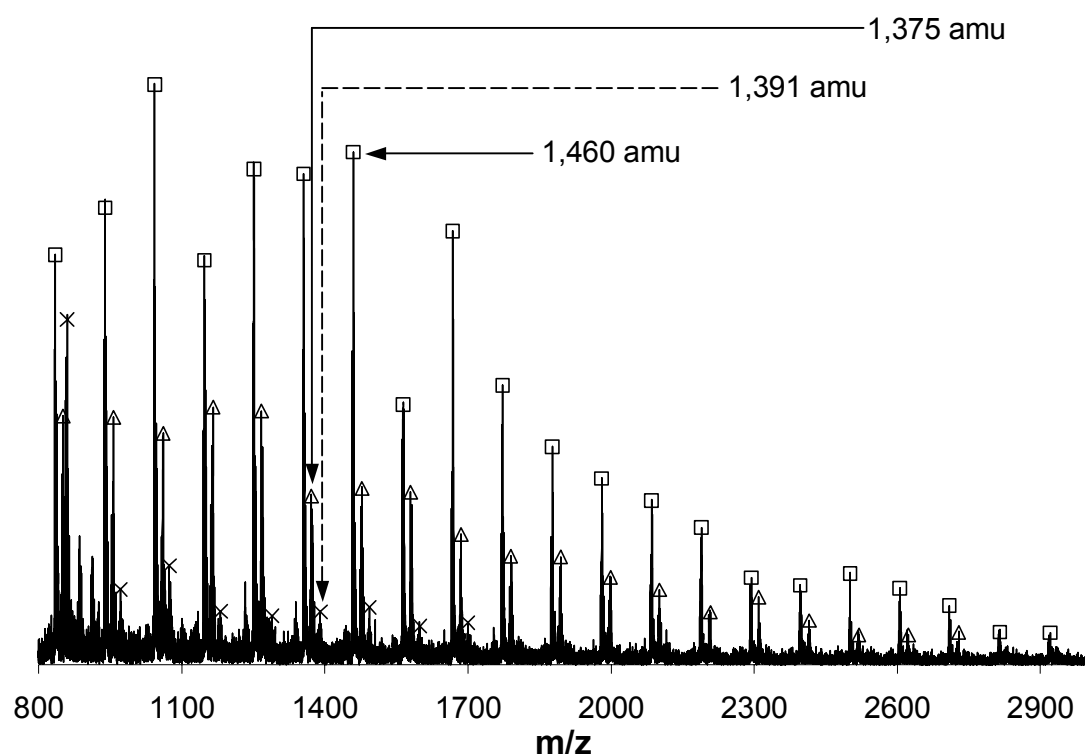
Figure 4.16 – MALDI-TOF mass spectrogram of the PS-DEG macrocycle. Species cationized with silver ions are designated with (•). Those cationized with sodium and potassium ion impurities are marked as (•) and (✕), respectively. The 3 peaks marked on the spectrogram are analyzed in Equations 4.1 – 4.3.

Each peak on the mass spectrogram corresponds to the combined mass of a polymer molecule and one of the 3 cations. To assign the peak to a particular topology, the number of repeat units of polystyrene is calculated by subtracting the ion mass, the initiator mass, and then the masses of other features (like the DEG linker or endgroups) from the mass of the peak to leave only the mass of the PS repeat units in the polymer. This number is divided by the mass of a PS repeat unit, and the result should be a whole number. Every possible permutation in polymer structure – linear PS, chain extended block copolymer, PS-DEG diblock macrocycle, etc. – is considered in these calculations, but the only structure that resulted in PS repeat units with whole numbers was the diblock PS-POE macrocycle, cationized with silver, sodium, or potassium. Sample calculations for the 3 spectrogram peaks identified in Figure 4.16 are shown in Equations 4.1 – 4.3.

23 amu (Na, ambient) + 104 amu (diethylene glycol linker) + 104 amu   (4.1)
(initiator) + x * 104 amu (PS repeat unit) = 1,375 amu

   x = 11 PS repeat units

39 amu (K, ambient) + 104 amu (diethylene glycol linker) + 104 amu   (4.2)
(initiator) + x * 104 amu (PS repeat unit) = 1,391 amu

   x = 11 PS repeat units

108 amu (Ag, ambient) + 104 amu (diethylene glycol linker) + 104 amu   (4.3)
(initiator) + x * 104 amu (PS repeat unit) = 1,460 amu

   x = 11 PS repeat units

The NMR spectra in Figure 4.17 reveals the presence of oxyethylene units at $\delta_H = 3.6$ ppm and aryl protons from 6.3-7.4 ppm. Taking a ratio of the integrals of these peaks gives a value of 1.00:11.1, very close to the expected value of 1.00:10.6, meaning that the PS and DEG are present in stoichiometric proportions. Furthermore, the protons from the tosyl groups can no longer be seen at $\delta_H = 2.5$, 7.4, and 7.8 ppm, further indication that diethylene glycol has been used as a linker to cyclize the PS. The ^{13}C spectrum appears very similar to that of the α,ω-dihydroxy PS. The main difference is that the carbon adjacent to the hydroxyl group in the linear PS is located at $\delta_C = 68$ ppm, and the peak for the carbons of the diethylene glycol ditosylate block of the macrocycle is at $\delta_C = 69$ ppm. Peaks from the tosylate groups are absent from their usual locations at 22, 142, and 147 ppm.
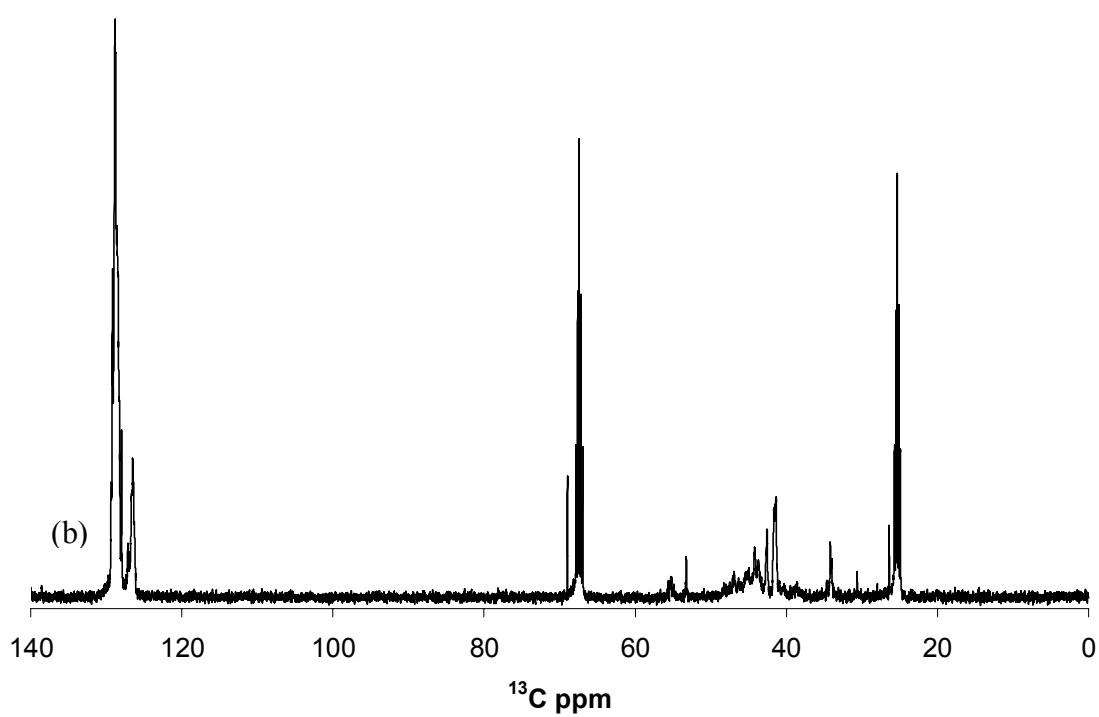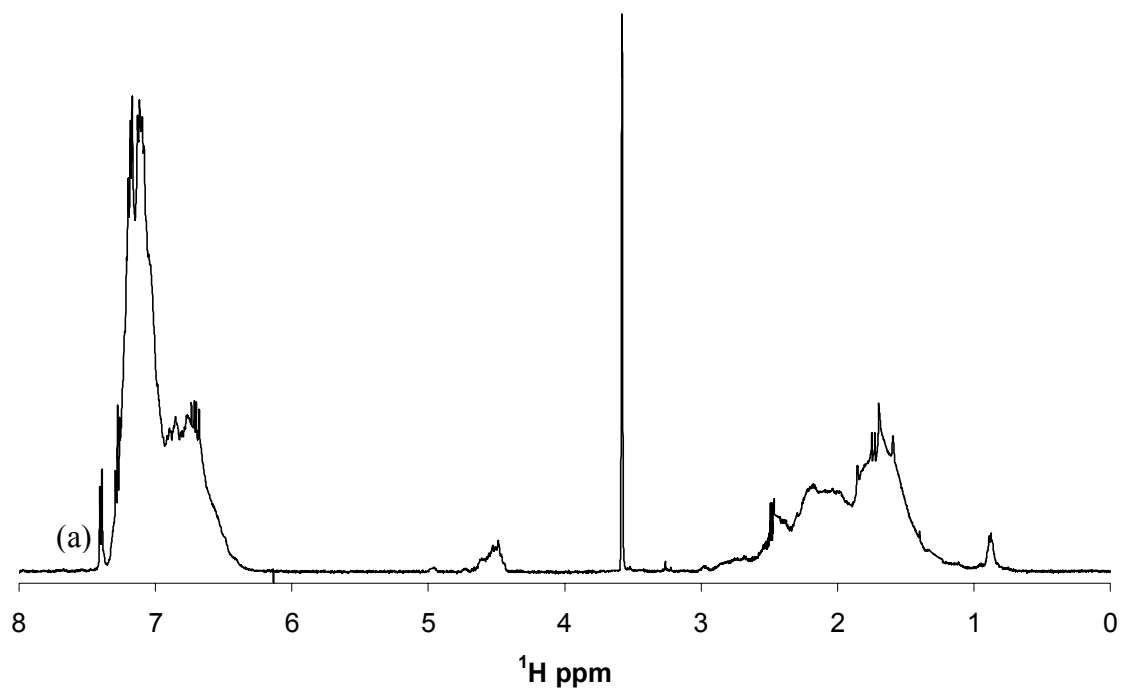
Figure 4.17 – ^{1}H (a) and ^{13}C (b) NMR spectra of the PS-DEG macrocycle in CDCl$_3$.

Two-dimensional diffusion-ordered NMR spectroscopy (DOSY) provides an even more compelling case by showing the diffusion coefficients of species as a function of their chemical shifts. DEG ditosylate in Figure 4.18 is much smaller than the dihydroxy PS in Figure 4.19(a), and this is reflected by DEG having the faster diffusion coefficient (-8.24 vs. -8.98). After the cyclization reaction, though, the chemical shifts for both styrene and ethylene glycol repeat units in Figure 4.19(b) are moving at the same diffusion coefficient (-8.97), indicating that they are now part of the same molecule. Again, shifts from the tosylate groups at δ_H = 2.5, 7.4, and 7.8 ppm are absent in the cyclic product, and the methylene protons in diethylene glycol are all now located at 3.6 ppm.
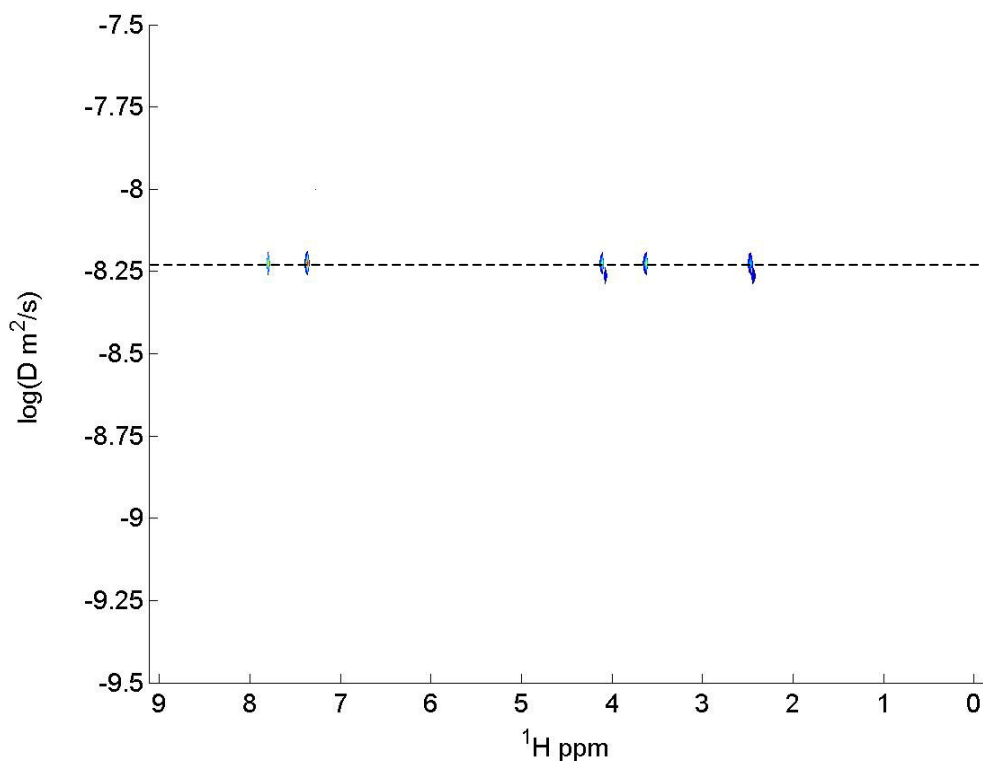
Figure 4.18 – 2D DOSY NMR spectrum of diethylene glycol ditosylate in CDCl$_3$.
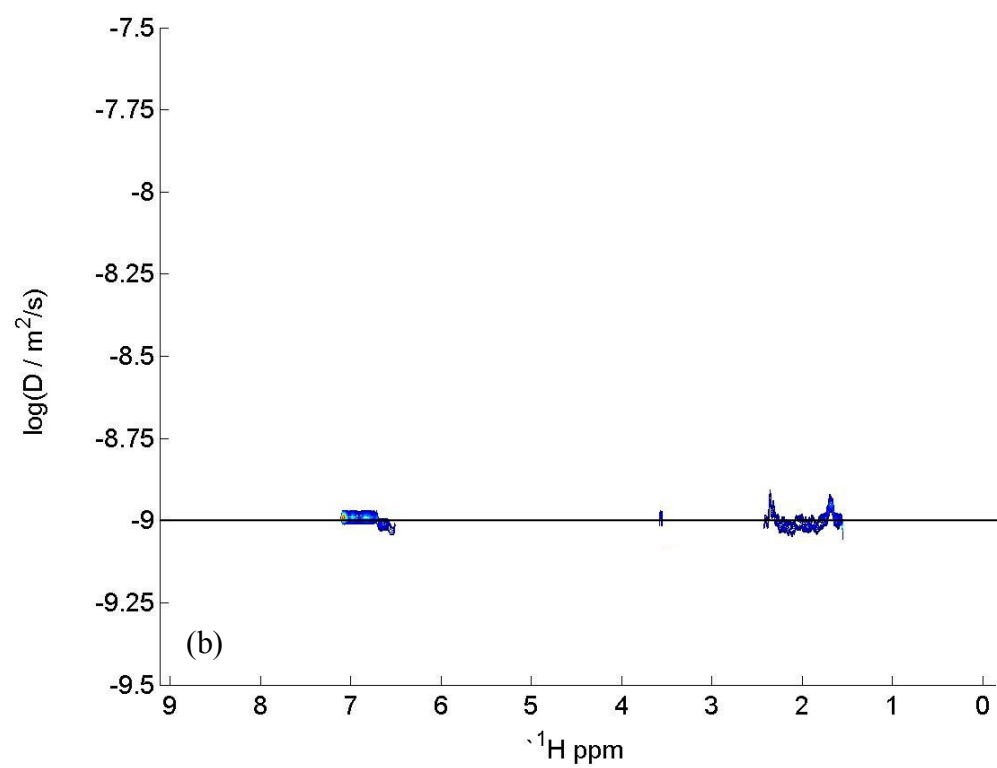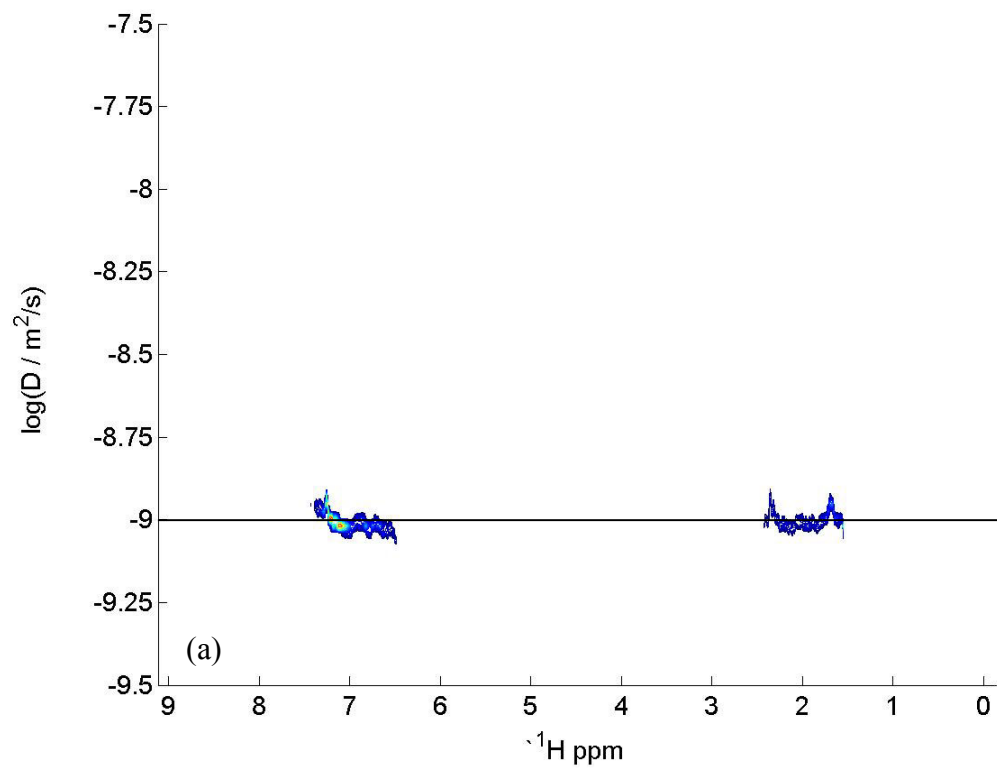
Figure 4.19 – 2D DOSY NMR spectra of α,ω-dihydroxy PS (a) and the PS-DEG macrocycle (b) in CDCl$_3$.

Although only 6% of the mass of the resulting PS-DEG macrocycle are stems from oxyethylene repeat units, small differences between the behaviors of the macrocycle and the linear PS precursor became apparent. For example, the α,ω-dihydroxy PS precipitated from a 15 wt% solution in acetone at room temperature, while the PS-DEG macrocycle remained in solution at the same concentration.

4.3.4. PS-*rotaxa*-cyclo(PS-*block*-DEG)

Unlike POE homocycles, the PS-DEG macrocycle was soluble in the styrene monomer, making the addition of a cosolvent unnecessary. Also, while the macrocycle is a soft solid at room temperature, the macrocycle exists as a liquid at the elevated reaction temperature. The GPC trace of the crude rotaxanation product in Figure 4.20 appears to be the superposition of 2 distributions of molecular weight, one of which lies in the same area as the GPC of the macrocycle. After fractionation, the distribution measured by the GPC narrowed, and a ^{1}H NMR of the removed polymer showed it to be the PS-DEG macrocycle.

Once purified, the rotaxane was analyzed with DOSY NMR to ascertain that the remaining macrocycles were threaded. As illustrated in Figure 4.21, all the components lie along the same diffusion coefficient, and the log of the diffusion coefficient for the rotaxane (-9.73) is lower than that of the macrocycle (-8.97), indicating that the macrocycle was mechanically incorporated into a larger polymer. The blocking group/ initiator, *meso*-4,4-bis(*p-tert*-butylphenyl)-4-phenylbutyl 4,4'-azobis[4-cyanopentanoate], has been empirically proven to block POE macrocycles up to 42 backbone atoms in size,

114

and it also blocks the PS-DEG cycle, which has approximately 40 atoms along its backbone.
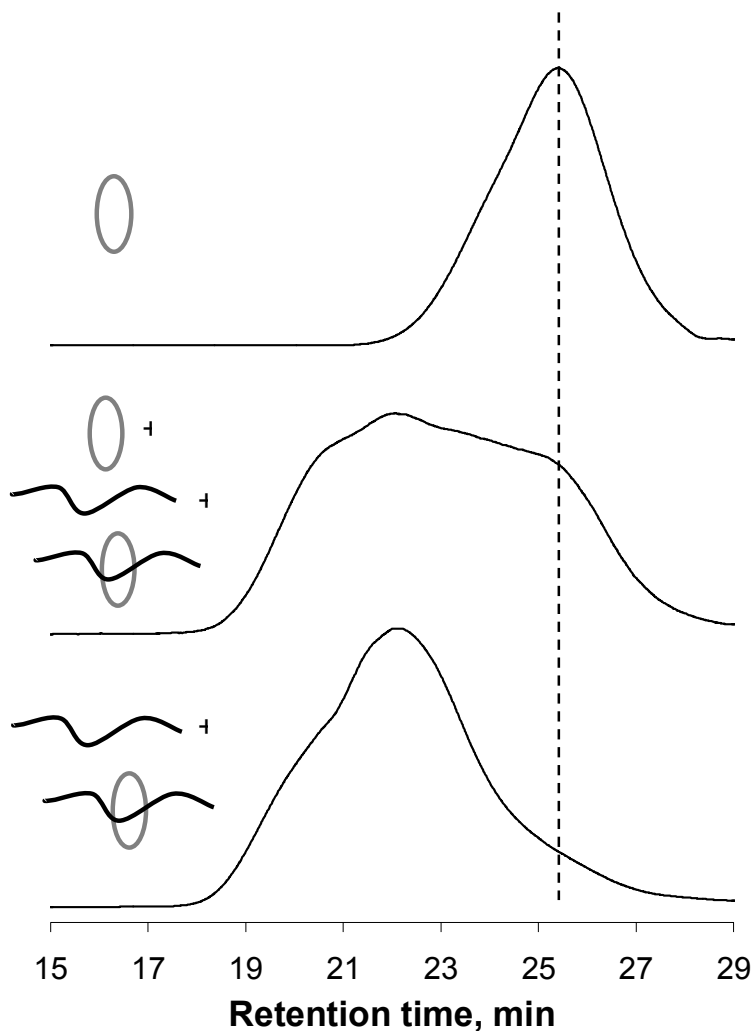
Figure 4.20 – GPC traces of the PS-DEG macrocycle (top), crude rotaxanation product (middle), and purified rotaxanation product (bottom). The crude rotaxanation product contains the rotaxane, unthreaded linear polymer, and unthreaded cycles. The purified rotaxanation product contains the rotaxane and unthreaded linear polymer.
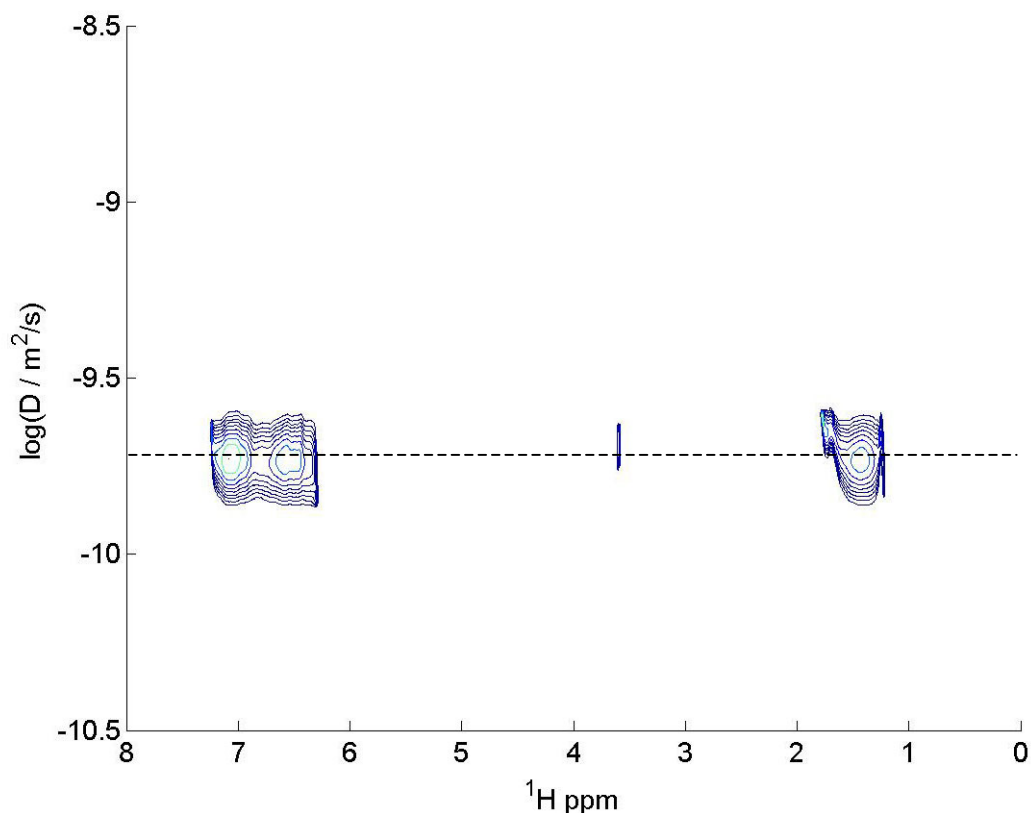
Figure 4.21 – 2D DOSY plot of poly(styrene)-*rotaxa*-cyclo[poly(styrene)-*block*-diethylene glycol] in chloroform-*d*.

Threading ratios were calculated from a quantitative ^{1}H NMR of the rotaxane in CDCl$_3$. The threading levels are commonly expressed as either the weight percent of macrocycle in the solid or by the m/n ratio, which is the ratio of macrocycles (m) to repeat units of the polymer (n). The polymer was determined to be 13% macrocycle by weight (0.78 wt% oxyethylene, taking into account that oxyethylene constitutes 6% of the mass of the cycle), with an m/n ratio of 0.010. This surpasses earlier work with rotaxanes from cyclic POE and linear PS, which had 5 wt% threading for 600 g/mol POE (42 backbone atoms) and a m/n ratio of 0.007.[40] Furthermore, this is one of the first

published accounts of a rotaxane using a hybrid macrocycle, with the other system having been prepared by Pugh et al.[21,37]

4.3.5. DSC analysis of linear PS, PS-DEG macrocycle and polyrotaxane

Thermal transitions of the linear PS precursor, PS-DEG macrocycle, and polyrotaxane were measured on a Seiko Instruments DSC 220C and are presented below in Figure 4.22. The α,ω-dihydroxy PS used as a cyclization precursor shows a T_g of 51 °C, while the macrocycle's glass transition temperature has decreased to 24 °C. Finally, the T_g of the PS-*rotaxa*-cyclo(PS-*block*-DEG) is at 79 °C. These changes in glass transition temperatures can be understood by the application of equations 4.4 and 4.5.[62-64]

$$T_g = T_{g,\infty} - \frac{C}{M_n} \tag{4.4}$$

$$\frac{1}{T_g} = \frac{w_A}{T_{g,A}} + \frac{w_B}{T_{g,B}} \tag{4.5}$$

Equation 4.4 can be used to verify that the T_g of the α,ω-dihydroxy PS is appropriate for a polystyrene chain of the same molecular weight. Besides the molecular weight, the only remaining values needed are the T_g of PS at infinite molecular weight, $T_{g,\infty}$, and an empirical constant specific for PS, C. These values have been determined to be 378 K[63] and 1.15×10^5 mol·K/g,[62] respectively, for PS. Substituting an M_n of 1,860 g/mol into equation 4.4, the result is a T_g of 43 °C (316 K), which is 8 °C lower than the observed value. Equation 4.4, however, does not take into account the effect of the hydroxyl

endgroups of the PS, which are capable of hydrogen bonding with other chains and increasing the glass transition temperature. This effect would be very large for a polymer with a low molecular weight such as 1,860 g/mol, allowing the conclusion that the measured T_g of 51 °C is reasonable for α,ω-dihydroxy PS.

Once the T_g of the PS precursor has been validated, equation 4.5 can be used to verify the glass transition temperature of the PS-DEG macrocycle. The weight fractions of PS and DEG in the macrocycle were calculated to be 0.940 and 0.060 in Section 4.3.3, so the only unknown is the T_g of diethylene glycol, which has not been measured in the scientific literature. Substituting the weight fractions of PS and DEG, as well as the T_g values of the PS and macrocycle, into Equation 4.5, the T_g of diethylene glycol was calculated to be -144 °C (129 K). The melting temperature for ethylene glycol is -10 °C (263 K), and it has been shown that the T_g of a polymer is typically between 1/2 and 2/3 of its T_m in Kelvin.[65] This places the T_g of diethylene glycol between -142 and -98 °C (132 and 175 K), very close to the T_g of -144 °C calculated using Equation 4.5. This close agreement is sufficient to verify the T_g of the PS-DEG macrocycle.

For the thermogram of the polyrotaxane, the most striking feature is that the supramolecular assembly only shows a single glass transition temperature, indicating that the linear and cyclic species are present in the same phase. The previously reported rotaxanation of PS and cyclic POE showed 2 glass transition temperatures, one for each component, and the rotaxane was only 5 wt% POE. By replacing the POE macrocycle with a hybrid macrocycle containing both styrene and oxyethylene units, the issues of phase separation that plagued the previous system have been eliminated.

Also, Equation 4.5 can be used to model the T_g of the polyrotaxane. The weight fractions of the linear and cyclic components of the rotaxane were calculated to be 0.87 and 0.13, respectively, in Section 4.3.2, and the T_g values of the macrocycle and rotaxane have been measured. Solving for the T_g of the linear component of the rotaxane, a value of 90 °C (363 K) is calculated, which is reasonable for linear PS with a molecular weight below 10,000 g/mol.[62]
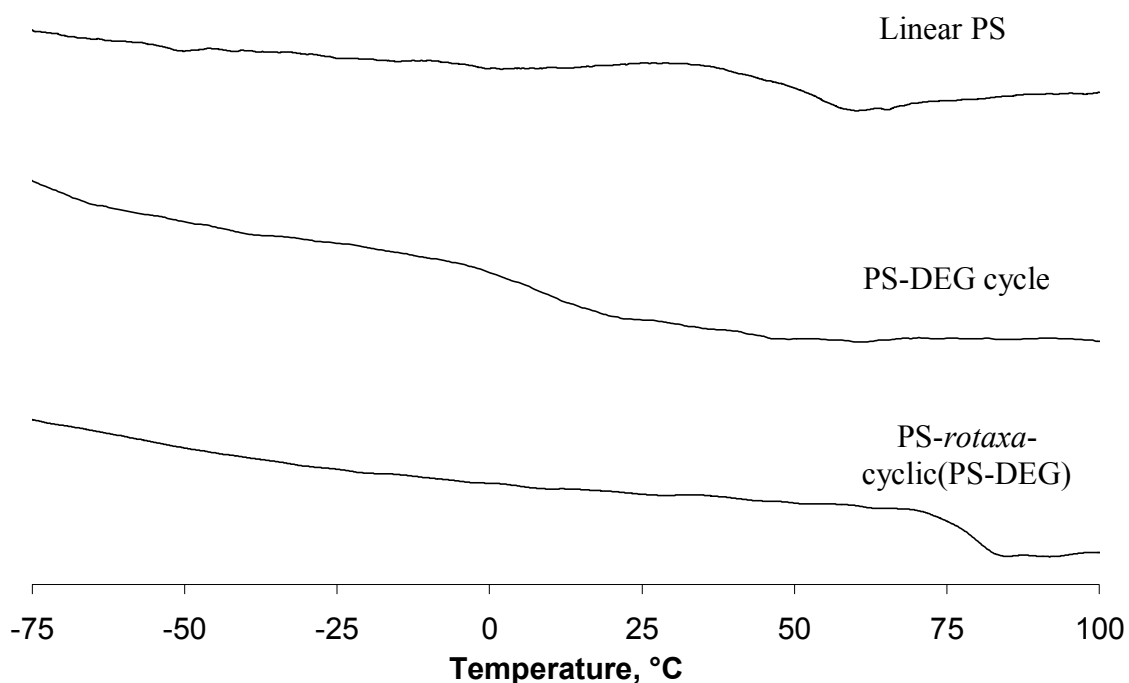

Figure 4.22 – DSC thermograms (second heating, 10 °C/min) for α,ω-dihydroxy PS, the PS-DEG macrocycle, and PS-*rotaxa*-cyclic(PS-DEG).

4.4 Conclusions

A rotaxane system was designed that consisted of linear poly(styrene) and a hybrid macrocycle containing styrene and oxyethylene blocks. Initially, the macrocycle was prepared by polymerizing styrene in the presence of ATRP agents to result in a difunctional, low molecular weight PS. The ATRP PS was functionalized with quinuclidine and reacted with functionalized POE via the self-assembly and covalent fixation cyclization methodology developed by Tezuka and Oike which typically results in quantitative cyclic yield. The most efficient method to simultaneously initiate polymerization and block the cycles from dethreading was to use *meso*-4,4-bis(*p-tert*-butylphenyl)-4-phenylbutyl 4,4'-azobis[4-cyanopentanoate], but it only stops macrocycles smaller than 42 backbone atoms from dethreading. Since the linking groups for the Tezuka scheme would then comprise nearly 40% the backbone atoms and potentially alter the thermodynamics of the macrocycle mixing with linear PS, another synthetic approach was needed.

A second cyclization pathway was developed, this time maximizing the repeats of styrene and oxyethylene in the macrocycle by directly reacting α,ω-dihydroxy PS with diethylene glycol ditosylate and using an ion-exchange resin to remove any linear species from the product mixture, resulting in a 79% yield in high purity. Next, the macrocycle was threaded by polymerizing it in the presence of styrene with the blocking group/initiator mentioned above. After removing the unthreaded macrocycle by fractionation with methanol, the polymer was determined to contain 13% of the macrocycles by weight (0.78 wt% ethylene glycol), with an m/n ratio of 0.010. The compatibilizing effect of the PS in the macrocycle allowed the rotaxane to surpass the

threading levels of a previous study which prepared a rotaxane from PS and a POE macrocycle with 42 backbone atoms, leading to 5 wt% threading and an m/n ratio of 0.007. Furthermore, thermal analysis reveals that the linear and cyclic components are present in a single phase, and the depression in the T_g of the linear polystyrene caused by the inclusion of the low-T_g macrocycles corroborates the NMR calculation of threading levels.

4.5 **References**

(1)   Gibson, H. W.; Bheda, M. C.; Engen, P. T. *Prog. Polym. Sci.* **1994**, *19*, 843.

(2)   Gong, C.; Gibson, H. W. *Current Opinion in Solid State & Material Science* **1997**, *2*, 647.

(3)   Nepogodiev, S. A.; Stoddart, J. F. *Chem. Rev.* **1998**, *98*, 1959.

(4)   Fyfe, M. C.; Stoddart, J. F. *Adv. Supramol. Chem.* **1999**, *5*, 1.

(5)   Gibson, H. W.; Engen, P. T.; Shen, Y. X.; Sze, J.; Lim, C.; Bheda, M.; Wu, C. *Makromol. Chem., Macromol. Symp.* **1992**, *54/55*, 519.

(6)   Frisch, H. L.; Wasserman, E. *J. Am. Chem. Soc.* **1961**, *83*, 3789.

(7)   Harrison, I. T.; Harrison, S. *J. Am. Chem. Soc.* **1967**, *89*, 5723.

(8)   Ogata, N.; Sanui, K.; Wada, J. *J. Polym. Lett. Ed.* **1976**, *14*, 459.

(9)   Harada, A.; Kamachi, M. *Macromolecules* **1990**, *23*, 2821.

(10)   Harada, A. *Coordination Chemistry Reviews* **1996**, *148*, 115.

(11)   Harada, A.; Li, J.; Kamachi, M. *Macromolecules* **1993**, *26*, 5693.

(12)   Zhao, T.; Beckham, H. W. *Macromolecules* **2003**, *36*, 6945.

(13)   Gong, C.; Gibson, H. W. *Macromolecules* **1998**, *31*, 1814.

(14)   Gibson, H. W.; Bryant, W. S.; Lee, S.-H. *J. Polym. Sci., Part A: Polym. Chem.* **2001**, *39*, 1978.

(15)   Wu, C.; Bheda, M. C.; Lim, C.; Shen, Y. X.; Sze, J.; Gibson, H. W. *Polymer Communications* **1991**, *32*, 204.

(16)   Harrison, I. T. *J.C.S. Perkin I* **1974**, 301.

(17)   Gibson, H. W.; Liu, S.; Gong, C.; Ji, Q.; Joseph, E. *Macromolecules* **1997**, *30*, 3711.

(18)   Gibson, H. W.; Lee, S.-H.; Engen, P. T.; Lecavalier, P.; Sze, J.; Shen, Y. X.; Bheda, M. *J. Org. Chem.* **1993**, *58*, 3748.

(19)   Yamagishi, T.-A.; Kawahara, A.; Kita, J.; Hoshima, M.; Umehara, A.; Ishida, S.; Nakamoto, Y. *Macromolecules* **2001**, *34*, 6565.

(20)   Lee, S.-H.; Engen, P. T.; Gibson, H. W. *Macromolecules* **1997**, *30*, 337.

(21)   Pugh, C.; Bae, J.-Y.; Scott, J. R.; Wilkins, C. L. *Macromolecules* **1997**, *30*, 8139.

(22)   Mason, P. E.; Bryant, W. S.; Gibson, H. W. *Macromolecules* **1999**, *32*, 1559.

(23)   Gibson, H. W.; Engen, P. T.; Lee, S. H. *Polymer* **1999**, *40*, 1823.

(24)   Ashton, P. R.; Balzani, V.; Kocian, O.; Prodi, L.; Spencer, N.; Stoddart, J. F. *J. Am. Chem. Soc.* **1998**, *120*, 11190.

(25)   Pease, A. R.; Jeppesen, J. O.; Stoddart, J. F.; Luo, Y.; Collier, C. P.; Heath, J. R. *Acc. Chem. Res.* **2001**, *34*, 465.

(26)   Harada, A. *Acc. Chem. Res.* **2001**, *34*, 456.

(27)   Anastasiadis, S. H.; Restos, H.; Pispas, S.; Hadjicristidis, N.; Neophytides, S. *Macromolecules* **2003**, *36*, 1994.

(28)   Gray, H. N.; Jorgensen, B.; McClaughtery, D. L.; Kippenberger, A. *Ind. Eng. Chem. Res.* **2001**, *40*, 3540.

(29)   Gibson, H. W.; Bheda, M. C.; Engen, P.; Shen, Y. X.; Sze, J.; Zhang, H.; Gibson, M. D.; Delaviz, Y.; Lee, S.; Liu, S.; Wang, L.; Nagvekar, D.; Rancourt, J.; Taylor, L. T. *J. Org. Chem.* **1994**, *59*, 2186.

(30)   Lecavalier, P. R.; Shen, Y. X.; Wu, C.; Gibson, H. W. *Polymer Preprints* **1990**, *31*, 659.

(31)   Gong, C.; Gibson, H. W. *Macromolecules* **1996**, *29*, 7029.

(32)   Gong, C.; Ji, Q.; Glass, T. E.; Gibson, H. W. *Macromolecules* **1997**, *30*, 4807.

(33)   Mason, P. E.; Bryant, W. S.; Gibson, H. W. *Macromolecules* **1999**, *32*, 1559.

(34)   Mason, P. E.; Parsons, I. W.; Tolley, M. S. *Polymer* **1998**, *39*, 3981.

(35)   Hodge, P.; Monisvade, P.; Owen, G. J.; Heatley, F.; Pang, Y. *New. J. Chem.* **2000**, *24*, 703.

(36)   Amabilino, D. B.; Anelli, P.-L.; Ashton, P. R.; Brown, G. R.; Cordova, E.; Godinez, L. A.; Hayes, W.; Kaifer, A. E.; Philp, D.; Slawin, A. M. Z.; Spencer, N.; Stoddart, J. F.; Tolley, M. S.; Williams, D. J. *J. Am. Chem. Soc.* **1995**, *117*, 11142.

(37)   Wollyung, K. M.; Xu, K.; Cochran, M.; Kasko, A. M.; Mattice, W. L.; Wesdemiotis, C.; Pugh, C. *Macromolecules* **2005**, *38*, 2574.

(38)   Zhao, T.; Beckham, H. W.; Gibson, H. W. *Macromolecules* **2003**, *36*, 4833.

(39)   Wimmer, R.: Dept. of Life Sciences, Aalborg University, Aalborg, Sweden. Class notes (PowerPoint file). http://dmailweb.bio.auc.dk/~rw/.

(40)   Singla, S. *Topological Effects on Properties of Multicomponent Polymer Systems*. School of Polymer, Textile and Fiber Engineering, Georgia Institute of Technology, 2004.

(41)   Pohl, M. C.; Espenson, J. H. *Inorg. Chem.* **1980**, *19*, 235.

(42)   Qin, S.; Saget, J.; Pyun, J.; Jia, S.; Kowalewski, T.; Matyjasewski, K. *Macromolecules* **2003**, *36*, 8969.

(43)   Francis, R.; Taton, D.; Logan, J. L.; Masse, P.; Gnanou, Y.; Duran, R. S. *Macromolecules* **2003**, *36*, 8253.

(44)   Roovers, J.; Toporowski, P. M. *Macromolecules* **1983**, *16*, 843.

(45)   Lepoittevin, B.; Dourges, M. A.; Masure, M.; Hemery, P.; Baran, K.; Cramail, H. *Macromolecules* **2000**, *33*, 8218.

(46)   Oike, H.; Hamada, M.; Eguchi, S.; Danda, Y.; Tezuka, Y. *Macromolecules* **2001**, *34*, 2776.

(47)   Yin, R.; Hogen-Esch, T. E. *Macromolecules* **1993**, *26*, 6952.

(48)   Hussman, M.; Malmström, E. E.; McNamara, M.; Mate, M.; Mecerreyes, D.;
        Benoit, D.; Hedrick, J. L.; Mansky, P.; Huang, E.; Russel, T. P.; Hawker, C. J.
        Macromolecules **1999**, *32*, 1424.

(49)   Hawker, C. J.; Bosman, A. W.; Harth, E. *Chem. Rev.* **2001**, *101*, 3661.

(50)   Hawker, C. J.; Barclay, G. G.; Orellana, A.; Dao, J.; Devonport, W.
        Macromolecules **1996**, *29*, 5245.

(51)   Matyjasewski, K.; Xia, J. *Chem. Rev.* **2001**, *101*, 2921.

(52)   Matyjasewski, K.; Wang, J.-S. *Macromolecules* **1995**, *28*, 7901.

(53)   Johnson, R. M.; Ng, C.; Samson, C. C. M.; Fraser, C. L. *Macromolecules* **2000**,
        33, 8618.

(54)   Johnson, R. M.; Corbin, P. S.; Ng, C.; Fraser, C. L. *Macromolecules* **2000**, *33*,
        7404.

(55)   Matyjaszewski, K.; Pintauer, T.; Gaynor, S. *Macromolecules* **2000**, *33*, 1476.

(56)   Oike, H.; Imaizumi, H.; Mouri, T.; Yoshioka, Y.; Uchibori, A.; Tezuka, Y. *J. Am.
        Chem. Soc.* **2000**, *122*, 9592.

(57)   Tezuka, Y. *Macromol. Chem. Phys.* **1997**, *198*, 627.

(58)   Tezuka, Y.; Oike, H. *Prog. Polym. Sci.* **2002**, *27*, 1069.

(59)   White, B. M.; Watson, W. P.; Barthelme, E. E.; Beckham, H. W. *Macromolecules*
        2002, *35*, 5345.

(60)   Singla, S.; Zhao, T.; Beckham, H. *Macromolecules* **2003**, *36*, 6945.

(61)   Karayianni, E.; Jerome, R.; Cooper, S. L. *Macromolecules* **1997**, *30*, 7444.

(62)   Fox, T. G.; Flory, P. J. *J. Polym. Sci.* **1954**, *14*, 315.

(63)   Liu, X.; Chen, D.; He, Z.; Zhang, H.; Hu, H. *Polym. Commun.* **1991**, *32*, 123.

(64)   Fox, T. G. *Bull. Am. Phys. Soc.* **1956**, *2*, 123.

(65)   Billmeyer, F. W., Jr. *Textbook of Polymer Science*; 3rd ed.; John Wiley & Sons:
        New York, 1984.

CHAPTER V

CONCLUSIONS AND RECOMMENDATIONS FOR FUTURE RESEARCH

5.1. Conclusions

The major findings of the work are summarized below:

Hydrosilane-functionalized cyclic PDMS was prepared from linear α,ω-dihydroxy PDMS and dichloromethylsilane, then purified by the addition of an ion-exchange resin to remove linear byproducts, resulting in a yield of 77%. The reaction product and purity were confirmed with ^{1}H NMR and IR spectroscopy, MALDI-TOF MS and GPC. The synthesis of vinylsilane-functionalized cyclic PDMS was attempted in a similar fashion from linear α,ω-dihydroxy PDMS and dichloromethylsilane, but ^{1}H and ^{13}C NMR showed that the many of the vinyl groups had been converted to alkenes during the reaction, presumably by nucleophilic attack of silanolate intermediates.

Linear α-allyl,ω-methoxy POE was synthesized from α-hydroxy,ω-methoxy POE and allyl bromide, and analyzed with ^{1}H and ^{13}C NMR.

Coupling the hydrosilane-functionalized PDMS and α-allyl,ω-methoxy POE moieties via a platinum catalyzed hydrosilylation reaction to make a tadpole macrocycle did not result in a product when the reaction was analyzed by GPC and NMR. Several platinum catalysts were tested under various conditions, but none resulted in a tadpole, even though they worked with the functionalized POE and α,ω-dihydrosilane PDMS to produce a linear triblock copolymer. It was theorized that the dimethylsiloxane repeat

units around the hydrosilane group were too bulky, preventing the platinum complex from reacting.

Linear α-methoxy,ω-allyl POE and hydrosilane-functionalized PS were successfully linked with a free-radical-catalyzed hydrosilylation reaction using di-*tert*-butyl peroxide, the first reported hybrid PDMS-POE macrocycle. The tadpole product was characterized with ^{1}H, ^{13}C, and ^{29}Si NMR spectroscopy, GPC and DSC. Thermal analysis showed that the POE and PDMS phases had undergone microphase separation in the solid state, allowing the POE to show a melting endotherm at 24 °C, 9 °C lower than the T_m of the POE starting material.

Since the tadpole was essentially a nonionic surfactant, the critical micelle concentrations in polar and nonpolar solutions were measured by surface tensiometry. Concurrently, the hydrodynamic radii of the tadpoles above and below the CMC were measured with dynamic light scattering. The tadpole had a CMC of 5.06 mg/mL in MEK, the most polar solvent that would dissolve the macrocycle without causing immediate micellization, and a CMC of 6.76 mg/mL in toluene, the most nonpolar solvent in which the tadpoles could exist as single molecules at low concentrations. The micelles were found to be an order of magnitude larger in size under polar conditions than under nonpolar conditions.

As a precursor for the PS-DEG macrocycle, styrene was polymerized via ATRP, resulting in a low molecular weight, low polydispersity, α,ω-difunctional polymer. The polymer structure was analyzed with ^{1}H and ^{13}C NMR, GPC, and DSC. The PS was then cyclized under dilute conditions with diethylene glycol ditosylate, and an ion-exchange resin was used to remove linear byproducts to give a macrocycle in 76% yield. The

cyclic structure was ascertained with ^{1}H, ^{13}C, and DOSY NMR, MALDI-TOF MS, GPC, and DSC. This marks the first reported instance of a hybrid PS-DEG macrocycle.

The PS-DEG macrocycle was statistically threaded by linear PS under neat conditions. To prevent the macrocycles from dethreading, a free radical initiator incorporating sterically bulky groups was used to catalyze the polymerization and cap the ends of the linear molecule. DOSY NMR was used to confirm that the rotaxane had been prepared, and ^{1}H NMR was used to calculate that the macrocycles were present in 13 wt%, with a threading ratio of 0.010. This is significantly larger than the previously reported PS-*rotaxa*-cycloPOE of a similar size, which was 5 wt% macrocycle and had a threading ratio of 0.007. The DSC thermogram of the rotaxane showed only 1 T_g, indicating that the macrocycles and linear polymer were completely miscible, unlike the PS-*rotaxa*-cycloPOE, which showed glass transition temperatures for both the linear and cyclic components.

5.2.   Recommendations for Future Work

Use surface tensiometry to study if the PDMS-POE tadpole undergoes transitions to differently-shaped micelles at higher concentrations. This would provide further information on its solution behavior that could be compared to other nonionic surfactants.

Perform tests to explore if the shapes of the micelles in polar and nonpolar solution have any effect on the uptake of small molecules into the micellar interior. This would benchmark the tadpole according to one of the most important criteria for surfactants.

Synthesize a range of PS-POE macrocycles with varying ratios of styrene and oxyethylene repeat units. To result in linear PS with lower molecular weights, it may be

necessary to replace the bipyridyl ligands on the ATRP catalyst with others that possess better solubility in toluene at high concentrations. These macrocycles could then be used to explore the solution properties of the system in a similar fashion to the ways mentioned for the PDMS-POE tadpole macrocycle. Furthermore, rotaxanes can be prepared from the macrocycles and characterized to determine the effects of the chemical structure of the macrocycle on threading levels and resultant physical properties.

VITA

Walter Philip Watson was born on January 20, 1978, in Greenville, South Carolina, and wanted to get started with life so quickly that he emerged a month prematurely. He was first exposed to chemistry his sophomore year at Eastside High School, under the guidance of his teacher Mrs. Claudia Timmons, and repeated viewings of *The Graduate* ("I just want to say one word to you – just one word – plastics") interested him in the chemistry of polymers (among other things).

After graduating in 1996, he attended Clemson University, majoring in Textile Chemistry and spending his summers researching conducting polymers for Dr. Richard Gregory. In 2000, he left Clemson to pursue graduate studies in Polymer Chemistry at the Georgia Institute of Technology, and vociferously denies that his departure catapulted Clemson into the "Top 20 Party Schools" list.[1] For his Ph. D., he worked under the guidance of Dr. Haskell Beckham, and his thesis was entitled "Amphiphilic Macrocycles for Supramolecular Assemblies." After meeting many people and having many adventures along the way, the most exciting of which involved marrying Cathy Lane in 2004, he completed his degree in March of 2005.

1. Princeton Review 2001 Edition – Not named in the "Top 20 Party Schools" list

   Princeton Review 2002 Edition – #2 party school in nation

   Princeton Review 2003 Edition – #2 party school, #1 in hard liquor consumption, #1 in beer

      consumption, and #1 for marijuana usage in nation